

MODELING AND UTILIZING A VANADIUM REDOX FLOW BATTERY
FOR EASIER GRID AND MARKET INTEGRATION OF WIND POWER

Vom Fachbereich Produktionstechnik
der
UNIVERSITÄT BREMEN

zur Erlangung des Grades

Doktor-Ingenieur

genehmigte

Dissertation

von

M. Sc. Burak Türker

Gutachter: Prof. Dr. Matthias Busse

Prof. Dr. Carsten Agert (Carl von Ossietzky Universität Oldenburg)

Tag der mündlichen Prüfung: 16. Dezember 2014

*"Nothing in all the world is more dangerous than
sincere ignorance and conscientious stupidity."*

Dr. Martin Luther King, Jr.

Acknowledgments

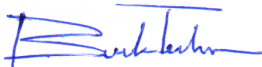
First of all, I would like to thank NEXT ENERGY - EWE Research Centre for Energy Technology at Carl von Ossietzky University and its director Prof. Carsten Agert for giving me the opportunity to conduct my doctoral research at the institute. Having already mentioned the research center, where I worked for almost 4 years, I would like to thank all my colleagues, fellow scientists, and other personnel, who have contributed greatly to my research. I must especially mention the priceless contributions by my colleagues Meinert Lewerenz, Lidiya Komsijska, and Ralf Dittmann.

I am also thankful to Prof. Matthias Busse and other valuable professors of the Department of Production Engineering at University of Bremen for their supervision and guidance throughout the research. A special gratitude goes to Mr. Sebastián Arroyo Klein, the first graduate student I supervised and whose work has been an integral part of this research. I am also grateful to the Oldenburg University Postgraduate Programme Renewable Energy (PPRE) team who kept on supporting me at every front since my graduation with a M.Sc. Renewable Energy degree back in 2008.

At the end of this acknowledgment, I must mention my family. I have always felt their support, even if it came from thousands of kilometers away. Furthermore, I am glad that I have had all these great friends around me. They really helped me out during the times when things looked a little shaky. Finally, the most special thanks to the most special person, my dearest girlfriend whom I met while approaching the final stages of the writing of this book. She kept me motivated with her utmost support and contributed to this work with her invaluable academic experience.

Erklärung

Ich erkläre, dass ich die Arbeit ohne unerlaubte fremde Hilfe angefertigt habe, keine anderen als die von mir angegebenen Quellen und Hilfsmittel benutzt habe und die den benutzten Werken wörtlich oder inhaltlich entnommenen Stellen als solche kenntlich gemacht habe.



Burak Türker

Abstract

Power grid and market integration of wind energy is a challenge due to the fluctuating and intermittent power output resulting from the variable nature of wind resource. Energy storage is a promising alternative for effective grid integration of renewable energy. One storage technology which is under the spotlight in the recent years is the vanadium redox flow battery (VRFB) which could have certain advantages when utilized at large-scale grid connected applications.

In this study, a megawatt scale VRFB was modeled based on experimental data with a kilowatt scale real life unit. The dependence of the overall system efficiency on the state of charge and power was determined. By using the model, optimal number of modules for certain power levels during charging and discharging operations were estimated for megawatt scale operations.

In order to evaluate the power grid integration of wind power at a single wind farm level, a second simulation model which combines the megawatt scale VRFB model and a medium sized (10 MW) wind farm was developed and the battery was utilized to compensate for the deviations resulting from the forecast errors in an electricity market bidding structure. Using an existing electricity market model based on deviation penalties and penalty multipliers, economics of the system were evaluated by determining the payback periods for a dedicated VRFB installation at this medium sized, single wind farm level.

Zusammenfassung

Durch ihre fluktuierende und unregelmäßige Energieerzeugung, resultierend aus der variierenden Verfügbarkeit der natürlichen Ressource Wind, stellt die Stromnetz- und Marktintegration von Windenergie eine Herausforderung dar. Vanadium Redox Flow Batterien (VRFB) werden in jüngster Zeit aufgrund bestimmter Vorteile in großmaßstäblichen Anwendungen als geeignete Technologie zur nötigen Speicherung elektrischer Energie und somit als vielversprechende Option zur Integration erneuerbarer Energieformen in bestehende Netze angesehen.

Im Rahmen dieser Studie wurde eine VRFB im Bereich von Megawatt anhand experimenteller Daten, welche mit einem System im Kilowattbereich erhoben wurden, modelliert. Dabei wurde die Abhängigkeit der Systemeffizienz vom Ladezustand und aktueller Batterieleistung miteinbezogen. Anhand dieses Modells wurde die optimale Anzahl der aktiven Module während der Lade- und Entladevorgänge ermittelt und in den Megawattbereich skaliert. Um die Netzintegration von Windenergie auf der Ebene einer einzelnen mittelgroßen Windfarm (10 MW) zu evaluieren wurde ein zweites Simulationsmodell erstellt, welches das skalierte VRFB-Modell zum Ausgleich der Abweichungen von der Windkrafthertragsprognose in einem Elektrizitätsmarkt verwendet. Innerhalb dieses Szenarios wurde die Wirtschaftlichkeit einer dediziert installierten VRFB durch die Berechnung der Amortisationszeit innerhalb eines existierenden Elektrizitätsmarktmodells mit Abweichungsstrafen überprüft.

Contents

List of Abbreviations	xi
List of Figures	xii
List of Tables	xiv
1 Introduction	1
1.1 Overview	1
1.2 Statement of problem	4
1.3 Objectives and scope	6
2 Background Information	11
2.1 Introduction	11
2.2 Power systems	11
2.3 Electricity markets	14
2.4 Wind power	16
2.4.1 The wind resource	16
2.4.2 Brief history of wind energy utilization	18
2.4.3 Wind farms	20
2.5 Wind power integration	22
2.5.1 Handling of wind power within the power systems	22
2.5.2 Wind power forecasting	24
2.6 Electrical energy storage	26
2.6.1 Overview	26
2.6.2 Benefits and uses of electricity storage	26
2.6.3 Energy storage technologies	26

2.6.4	Vanadium redox flow batteries	33
3	Vanadium Redox Flow Battery Model	39
3.1	Introduction	39
3.2	Experimental characterization of a VRFB unit	40
3.2.1	Overview	40
3.2.2	Description of the battery unit	40
3.2.3	Measurement strategy	42
3.2.4	Efficiency calculations	43
3.3	Megawatt scale VRFB model development	49
3.3.1	Overview	49
3.3.2	Design criteria	50
3.3.3	General assumptions	50
3.3.4	The software model	51
3.4	Results and discussion	52
3.4.1	Overview	52
3.4.2	Operating range of a string	52
3.4.3	Efficiency of a string	54
3.4.4	Choosing the number of modules	61
3.4.5	Test runs with the model	63
3.5	Summary	65
4	Wind-VRFB Model	67
4.1	Introduction	67
4.2	Input data and parameters	67
4.2.1	Wind power data	67
4.2.2	VRFB data	71
4.3	Simulation model and methodology	78
4.3.1	Wind power forecasts	78
4.3.2	Market structure and deviation penalties	79
4.3.3	Power dispatch strategy by utilizing the VRFB unit	79
4.4	Results and discussion	82
4.5	Summary	88
5	Conclusion and outlook	89

CONTENTS

6 Zusammenfassung und Ausblick	93
Bibliography	97
Biography	109

List of Abbreviations

Abbreviation	Description
GHG	greenhouse gas
VRFB	vanadium redox flow battery
TSO	transmission system operator
RESA	Renewable Energy Sources Act
SOC	state of charge (of a battery)
O&M	operation and maintenance
AGC	automatic generation control
ACE	area control error
DC	direct current
AC	alternating current
CF	capacity factor (of a power plant)
FIT	feed-in tariff
RO	renewables obligation
DSM	demand side management
NWP	numerical weather predictions
RMSE	root mean square error
MAE	mean absolute error
ESS	energy storage system
PHES	pumped hydro energy storage
CAES	compressed air energy storage
SMES	superconducting magnetic energy storage
rpm	rounds per minute
UPS	uninterruptable power supply
SLI	starting, lighting, ignition
EV	electric vehicle
PVC	polyvinyl chloride
OCV	open circuit voltage
BMS	battery management system
DWD	Deutscher Wetterdienst

List of Figures

1.1	World total primary energy supply by fuel (Mtoe) [1].	2
1.2	World electricity generation by fuel (TWh) [1].	2
1.3	World electricity generation by source [2].	3
1.4	Share of renewables in global final energy consumption (2011) [2]. . .	4
1.5	Global installed wind power capacity growth [3].	5
1.6	Diagram illustrating the objectives and the results of the study.	10
2.1	Sample daily load profile for Germany.	13
2.2	Control actions starting with the system frequency [ENTSO-E].	15
2.3	Weibull distribution samples [4].	17
2.4	Remains of an early horizontal axis sail-wing windmill in Datca, Turkey. 18	
2.5	Predicted and measured wind power values for TenneT control area in Germany for the first 2 weeks of April, 2009 [TenneT Holding B.V.]. . .	25
2.6	Working principle of an electrochemical cell.	30
2.7	Schematic representation of a flow battery.	33
2.8	VRFB redox reactions during charging and discharging.	35
3.1	CellCube Schematic [5].	40
3.2	OCV vs SOC for a VRFB cell (2 M vanadium electrolyte, $E_{cell}^0=1.4$ V) 42	
3.3	Operating range of a string [6].	53
3.4	Voltage efficiency of a string as a function of SOC and power [6]. . . .	54
3.5	Voltage efficiency of a string as a function of SOC and power (with corrections and extrapolation to cover the entire operating range) [6].	56
3.6	Pumping power demand of the battery as a function of SOC and power [6].	57

3.7	Pumping power demand of the battery as a function of SOC and power (with corrections and extrapolation to cover the entire operating range) [6].	58
3.8	Pumping power demand for one string as a function of SOC and power [6].	58
3.9	String efficiency as a function of SOC and power [6].	60
3.10	Number of utilized modules as a function of SOC and power [6].	63
3.11	Full cycle simulation of a 2.5 MW/20 MWh VRFB [6].	64
3.12	Overall system efficiency as a function of SOC at megawatt scale.	65
4.1	Objectives diagram with highlighted Wind-VRFB model inputs.	68
4.2	Wind farm layout.	69
4.3	Quarterly wind power output patterns for 2009 [7].	70
4.4	Power output histogram for 2009 [7].	70
4.5	Hourly power output averages for 2009.	71
4.6	Monthly wind energy generation for 2009.	72
4.7	Capital cost breakdown for a 1 MW, 8 MWh unit [8].	74
4.8	Cost breakdown for vanadium based electrolyte [8].	74
4.9	Cost breakdown for vanadium redox battery cell stack [8].	75
4.10	Battery (4 MW/100 MWh) response to deviations between forecast and actual output.	83
4.11	Yearly duration curve of the wind power deviation (without battery) [7].	85
4.12	Avoided deviations, battery losses, and capital costs for different battery capacities [7].	87
4.13	Payback periods for different penalty multipliers and electricity price scenarios [7].	87

List of Tables

2.1	Installed wind power capacity by country as of May 2012 [3].	20
2.2	Typical capacity factor values for different generation types.	21
2.3	VRFB vs Lead-Acid Battery.	33
3.1	Variables recorded during the measurements.	43
3.2	Effect of battery power on efficiency.	62
3.3	Effect of module/string configuration on efficiency.	62
4.1	Estimated cost information for a megawatt scale VRFB unit.	78
4.2	Comparison of energetic values with and without a battery.	84

Chapter 1

Introduction

1.1 Overview

Energy is one of the most important and most widely discussed subjects of our time. People need energy in order to sustain their current comfort levels. Energy is needed to heat up or cool down our houses, to get from one point to another in a fast and convenient manner, to run our industries, to communicate with each other, and to have access to information using today's high technology services such as the Internet.

Highly increasing demand for energy started with The Industrial Revolution in the late 18th century and has been going on ever since due to constantly growing world economies. Although coal was the main fuel in the beginning of the industrial revolution, energy production gained a bigger momentum with the vast discovery of oil. Despite the energy crises, which caused the fossil fuel prices to rise during the past 50 years, fossil fuels such as oil, natural gas, and coal have maintained their global positions as dominant sources of energy. Although nuclear energy and renewable energy sources such as wind and hydro took their shares in the world electricity production later on, fossil fuels, especially oil, still dominate the primary energy supply for transportation sector while natural gas play a huge role in supplying energy for heating demand. Figure 1.1 shows the evolution of world primary energy supply by fuel from 1971 to 2011 while the share of sources for electricity generation can be seen in Figure 1.2 for the same time frame.

In the last 20 years, concerns over climate change and man made greenhouse gas (GHG) emissions along with depletion of world's fossil fuel resources and energy independence issues accelerated the research and development in energy production from renewable resources. Furthermore, countries and international organizations such as the European Union (EU) introduced long-term plans to increase the share of renewable energy in electricity production. In order to accelerate the process,

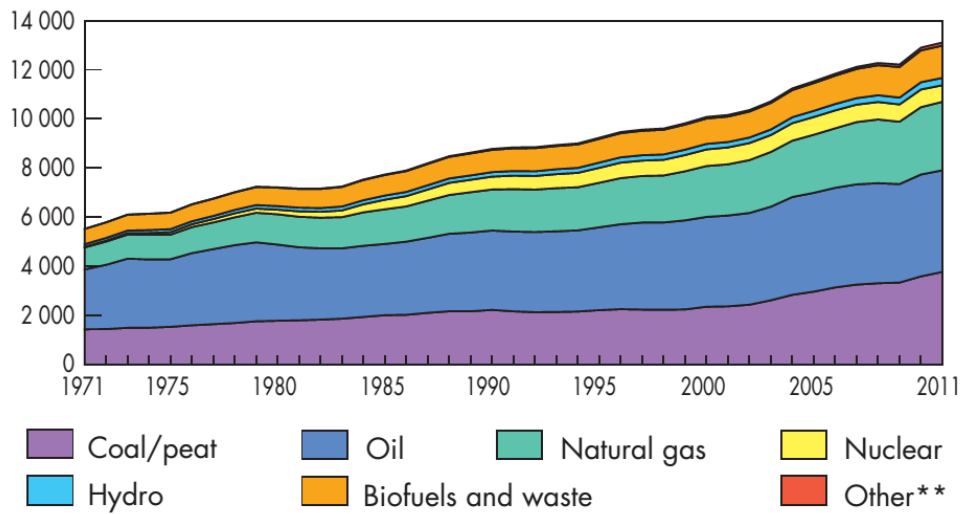


Figure 1.1 World total primary energy supply by fuel (Mtoe) [1].

** Other includes geothermal, solar, wind, heat, etc.

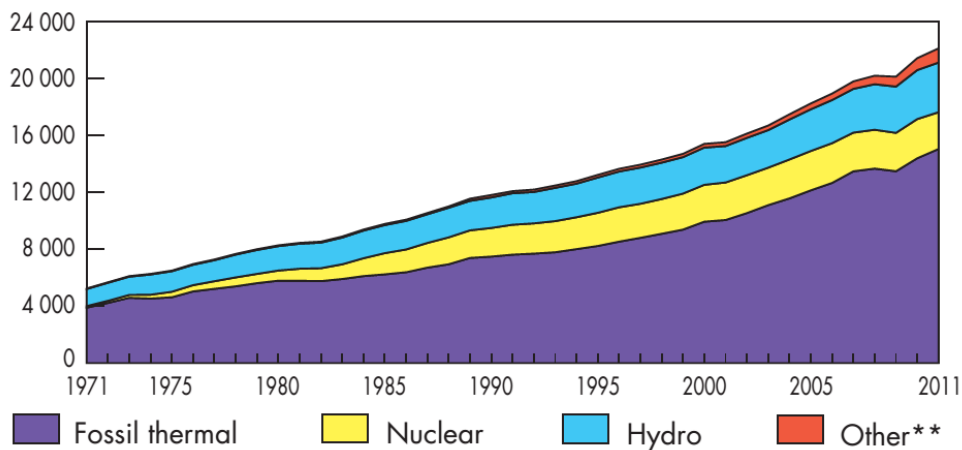


Figure 1.2 World electricity generation by fuel (TWh) [1].

** Other includes geothermal, solar, wind, biofuels and waste, and heat.

many countries developed renewable energy support schemes so that the renewable energy sources could become economically competitive against their fossil fuel counterparts, which have been receiving subsidies for almost a century. As a result, electricity generation from renewable sources significantly increased in some countries where the support schemes functioned well and the available renewable sources were successfully utilized. Countries with good wind potential such as Germany and Denmark built many wind farms in the last 10 years accounting for gigawatts of installed generation capacity while Spain increased its installed solar and wind power capacity drastically. As of 2012, the global installed wind and solar PV capacities accounted for 283 GW and 100 GW respectively. Figure 1.3

shows the world electricity generation shares by source while share of renewables in global final energy consumption can be seen in Figure 1.4. It should be noted that almost half of this renewable energy consumption in global final energy is traditional biomass.

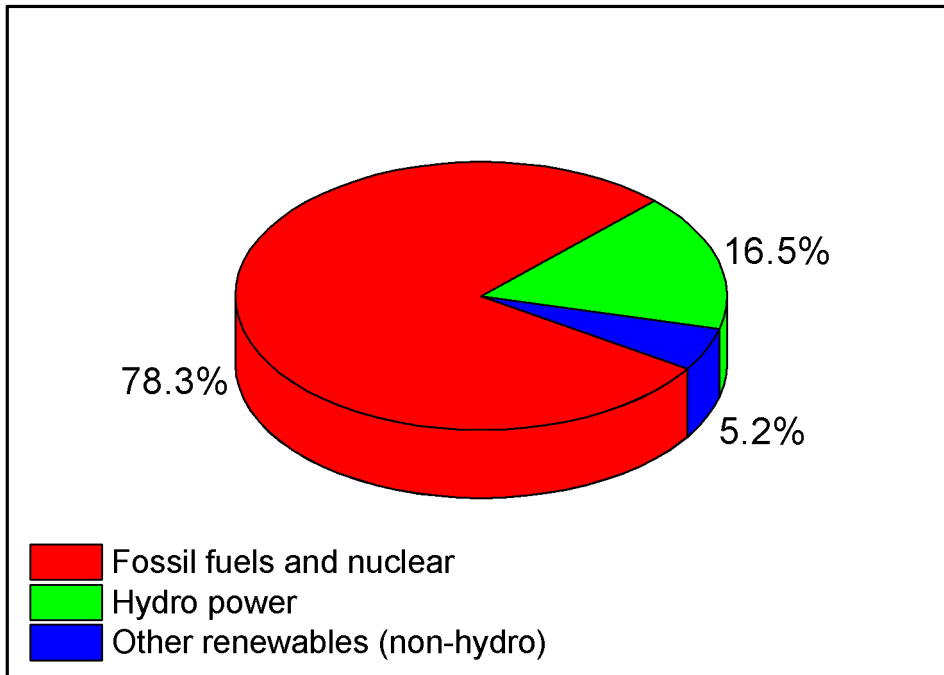


Figure 1.3 World electricity generation by source [2].

Nuclear energy has also been within the long-term plans of many countries for emission-free electricity generation. However, the Fukushima Dai-ichi nuclear power plant accident in Japan, which caused the first ever triple-core meltdown in the history after an extreme event of an earthquake and tsunami on March 11th, 2011 changed the global look on nuclear energy once again. Many countries reconsidered their nuclear energy plans after the event and some of them already decided to phase out nuclear energy. Germany announced that it would shut down all its nuclear power plants by 2022 and the phaseout began immediately after the Fukushima incident. Countries which decided to abandon nuclear power in the mid to long-term see the renewable energy sources and natural gas as the most appropriate candidates to compensate for the power deficit caused by the nuclear phaseout. Therefore, the shares of renewables and natural gas in electricity generation are expected to grow at an accelerated rate in the coming years, provided natural gas prices do not see extreme increases.

Among renewable energy sources excluding traditional large-scale hydro power, wind power has shown the biggest development in the last 20 years. Research and

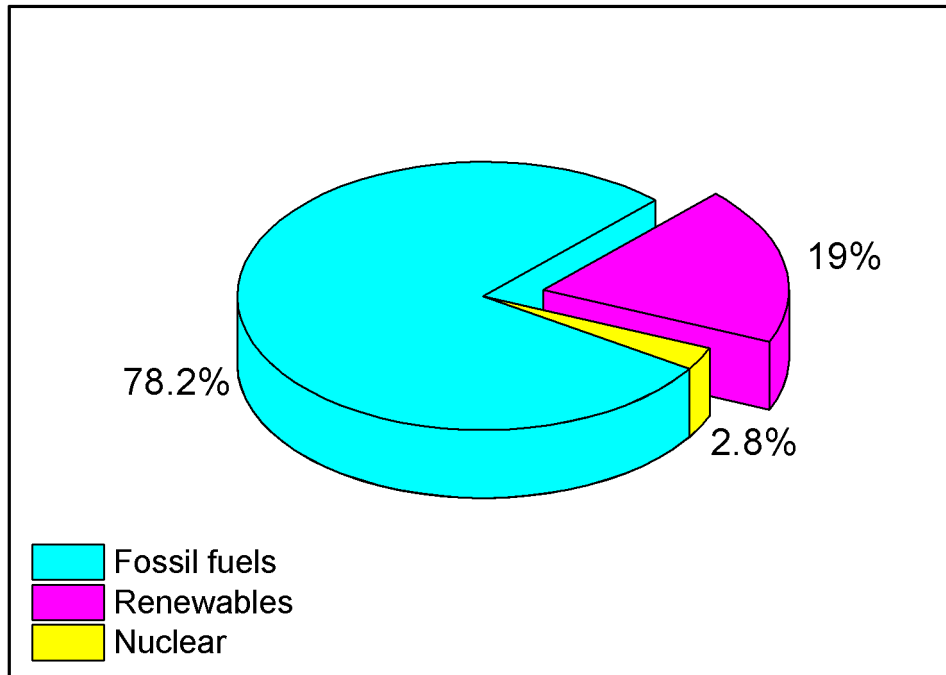


Figure 1.4 Share of renewables in global final energy consumption (2011) [2].

development in the wind energy area resulted in today's high power wind energy converters, which are installed on land or offshore. With wind turbine technology reaching a mature level and wind power becoming economically competitive for electricity generation, thanks to renewable energy support schemes, many local and global players entered the wind power business. These players include wind turbine manufacturers, wind farm operating energy companies, wind farm planning and consultancy companies, and wind power forecasting businesses. As a result of this trend, wind energy became the most widely exploited source of renewable energy with a constantly growing installed capacity worldwide. Top 5 countries with the largest amounts of installed wind capacities are China, USA, Germany, Spain, and India while Denmark, Spain, Portugal, and Germany constitute the top 4 in installed wind capacity per capita. Figure 1.5 shows the development of global installed wind power capacity from 2001 to 2010.

1.2 Statement of problem

While renewable energy resources enable clean electricity generation without green house gas (GHG) emissions, they come with problems such as interruptions, fluctuations and variability in supply. Solar power plants can only generate electricity as long as the solar radiation is at a certain level while power output

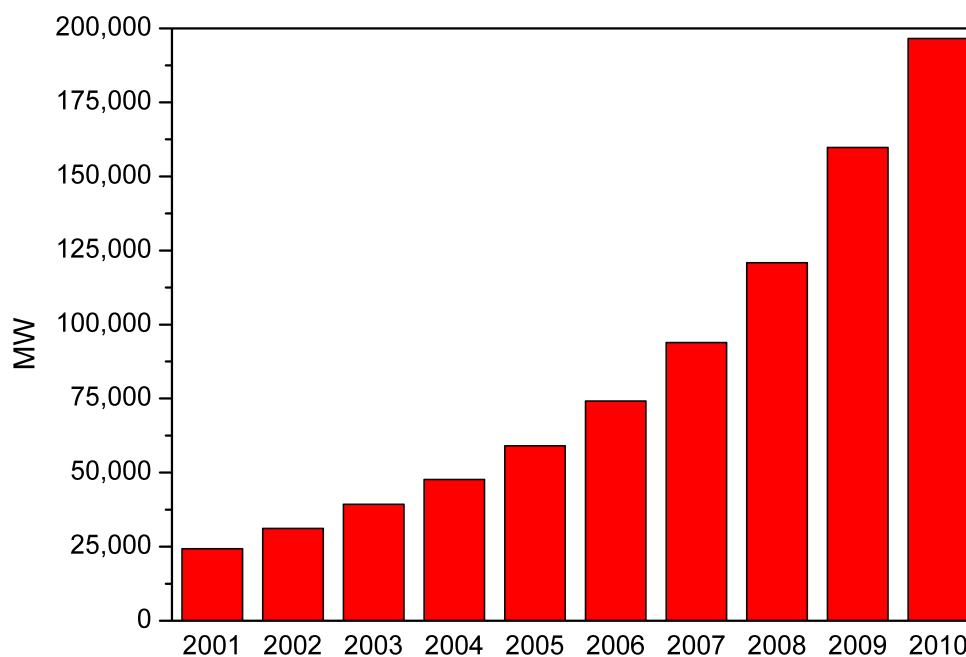


Figure 1.5 Global installed wind power capacity growth [3].

levels from a wind power plant depends strongly on wind speeds, which are hardly ever constant. Back to back cloudy days could hinder electricity generation of a solar unit drastically and wind turbines could stay idle for days if the wind does not blow. It is also clear that renewable energy sources as of date are far from being sufficient by themselves to fulfill world's increasing energy demand. However, despite their drawbacks, share of renewables in our electricity generation systems will and should keep increasing if we would like to move toward a global carbon-free economy. Therefore, power systems in the world will need to adapt accordingly, which would mean modifications and improvements of the current power generation, transmission, and distribution infrastructure.

General perception in the world is that our current power transmission systems are not suitable for handling large shares of renewable energy in the near future and need to be improved. This means building thousands of kilometers of new transmission lines for a better exchange of variable output renewable energy in the power systems. Another approach for handling high shares of renewables is to build more grid connected energy storage systems, which would help balancing out the fluctuations in the renewable electricity generation. Although various types of energy storage technologies such as batteries, compressed air, hydrogen, and pumped hydro exist, available grid connected storage capacity is somewhat limited.

Both the grid upgrade and adding more energy storage approaches have

their advantages as well as their drawbacks over one another. They are both technologically realizable, yet come with very high costs. Ultimately, future power systems with higher shares of renewable energy will probably require the pursuing of both approaches rather than picking one.

1.3 Objectives and scope

Aim of this study is to investigate the possibility of better power grid and accordingly market integration of wind energy by evaluating the option of utilizing an energy storage system coupled to a wind farm. Energy storage type to be evaluated in this study for such an application is "Vanadium Redox Flow Battery (VRFB) Storage", which is a promising technology for large-scale stationary energy storage applications.

This idea essentially suggests operating a decentralized storage system dedicated to a single wind power plant, rather than a storage system utilized for tasks such as grid balancing, providing reserve power, and similar. Larger scale storage systems require higher capacities and more complex control systems whereas a storage unit dedicated solely to a single power plant would have a much simpler operation scheme making the design and operation easier. Furthermore, a well designed dedicated storage system could help a variable output renewable energy power plant to be operated in a similar way to a conventional fossil fuel power plant. This operational similarity lies within the aspect of market integration of the generated power. Currently, participation of renewable generation in the electricity markets and power exchanges is more complicated and troublesome compared to conventional generation units. The main reason behind this is the existence of variations, fluctuations, and intermittency in renewable generation, as explained above.

Even though the challenge of variability is valid for various types of renewable generation, this study focuses on wind power and better integration of it into the power grids and the electricity markets by utilizing a dedicated storage unit. Problem of variability and integration of wind power has been discussed in several studies from a technical and economic point of view [9–11]. This variable nature of wind power has a significant effect on its relative market price [12]. Additional backup capacities and regulation measures might often be necessary to deal with the fluctuations and variability [13]. Currently, wind power forecasting plays an important role in facilitating the wind power integration by helping the wind farm operators and transmission system operators (TSO) with their dispatch planning [14–16]. Furthermore, forecasting enables the participation of wind power in certain market mechanisms as in the example of Spain, where selling wind power in the wholesale market is most of the time more profitable than selling according to the fixed feed-in tariffs for wind power generators [14, 16, 17].

As increasing wind power capacity also increases the requirements for efficient grid integration of this variable resource, countries which have high wind power share in their energy mix introduced grid integration standards for wind power plants. Grid integration measures also made wind power generators balance responsible parties in some countries such as Spain [15]. Furthermore, participation of wind power in the electricity market also varies from country to country. For instance, most wind power producers do not actively participate in the wholesale electricity market in Germany and they get paid according to the fixed feed-in tariff they are entitled to although this could also be expected to change in the near future due to the recent changes in Renewable Energy Sources Act (RESA) [18]. On the contrary, most Spanish wind power generators participate in the wholesale market using the feed-in premium option rather than the also available fixed feed-in tariff due to the fact that the former option became more profitable after the new feed-in tariff regulations introduced in 2004 [14, 19, 20]. This type of energy selling mechanism requires day-ahead bidding and correction of the bids in intraday markets within the wholesale electricity market. However, as wind power generators cannot predict the amount of energy they can deliver as easily as conventional generators, wind power forecasting becomes a very important market component in Spain. In order to sustain an efficient grid management by using the most accurate power forecasts, Spanish market regulation induces a deviation penalty for wind power (and other renewable energy) generators when there is a deviation between the forecast and the actual energy sold in the market. In the regulation, deviation cost was defined as 10% of the market price multiplied by the deviation [17, 19, 20].

Energy storage is expected to play an important role in the grid and market integration of renewables in the future [21]. Therefore, studies have been carried out in order to evaluate the benefits of utilizing energy storage technologies to wind power [22–27]. Combining wind power with other generation technologies in order to balance out the fluctuations has also been considered by several studies [28–31]. Since choosing the right storage technology for a grid connected application is not only a technical but also an economic challenge, possibilities of profitable energy storage applications within the appropriate market mechanisms have also been discussed in various publications [32–36]. General conclusion reached by most of the cited studies was that both electrical and thermal energy storage would be beneficial to the grid integration of renewables. Nevertheless, the costs of storage technologies, value of wind power and CO₂ mitigation costs would play an important role in the introduction of large-scale storage systems to the existing power grids.

Only way of operating renewable power plants as conventional generation units is to mitigate the problems caused by variability and intermittency. Dedicated energy storage units would stand out as the most obvious solution even though

selecting the right storage system for a specific renewable energy power plant would require elaborate technical and economic evaluations. After all, giving a renewable power plant operator the capability of participating in power exchange auctions as freely and comfortably as conventional generation operators should not cause additional technical and economic burdens due to the presence of a dedicated storage unit. Extra investment on a storage system should eventually pay off and keep the power plant it supports financially competitive in a market structure. Several approaches could be taken to justify the technical and economic benefits of integrating a dedicated energy storage unit into a wind farm. The approach in this study combines the idea of easier power grid and market integration of wind farm output by utilizing wind power forecasting techniques and a dedicated storage unit. Wind power forecasting has become a very important tool in the past years for grid and market integration of wind power. Wind farm operators as well as transmission system operators (TSO) utilize wind power forecasting data for dispatch planning in an effort to maximize the financial benefits and minimize the technical difficulties encountered during power dispatch. Despite the significant improvements in power forecasting technology based partly on weather predictions, forecasting errors are still a part of the business and might come costly in power grid and market integration.

This study aims to evaluate the benefits of utilizing a dedicated VRFB system to mitigate the wind power forecasting errors through two interconnected tasks. It has already been demonstrated in a number of projects in various locations that the VRFB technology can be successfully utilized in applications ranging in sizes from several kilowatts to some megawatts [37]. Since the technological applicability of the VRFB technology was successfully demonstrated, a more detailed evaluation and precise upscaling at the system level are needed. Several modeling studies have been carried on single cell level dealing with electrochemical phenomena and hydraulic behavior [38–43]. There has also been modeling studies which focus on self-discharge behavior of VRFBs [44, 45]. However, there has been only a small number of reported studies dealing with modeling on a system level [46]. Therefore, the initial task of this study focuses on building a megawatt scale software model for simulating a wind farm integrated VRFB unit. Modeling was necessary as no commercial megawatt scale units of the required size for the calculations in this study exist as of today. In order to base the computer model on real life data, experimental work with a kilowatt scale (10 kW) commercially available VRFB unit was done. Using the characterization results based on these experiments, the megawatt scale model was developed. The model performs upscaling of a VRFB unit to represent various system sizes via a modular battery approach. Using the model, optimal number of modules for certain power levels during charging and discharging operations were estimated. In addition, the dependence of the system efficiency and the battery SOC was demonstrated.

Further details on this part can be found in Chapter 3.

Once the VRFB software model was established and tested with arbitrary charge-discharge simulations, the next step was to utilize it for power grid and market integration of wind power at a single wind farm level. Real life power data from a 10 MW wind farm in Germany were used for the calculations. Furthermore, wind power forecasting data were generated for the wind farm by considering the location, wind speeds, and the power output. For the economic evaluations, a market model was chosen, in which wind farm operators are penalized for deviations between bid and delivered power, similar to the Spanish market model explained above. Hypothetical VRFB unit was then utilized to mitigate the deviation penalties and make financial assessments on the use of a dedicated VRFB storage based on installation and O&M costs along with market prices of electricity. Assessments were based on an existing economic model and VRFB financial data based on existing literature and self evaluations were used. Self evaluations on VRFB economics were necessary as the market for this technology is not mature (as opposed to other energy storage technologies) and it is extremely difficult to put hands on already published financial data. The main aim of the power plant and integrated VRFB simulation and the economic assessments were to determine the expected payback periods of an additional VRFB investment as a function of the penalty multiplier value used in the suggested market model. Details on this part concerning the dedicated utilization of the VRFB system with a medium sized wind farm can be found in Chapter 4. The diagram in Figure 1.6 illustrates how the objectives and results of the study are connected to each other.

The studies and results from both the first task, which focuses on the megawatt scale software model and the second task, which evaluates the dedicated storage approach of a hypothetical VRFB unit by using the developed software model were published in the peer reviewed articles [6] and [7] respectively. Prior to these publications, the preliminary results from the integration study were presented at the 2011 International Flow Battery Forum in Edinburgh, United Kingdom.

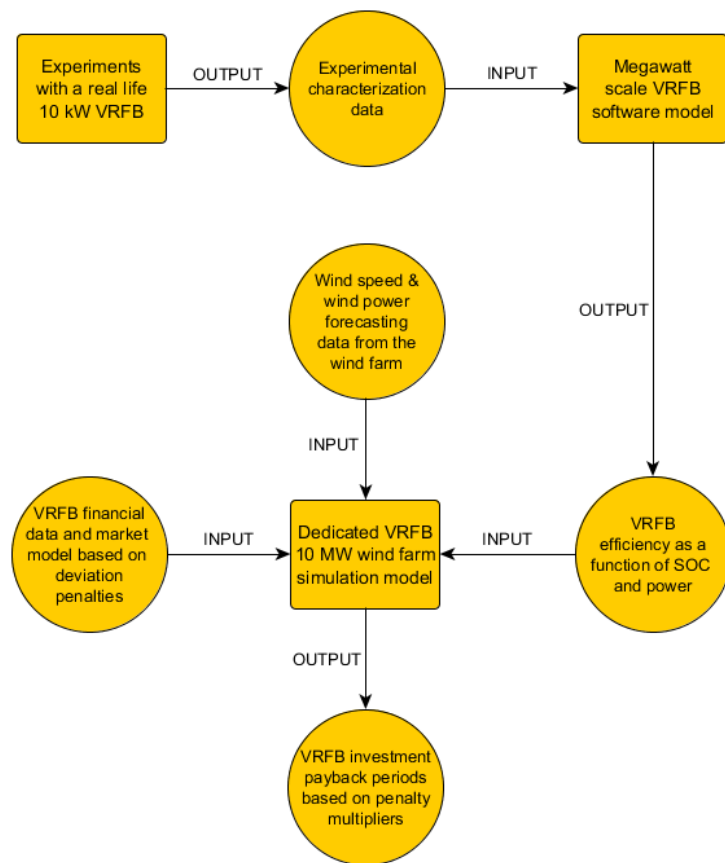


Figure 1.6 Diagram illustrating the objectives and the results of the study.

Chapter 2

Background Information

2.1 Introduction

This chapter aims to provide an overview on the technologies which are discussed within this study. In order to fully understand the proposed idea of the wind farm dedicated VRFB storage unit for easier wind power integration, basic theoretical information on the involved technologies should be reviewed. Accordingly, wind power and energy storage (VRFB in particular) technologies are discussed in the following sections. Furthermore, in order to make the wind power integration problem crystal clear to the reader, some insight information on power systems including the power system reserves, electricity markets, and currently practiced methods for grid integration of wind power is provided.

2.2 Power systems

Most of the world's electric energy is supplied to the users by power grid systems. This is a natural result of the location of electricity production usually being different than the location of consumption. Large production facilities such as coal, nuclear, natural gas, and oil power plants as well as wind farms are usually far from regions such as densely populated big cities where most of the energy consumption takes place.

Main components of a power grid are the power plants, energy transmission lines, and consumers. Side components include transformer stations, which regulate the voltage levels within the grid, safety systems such as circuit breakers, and control systems that guarantee uninterrupted and safe operation. Generated electric energy is transmitted to the point of consumption via transmission lines and at high voltages in order to minimize the transmission losses.

Quality and stability of a power grid is the key to uninterrupted supply of energy to the consumers. This requires an elaborate control and management of the grid. This essential control should ideally be carried out at both production and consumption side. However, utility companies operating the power grids do not have much influence on the demand side as this corresponds to the load profiles depending on users' energy needs. Accordingly, more control over the power grid can be provided at the generation side.

Different types of energy production facilities have different properties in terms of power levels, response times, and yearly hours of operation. Accordingly, some are only suitable to supply the base load while some can respond to short-term peak power demands. For example, large coal and nuclear power plants are only suitable to supply the base power as it takes considerable amount of time (many hours to days) to bring them into full operation. These power plants can be operated throughout the year except the periods of maintenance as they are only dependent on fuel supply. Energy production from renewable energy sources such as wind and solar power plants on the other hand depend heavily on the availability of wind and solar resource. Therefore, these power plants produce energy only when there is enough wind or solar radiation. Hence, they are far from being reliable for supplying the base power by themselves no matter how big their installed capacity is [9]. They can however be part of an energy mix, which supplies the base power at certain periods of time. Figure 2.1 shows a typical daily load profile in Germany and how the power for this load profile is supplied. Smaller peaks in the load profile can only be supplied by production units, that can be brought into operation within a few minutes. These include gas turbines, hydroelectric generation running on stored water, and other fast responding energy storage units.

Another issue with the power grid is maintaining the stability of its voltage and frequency levels. Due to varying power requests from the grid, voltage and frequency might deviate from their desired values. In this case, grid operators must take action at the production side to regulate the voltage and frequency of the power grid. This is realized by utilizing power system reserves, which are components of the supply side management of a power system. They are online or offline additional generation units, which are used in case of losses of main generation units. Loss of a generation unit can be caused by a failure in a power plant, during scheduled maintenance periods, or due to lack of primary energy source (e.g. problems with supply of natural gas to run a natural gas fired power plant, lack of wind for a wind power plant, an overcast day for a solar photovoltaic or solar thermoelectric power plant). As the system load must be met in any case due to the principle of secure supply of energy, power systems reserves (also called operating reserves) play their part in such a failure of a single generation unit or multiple units. Similarly, sometimes downward regulation in power system

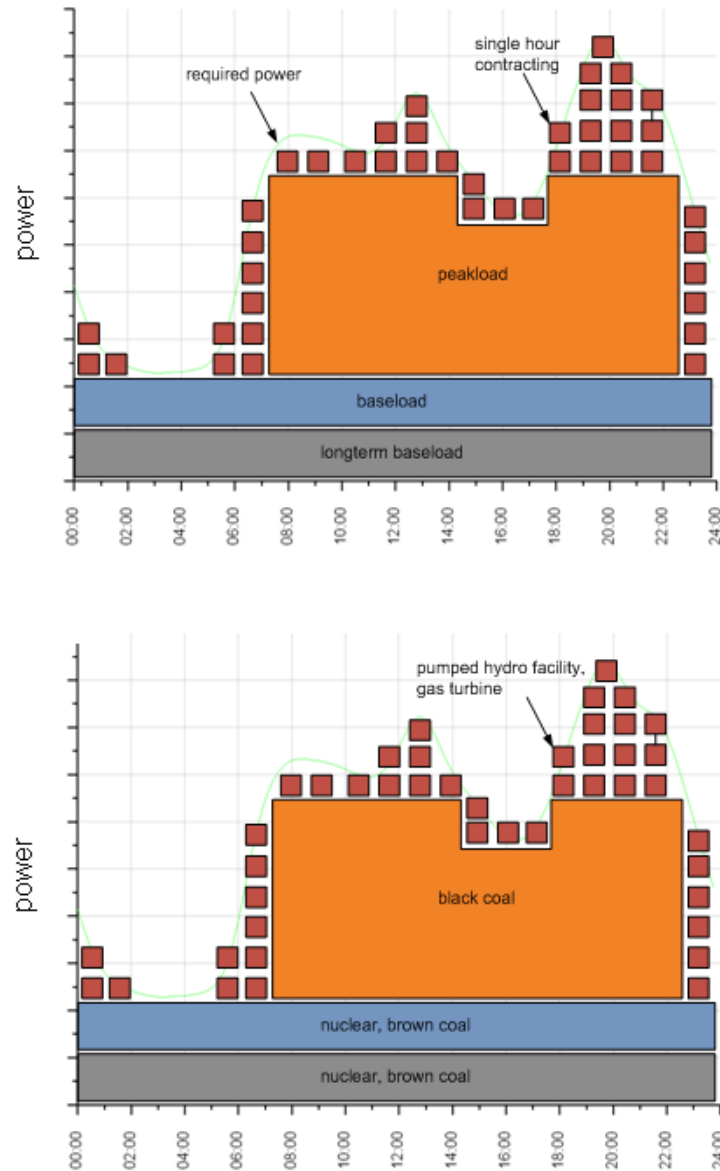


Figure 2.1 Sample daily load profile for Germany.

might be necessary in the case of generation exceeding the actual load due to large loads unexpectedly going offline. Downward regulation is done by decreasing the output by shutting down power plants or running them at lower output levels. Main parameter in controlling a power system's balance is the frequency. System frequency deviates from its nominal value (50 Hz or 60 Hz depending on the geographic area) when there is a mismatch between generation and system load.

Sizes and reaction times of power system reserves vary depending on their types and intended operation. Names and definitions of power system reserves vary

quite a bit from region to region or country to country although their functions are similar. Operating reserves are defined in three categories in Europe by the European Network for Transmission System Operators (ENTSO-E). These are primary control, secondary control, and tertiary control reserves. Purpose of primary control is to limit the frequency deviation in the entire high-voltage grid in case of a contingency event and maintain a balance between generation and consumption within a synchronous area. Primary control can be supplied by spinning and non-spinning generation units and they are activated automatically when the system frequency deviates by 20 mHz from its nominal value of 50 Hz. Primary control starts within seconds and 50% of the total primary reserve must be deployed within maximum 15 seconds while it must reach fully operational state within 30 seconds. Primary control must be available until secondary and tertiary control completely offset the power deviations in the interconnected area. Secondary control is mainly made up of automatic generation control (AGC)¹ units and it maintains the balance between generation and consumption in a control area under the responsibility of a TSO. These units must be available within seconds after a contingency and up to a time frame of 15 minutes. Ultimate goal of secondary control is to return the frequency to its nominal value and reduce the area control error (ACE)². Secondary control consists of spinning reserves, which are usually hydro and thermal power plants in part load and standing reserves, which are fast starting gas turbine power plants. Tertiary control is primarily used to free up the secondary reserves and their response time is longer than that of primary and secondary reserves. However, tertiary control is also activated in case secondary control is not sufficient to restore the system balance within a control area. Tertiary reserves are activated by changing the generation or load within a control area. Figure 2.2 shows the ENTSO-E control actions performed by operators in case of imbalances and accordingly frequency deviations.

2.3 Electricity markets

Electricity is considered as a commodity, which can be traded under various market structures. However, electricity has some unique properties compared to other goods. First of all, it is a product, which must be available at the time of demand and it is difficult and expensive to be stored. In addition, electricity demand is also volatile on a daily, weekly, monthly, and yearly basis. In general

¹An AGC system can regulate the outputs of connected generators depending on short-term changes in load or production. An AGC consists of hardware and software, which can receive and transmit signals from and to the generators connected to it.

²Area control error (ACE) is calculated as the deviation of generation from load in a power system area. The total ACE is subdivided into a schedule of station control errors and transmitted to power plants for the readjustment of specific generators.

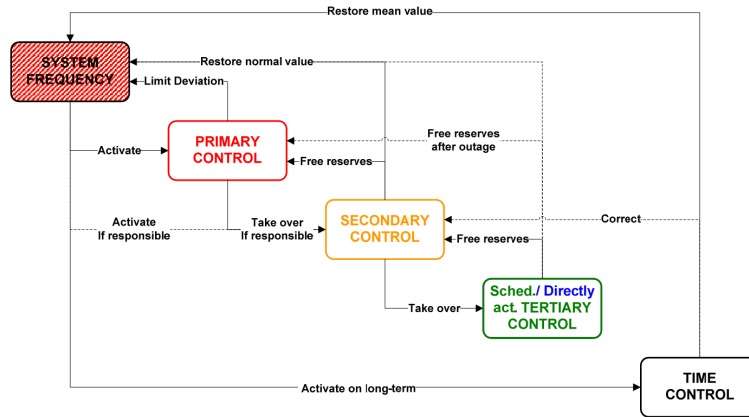


Figure 2.2 Control actions starting with the system frequency [ENTSO-E].

terms, it can be supposed that the supply-demand relation defines the price of electricity although it should be realized that the demand curve for electricity has a very inelastic nature. Cost of production of electricity is determined by various variables such as the generation technology, fuel prices, demand, and even weather conditions. All these lead to large variations in electricity generation costs, which play an important role in determination of electricity price to end-users.

The concept of energy markets was first introduced in Chile in 1980s and the idea of trading electricity similar to other commodities was born. Chilean model went through many modifications and refinements in other places and today many countries have similar energy markets where electric energy is traded between electricity generators and consumers. Retailers buy electricity from generators and sell to end-users in an established power exchange or with bilateral contracts. Bilateral sales and wholesale market usually co-exist in electricity markets. Shares of electricity sold under bilateral contracts and power exchanges vary from country to country. In countries with mature power exchange structures, electricity sales via a power exchange is on the rise and has a potential to take over bilateral contract sales in the near future [47].

Electricity markets operate in an auction mechanism where sellers and buyers of electricity participate in bidding structures, which determine the price of energy. Types of auctions and bidding mechanisms vary from market to market. Most important criteria defining an auction are number of bidding sides and pricing rule of the market. Number of bidding sides is defined by the "one-sided" and "double-sided" auction types where the former allows only one market side (usually sellers) to bid and the latter two (sellers and buyers). Pricing rule of a market is the second important criterion. The most commonly used pricing rule is uniform pricing where the market clearing price of electricity is in simplest terms decided by the intersection of aggregated supply and demand curves after bidding is completed. However, further pricing actions and adjustments might be necessary

to reach a final price after bidding is complete as electricity demand is very inelastic and has to be met in any case. Bids in a power exchange are usually collected for each hour in a day-ahead auction and are valid for the next day.

2.4 Wind power

2.4.1 The wind resource

Wind is in fact a form of solar energy as winds are caused by the uneven heating of the atmosphere by the sun, the irregularities of the earth's surface, and rotation of the earth. Furthermore, wind flow patterns are modified by the earth's terrain, bodies of water, and vegetative cover.

The energy available in the wind varies as the cube of the wind speed and the most striking characteristic of the wind resource is its variability. The wind is highly variable, both geographically and temporally. On a large-scale, spatial variability describes the fact that there are many different climatic regions in the world, some much windier than others. These regions are largely dictated by the latitude, which affects the amount of insolation. Furthermore, within any one climatic region, there is also a variation on a smaller scale, largely dictated by physical geography. The type of vegetation may also have a significant influence by affecting absorption or reflection of solar radiation, which in the end affects surface temperatures and humidity. More locally, the topography has a major effect on the wind climate. For instance, tops of hills and mountains are generally windier locations. In addition, trees and even man made structures such as buildings affect wind flow patterns significantly.

Temporal variation of wind speeds can be broken down into three subcategories:

- Long-term wind speed variations
- Annual and seasonal variations
- Diurnal variations

It is a common acceptance that wind speed at any particular location may be subject to very slow long-term variations. However, there is not enough historical wind speed data for evaluation of wind speed trends for many locations. This makes the prediction of annual yearly mean speed values hard to predict. On the other hand, wind speed variations during the year can be characterized by a probability distribution. For many sites around the world, The Weibull distribution was found to reflect the probability distribution of wind speed data very well. The Weibull distribution goes as follows:

$$F(U) = \exp\left(-\left(\frac{U}{c}\right)^k\right) \quad (2.1)$$

where $F(U)$ is the fraction of time, for which the hourly mean wind speed exceeds U . c is called the "scale parameter" and k is called the "shape parameter" of the Weibull distribution. Rayleigh distribution is a special case of the Weibull distribution when $k = 2$. Lower values of k indicate greater variability of wind speed about the mean while k values higher than 2 indicate that the variation hourly mean wind speed about the annual mean is small. Figure 2.3 shows some examples of Weibull distribution for different k values. Although a Weibull distribution gives a good representation of the wind regime at many locations, some sites showing distinctly different wind climates in summer and winter can be represented in a better way by a double-peaked "bi-Weibull" distribution, which has different scale and shape factors for the two seasons.

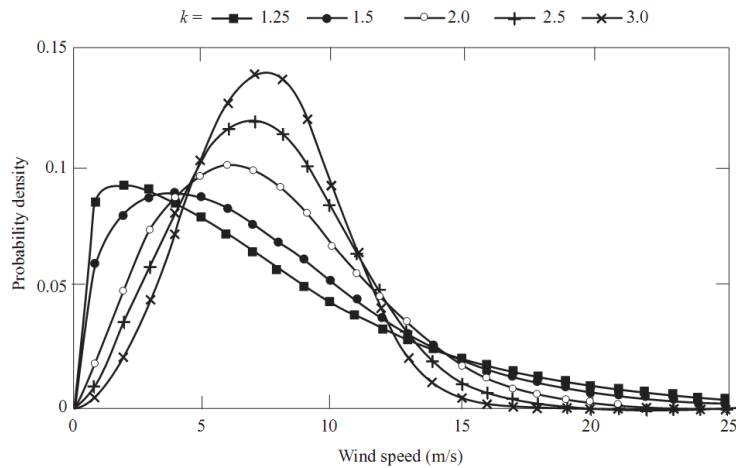


Figure 2.3 Weibull distribution samples [4].

On shorter time scales such as daily and weekly intervals, wind speed variations are more random and less predictable. Nevertheless, these short time scale variations also have some definite patterns, which result from the large-scale weather patterns moving across the earth. These patterns usually take a few days to pass over a given point. Air temperatures between the day and night time also contribute significantly to the diurnal wind speeds. Furthermore, land and sea breezes, caused by differential heating and cooling between land and sea also play a role. When all these factors are combined, diurnal wind patterns for a given geographical location can be characterized and wind speeds can be predicted to a certain extent [4].

Another important phenomenon that affects the wind speed variations in short time scale is turbulence. Turbulence refers to fluctuations in wind speed on a fast time scale, which is typically less than 10 minutes. Turbulence is generated by the friction with the earth's surface and thermal effects. Friction is caused by the topographical effects such as hills and mountains while thermal effects consist of

variations of temperature in the short time scale. Turbulence is a complex process and it is very difficult to characterize it by its physical properties. Hence, it is considered more useful to evaluate it based on its statistical properties. There are many statistical descriptors of turbulence, ranging from simple turbulence intensities and gust factors to detailed descriptions of the way, in which the three components of turbulence vary in space and time as a function of frequency. However, turbulence and further details about the wind resource are not discussed in this book as they are beyond the scope of this study.

2.4.2 Brief history of wind energy utilization

According to historical records and evidence, history of wind energy utilization dates back to at least 1000 B.C. The first windmills were developed to automate the tasks of grain grinding and water pumping and the earliest known design is the vertical axis system developed in Persia about 500-900 A.D. The first known documented design is also of a Persian windmill, which has vertical sails made of bundles of reeds or wood, which were attached to the central vertical shaft by horizontal struts. These vertical axis turbines made use of the drag force instead of the lift force as in today's modern turbines. Besides the tasks of grain grinding and water pumping by utilizing wind turbines, wind also became an important energy source for mobility applications with the introduction of sail ships.

First wind turbines to appear in Europe by the 13th century A.D. were using the horizontal axis design, which used the aerodynamic lift for rotation. Their applications stayed pretty much the same with grain grinding and water pumping remaining as the main purposes of utilization.



Figure 2.4 Remains of an early horizontal axis sail-wing windmill in Datca, Turkey.

Between 1850 and 1970, many mechanical output wind machines were installed worldwide, and especially in the United States with the primary application being water pumping. The first use of a large windmill to generate electricity was a system built in Cleveland, Ohio, in 1888 by Charles F. Brush. The first small electrical-output wind turbines simply used modified propellers to drive direct current generators. These systems were installed at first to provide lighting for farms and to charge batteries used to power several simple electrical appliances of the time. Later on, they were used to power further DC motor appliances such as refrigerators, freezers, and power tools. By the 1950s, utilization of wind energy for electricity generation declined significantly in the United States mainly due to the availability of vast fossil fuel resources for electricity generation. In Europe on the other hand, wind power trend continued to a certain extent.

The development of bulk-power, utility-scale wind energy conversion systems was first undertaken in Russia in 1931 with the 100 kW Balaclava wind generator. Subsequent experimental wind plants in the United States, Denmark, France, Germany, and Great Britain during the period 1935-1970 showed that large-scale wind turbines would work, but failed to result in a practical large electrical wind turbine.

After the World War II, developments in wind power technology accelerated in Europe, mainly due to shortages of fossil fuels. Post war activity in Denmark and Germany largely dictated the two major horizontal-axis design approaches that would emerge when attention returned to wind turbine development in the early 1970s. The Danes refined the already utilized wind turbines by introducing advanced materials, improved aerodynamic design, and aerodynamic controls. The engineering innovations in Germany also led to higher efficiency wind turbine generators.

In the 1980s, world wind energy market saw a big development led by the United States and Europe markets. Grid connected wind farms started to be built and operated utilizing technologically the most advanced turbines of the time at power scales ranging from 50 to 500 kW. In the early 90s, the development in the US declined and most of the market activity shifted to Europe and Asia. Later on, with the introduction of laws and regulations as part of the efforts to promote renewable energy, wind power market saw a big boom from late 90s to the present day. This era brought the first megawatt scale turbine generators into the market. A lot of megawatt scale wind farms were built after the year 2000 in pioneer countries such as Denmark, Spain, and Germany. United States also caught up in the last few years while Asian market grew rapidly with new installations in China and India. Most recently, South America started building up wind power capacity with the leadership of Brazil. Refer to Figure 1.5 in Chapter 1 for the development in installed wind capacity worldwide from 2001 to 2010. Table 2.1 shows the installed wind power capacity by country as of May 2012.

Table 2.1 Installed wind power capacity by country as of May 2012 [3].

Country	Installed wind power capacity (MW)
China	67,774
United States	49,802
Germany	30,016
Spain	22,087
India	17,351
Italy	7,280
France	7,182
United Kingdom	6,840
Canada	5,511
Portugal	4,398
Rest of the World	35,500

Other than the grid connected large-scale wind power, kilowatt scale wind power with small, rooftop type wind turbine generators has recently become popular for off-grid as well as for grid connected systems. These can offer solutions for providing electricity in rural areas where the power grid is too far away. Furthermore, small scale wind power could be an approach for clean and cheap electricity alternative for grid connected private households.

2.4.3 Wind farms

A wind farm is a certain number of wind turbine generators grouped together in a geographical area, size of which depends on the number of wind turbines and their rated powers. Essentially, a wind farm is an electricity generating power plant, output of which depends on the wind speeds the turbines face at a given interval.

Locations of wind farms are determined by site assessment studies, which take into consideration several parameters regarding the wind resource and its possible conversion into electricity by utilizing wind turbine generators. These parameters include the topography of the considered site, annual average wind speed values as well as the ease of grid connectivity. Furthermore, ease of access to a wind farm is critical as far as the maintenance and repair works are concerned. Positioning of the wind turbines within a wind farm is also important as wake effects and shadowing phenomena could affect the output of the turbines significantly. Wind farms can be built on the land (onshore) as well as offshore in order to benefit from the high wind speeds over the surface of the oceans, seas and lakes.

Wind farm capacities worldwide have a wide range. They can have capacities as small as 1-5 MW and as big as hundreds of megawatts. Offshore wind farms

have the potential to reach even higher capacities in the future although currently the largest offshore wind farm³ has an installed capacity of 630 MW.

Capacity factor

Capacity factor of a power plant is described as the amount of generated energy over a certain period of time, divided by the amount of energy, which would have been generated if the power plant had run at its rated power capacity continuously in that same period. It is common to take a one year period when calculating capacity factors of power plants. Capacity factor of a power plant can be expressed by the following equation:

$$CF = \frac{\sum_{h=1}^H P_h}{H \times P_{rated}} \quad (2.2)$$

where CF is the capacity factor, P_{rated} is the rated capacity of the power plant, P_h is the power output for the hour h and H is the number of hours, for which the capacity factor is calculated.

In practical terms, no power plant can achieve a 100% capacity factor as there are always interruptions in power generation throughout the year. Furthermore, sometimes power plants might be generating electricity at a lower level than their rated power even though the power generation does not come to a complete halt. In thermal power plants, these interruptions or lower level operations could result from planned or unplanned maintenance works, failures or unavailability of fuel. In renewable energy generation, capacity factor is directly determined by the availability of the renewable resource.

Wind power plants can generate electricity as long as the wind is blowing and they can reach their rated output power only if the wind speeds are at a sufficiently high level. Therefore, capacity factor of a wind power plant is strongly affected by its location. Table 2.2 provides some typical capacity factor value ranges for different types of electricity generation.

Table 2.2 Typical capacity factor values for different generation types.

Power plant type	Capacity factor
Coal	0.60-0.80
Nuclear	0.80-0.90
Hydro	0.40-0.90
Wind (onshore)	0.20-0.40
Wind (offshore)	0.35-0.50
Photovoltaic	0.10-0.20

³London Array wind farm off the southeast coast of Great Britain.

2.5 Wind power integration

Due to its fluctuating nature, participation of wind power in the power markets is a lot more difficult than conventional power sources, which are a lot more predictable at a given time scale [9]. Hence, it is difficult to bring bids to the market for wind power plant operators [10, 48]. Requirements for wind power participation in power markets vary from country to country. Some countries require the wind power plant operators to bid for their generation while some give them priority and try to purchase any production [14]. In markets that require bidding for wind power, wind power forecasting becomes important for wind power producers. Wind power forecasting is explained in more detail in the next section. Common worldwide practice for wind energy and other renewable sources market integration is applying feed-in tariffs or other support schemes such as premium tariffs or renewable obligation quotas. Support schemes are introduced by policy makers in order to encourage renewable energy investments in attempts to increase the share of power production from renewable sources. In the existence of feed-in tariffs, renewable energy producers have a guaranteed price per unit of generated energy for a certain amount of time (e.g. 10 years) specified by the legislation. Wind power producers are not obliged to participate in market actions such as bidding as other power plant operators do. Another example of support schemes is premium tariffs where the renewable energy producers receive an additional bonus on top of the market price for the energy they sell. In this scheme, wind power producers still take part in market actions and bid the amount of energy they want to sell. As mentioned above, wind power forecasting becomes important for wind power plant operators in this scheme as they become responsible for market imbalances. A third example of renewable energy support schemes is renewables obligation or quotas where the authorities set objectives such as a certain share of delivered energy being provided from renewable sources. While some countries apply one of these support scheme models, some use combinations of them. Germany applies the feed-in tariff (FIT) model while Spain prefers premium tariffs and the United Kingdom has a renewables obligation (RO) support scheme. One way of dealing with wind power integration is imposing imbalance penalties to the wind power producers. In this case, the wind power plant operators are responsible for imbalances resulting from forecasting errors are liable to paying penalties. Spanish power market is one of the markets, which apply imbalance penalties to wind power producers where they pay a penalty if there is a minimum of 5% error between their forecasts and power production [14, 15, 19].

2.5.1 Handling of wind power within the power systems

Imbalances caused by wind power in the generation mix is not something that is dealt separately with but it rather affects the use of power system reserves

to a certain extent along with many other factors such as contingencies from generation and demand side [11].

There are several ways of dealing with variable and unpredictable wind power generation in the power dispatch system. In case of more wind power generation than required or absorbed by the power grid due to the demand situation and outputs of other generation units, one alternative would be not to buy the extra production of wind power and waste it by shutting down wind energy converters despite the presence of enough wind to produce energy. Although this alternative is simple and problem free for the TSO, it is not environmentally desirable. Another alternative in the presence of too much wind power is to bring this power into the grid by reducing the output of other generation units, which are mainly the conventional power plants running on coal, natural gas, and nuclear fuel. Although this is the most environmentally friendly way of dealing with the situation, it is usually not the most economic option as reducing the output of conventional generation units is costly due to decreases in generation efficiency at part load as well as difficulties and time constraints in bringing these generation units back to their nominal output values. This is where power system reserves and balancing power play a role in integrating the wind power into the grid. TSO tries to respond to the fluctuations in system, which is partly due to wind power generation by utilizing power system reserves. One important tool for TSOs in managing the wind power in the system is wind power forecasting. By using forecasting information, they can plan the dispatch and reserve requirements more easily.

Wind power added to the generation mix has impacts on the power system just like any other generation type. However, it is not clear exactly how much (if any) extra power system reserves must be made available for extra installed wind capacity and there have been various studies on determining reserve needs related to wind power. Power system reserves are in principle assigned and operated to deal with the overall system imbalances rather than to deal with a certain type of generation technology. As concluded in several studies [11, 49] and stated in the European Wind Energy Association (EWEA) report entitled "Large Scale Integration of Wind Energy in the European Power Supply", wind power development have little to no influence on the primary reserves as primary reserves are assigned according to larger power plant outages and therefore large enough to cover imbalances resulting from wind energy generation. Additional secondary and tertiary control reserve requirements on the other hand depend on wind power penetration level in the system and wind power forecasting information used by the TSOs. According to EWEA, effect on secondary and tertiary reserves is 2% at low wind penetrations and 4% at higher penetration levels.

An alternative to traditional power system reserves can be the utilization of grid connected energy storage in interconnected energy systems. With the help of

storage systems, electric energy can be stored when the generation is more than the demand and this stored energy can be dispatched later when the demand exceeds generation. Storage systems can be designed for short-term and long-term applications. Short-term storage could serve a similar purpose as power system reserves while long-term storage could be utilized to balance the generation and demand on a larger time scale.

Another way of mitigating the imbalances resulting from generation and demand mismatch is demand side management (DSM). This is in simplest terms, switching the electrical loads on and off and changing the instantaneous power demand in order to cope up with the imbalances. Current developments in smart grid systems with smart metering and advanced grid-user interaction could make DSM a strong alternative in managing the grid in the near future.

2.5.2 Wind power forecasting

Wind power forecasting is predicting the power output of a turbine or set of turbines for a certain time interval. With the increasing wind power penetration, it has become an important tool for integration of variable wind power to power systems and electricity markets.

Forecasting of wind power output is in direct relation to forecasting of atmospheric variables such as wind speed, wind direction, and air density. It is in general terms a two step process of data acquisition and data processing. Data acquisition is mainly gathering the necessary atmospheric data through measurements as well as historical information while data processing is evaluating the acquired data by various software. Wind power forecasting can be done by using physical models or statistical models. Physical models mainly rely on physical information from numerical weather predictions (NWP) while statistical models rely mainly on statistics from historical data. There are many different approaches in the area of wind power forecasting and all of the developed tools use complex models and calculations to reach good forecast accuracies [50].

Various parties related to wind power generation can benefit from wind power forecasts depending on the regulations at regional or national levels. For example in countries where wind power plant operators are obliged to declare their output in advance for market operations, they can strongly benefit from forecasting services. Transmission system operators (TSO) benefit from wind power forecasting in any case as they can plan the flow of energy in the transmission system much more easily and they can reduce the balancing costs resulting from imbalances caused by wind power variability.

Wind power is usually forecast 2 to 40 hours ahead and the error increases with time. In short-term forecasting, the largest source of error is the NWP input. Wind power forecast accuracy can be quantified with various error functions although the root mean square error (RMSE) of the forecasts normalized to the

installed wind power capacity is the most common one. Other indicators include mean absolute error (MAE) and correlation coefficient between forecast and actual generation [51]. Wind power forecast error decreases with increasing area and number of turbines, outputs of which are being forecast. This is called the smoothing effect where negative and positive forecast errors cancel each other out in a distributed forecast, which includes many wind turbines. As the prediction area gets larger, the predictions become better. With the current state-of-the-art wind power forecasting techniques, forecasting error (RMSE) is usually below 10% for a 1-year interval in a region. However it can be much bigger or much smaller as the calculation interval changes [52–55]. Figure 2.5 shows an example deviation of wind power output from the forecast based on real forecasting and actual production data from the TenneT TSO⁴ control area in Germany for the first two weeks of April in 2009.

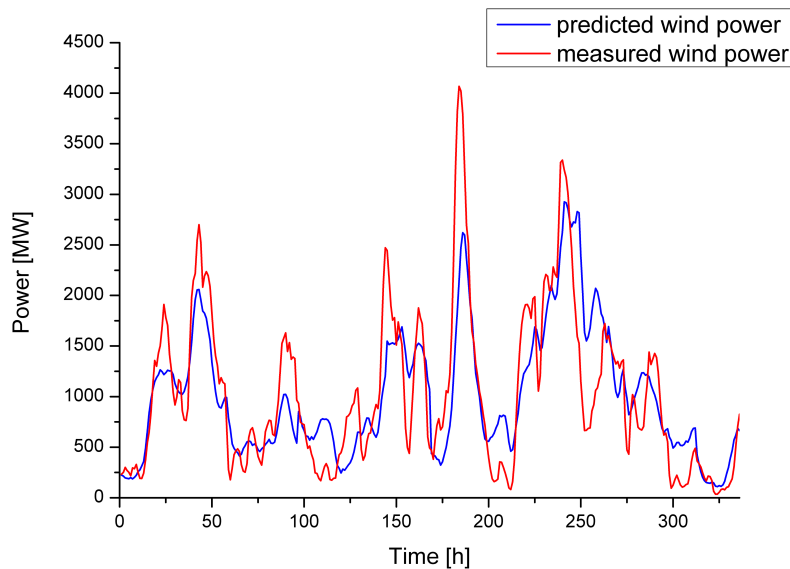


Figure 2.5 Predicted and measured wind power values for TenneT control area in Germany for the first 2 weeks of April, 2009 [TenneT Holding B.V.].

Within this two week period, wind power prediction error normalized to the installed power has a root mean square error (RMSE) of 4.76% . Amount of imbalances within this period accounts for 54 GWh of overprediction and 63 GWh of underprediction of wind energy.

⁴TenneT TSO operates as the TSO in German federal states of Schleswig-Holstein, Lower Saxony, Bremen, North Rhine-Westphalia, Hesse, and Bavaria. (<http://www.tennet.eu>)

2.6 Electrical energy storage

2.6.1 Overview

Although electricity storage with batteries at low power levels has been around for many decades, electricity is generally consumed as it is generated. Total globally installed on-grid storage capacity is quite small compared to the installed reserve capacity and consists mostly of pumped hydro storage. However, with the increasing share of renewable energy and distributed generation units, electrical energy storage is becoming more important every day. Current worldwide perception suggests that high (and one day possibly 100%) shares of renewable power could only be possible with the coexistence of improved power grids and adequate storage facilities [25, 56].

2.6.2 Benefits and uses of electricity storage

Grid connected energy storage systems (ESS) have a wide range of potential applications. Power and energy capacities of an ESS specify the suitable applications. In the most general case, applications can be classified as the short-term utilization and mid to long-term utilization of an ESS.

In short time periods, an ESS could provide power and energy for power quality control and grid stabilization, potentially replacing the traditional primary control units, which burn fossil fuels and are therefore expensive and environmentally unfriendly to operate. As investigated in this study, an ESS can also help mitigating the fluctuations and variability in the output from renewable energy sources.

Mid to long term applications of ESS could include backup power supply for a specific facility (e.g. hospitals, airports, military facilities etc.) or a region in case of a power system failure. ESS can also be used as an alternative tool to power system reserves in order to maintain generation and load matching. Furthermore, energy storage can be used for arbitraging in the energy market, which means buying and storing power when cheap and selling it when more expensive.

2.6.3 Energy storage technologies

Energy storage technologies can be classified in three categories according to the form of energy electricity is stored in:

- Mechanical energy storage systems
- Electrochemical energy storage systems
- Electrical energy storage systems

Mechanical EES include pumped hydro energy storage (PHES), compressed air energy storage (CAES) and flywheels. Batteries and double-layer capacitors⁵ store energy in an electrochemical form. Storing electricity in the same form, without any conversion is only possible with superconducting magnetic energy storage (SMES).

Pumped hydro energy storage

Pumped hydro storage system (PHES) relies on the principle of storing electrical energy in the form of potential energy by utilizing two water reservoirs at different heights. During charging, water is pumped from the lower reservoir to the higher one using an electric motor. When electricity needs to be generated, storage is discharged by releasing water from the higher reservoir back to the lower one through a pen stock and running a hydro power turbine/generator set.

Pumped hydro facilities currently constitutes most of the installed energy storage systems for power grids. There is more than 100 GW of pumped hydro storage capacity installed worldwide while installations in Japan account for about a quarter of it. Pumped hydro storage systems can have discharge times ranging from several hours to days and weeks. Typical efficiencies are between 75% to 85%. They can also be built at a wide range of power and energy levels depending on the reservoir volumes and the height difference between the upper and lower reservoirs. Biggest disadvantage of PHES is that they can only be built at locations where the geography is suitable. Large-scale pumped hydro storage facilities could also have a big environmental impact at the location they are built.

Compressed air energy storage

Compressed air energy storage (CAES) systems store electrical energy by compressing air and storing it at high pressure in caverns, which could be geological underground formations or abandoned mines. In order to discharge energy from the system, air at high pressure is released to run a gas turbine cycle. In a conventional gas turbine cycle, about 2/3 of the fuel is consumed to compress the air while the rest does the useful mechanical work of running an electrical generator. In a CAES gas turbine cycle, pre-compressed air stored in the cavern can be used in the combustion process to avoid the compression step.

As of date, worldwide there are only two CAES facilities in operation. These are located in Huntorf, Germany and McIntosh, Alabama, USA. Having been built in 1978, Huntorf plant was the first CAES facility and it has an installed power capacity of 290 MW. CAES plant in McIntosh, which was built in 1991 has an installed power of 110 MW. Like PHES, disadvantages of CAES are geographical

⁵Some sources classify double-layer capacitors as electrical energy storage units. However, due to the existence of the electrochemical double-layer, in this study they are classified as electrochemical storage units.

dependence and high capital costs. Furthermore, conventional, adiabatic designs still require fuel for the gas turbine operation and therefore create emissions.

Flywheels

Flywheels store the electrical energy in the form of kinetic energy of a spinning mass. An electric motor-generator unit is coupled mechanically to a flywheel. In order to charge the storage, electric motor spins the flywheel until it reaches a certain speed. Stored energy can later be released by inverting the operation and running the electrical machine as an alternator to generate electricity. Spinning part of a flywheel unit is in a low vacuum environment in order to reduce drag and keep the losses at a minimum. Furthermore, magnetic bearings are used to increase efficiency and lifetime, again by reducing drag and wear.

Although flywheel technology has been around for many decades, only after the development of composite materials, flywheels of very high efficiency were developed and utilized. Modern flywheels can reach up to 20,000 rpm and round trip efficiencies of 85-90%. Main disadvantage of flywheels is their self discharge rate, which make them unsuitable for long-term energy storage. Therefore, flywheels are mainly used in fast response, short-term applications such as frequency regulation, short-term backup power, and regenerative braking in electric vehicles. Flywheels have long cycle life with modern systems reaching 20 years or 30,000 cycles of operation.

Electric double-layer capacitors

Electric double-layer capacitors (aka Supercapacitors) have very high capacitances compared to traditional capacitors. This property is achieved by the utilization of an electrolyte material, which creates the electrochemical double-layers (Helmholtz layers) between the two electrodes of a capacitor. So in double-layer capacitors, an electrolyte takes the place of the classical dielectric in regular capacitors and forms the double-layers. Due to the existence of double-layers, a supercapacitor can be considered as two capacitors in series with a series resistor in between. This series resistor represents the ionic resistance of the electrolyte. In order to achieve high capacities, large electrode surface areas should be available. Activated carbon is often utilized as electrode material.

Double layer capacitors are suitable for fast response, short term (from milliseconds to some minutes), applications due to their high power but low energy capacities. They are mainly used for applications that require high power peaks within short time intervals such as uninterruptible power supply (UPS) systems and regenerative braking in electric vehicles.

Superconducting magnetic energy storage

Superconducting magnetic energy storage (SMES) systems store electrical energy in the magnetic field created by the flow of direct current through a superconducting coil. Superconducting coils are made up of special materials, which lose their resistance to electricity at very low temperatures. The most typical material used for superconducting coils is niobium, which usually alloys with tin or titanium to manufacture superconductive coils. Superconducting coil is placed in a vacuum-insulated vessel and cooled down to very low temperatures using liquid helium so that it reaches its superconducting stage. Electronic equipment is used to make AC/DC conversions and to charge and discharge the coil.

Although electrical losses in the system are quite low, energy consumed for the cooling process drives down the efficiencies of SMES systems. Despite the ongoing research in the field of high temperature superconducting materials, which would not require extreme cooling and can be cooled by using liquid nitrogen, there is no commercially available unit as of date.

Batteries

Batteries are electrochemical devices designed to store electric energy. Battery technology has been around for more than a century. Although the first modern batteries were invented by Luigi Galvani in 1780 (Galvanic cell) and by Alessandro Volta in 1800s (Voltaic pile), some historical artifacts such as the Baghdad battery suggests that there could be earlier attempts to store electricity by utilizing primitive batteries or battery like devices.

A battery cell essentially consists of two electrodes and an electrolyte. Electrodes store the electrons through electrochemical reactions while electrolyte acts as a medium, which enables the reduction and oxidation reactions at the positive and negative electrodes by ion transfer. As the ions flow through the electrolyte from one electrode to the other, released electrons flow through an external circuit to generate electric current and supply a load. In secondary (or rechargeable) cells, electrochemical reactions, which take place during discharging can be reversed by supplying a direct current to the electrodes and electric energy can be restored in the battery. Figure 2.6 shows the basic principle of an electrochemical cell during discharging and charging.

There are various types of batteries depending on their chemical composition based on the utilized electrode and electrolyte materials. Most commonly used secondary battery technologies are described briefly in the following paragraphs while vanadium redox flow batteries, which are the main scope of this study, are explained in more detail in the next section.

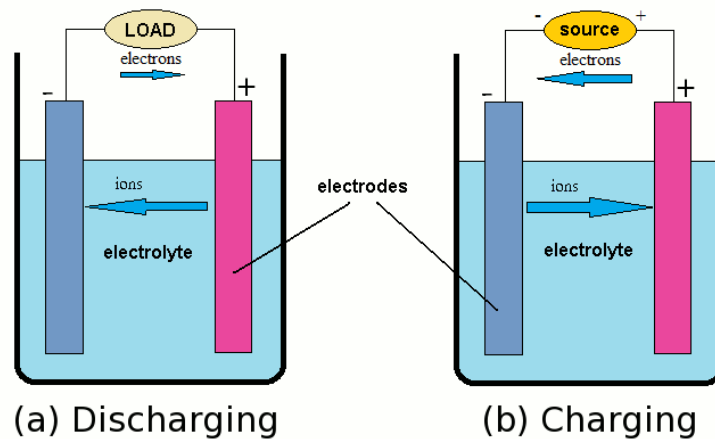


Figure 2.6 Working principle of an electrochemical cell.

Lead-acid batteries

Lead-acid battery technology is one of the oldest and arguably the most mature electrochemical energy storage technology. A lead-acid cell has electrodes made up of metallic lead (Pb) and lead dioxide (PbO_2) in an aqueous solution of sulphuric acid (H_2SO_4) electrolyte. Lead-acid batteries have a nominal voltage of 2.1 V per cell and gravimetric energy densities ranging from 35 to 60 Wh/kg.

Lead-acid batteries have found their main application area in the automobile industry for many decades as SLI (starting, lighting, ignition) batteries. They are also mainly used in solar home system applications coupled to photovoltaic modules and for backup power applications in rural areas with no or limited power grid access. One reason that makes them popular is their relatively low price. Main disadvantage of lead-acid batteries is their short cycle life, which is highly affected by operation modes. Cycling these batteries at low states of charge decrease their life significantly. Furthermore, they should always be kept under charge and at a high SOC in order to maintain usable capacity.

Nickel-cadmium batteries

Nickel-cadmium (NiCd) batteries use nickel oxide hydroxide (NiOOH) and metallic cadmium as electrodes. Electrolyte material is usually potassium hydroxide (KOH). NiCd batteries have a nominal voltage of about 1.25 V per cell and their gravimetric energy density varies between 45 and 80 Wh/kg. Main advantages of NiCd batteries include long cycle life, tolerance to deep discharging and high discharge currents. They have been widely used for consumer electronics applications in the 1990s but recently have been replaced by NiMH and Li-ion technologies due to some disadvantages such as memory effect, toxicity of cadmium, and high self discharge rates.

Nickel-metal hydride batteries

Nickel-metal hydride (NiMH) battery is chemically similar to a NiCd battery, also using a NiOOH electrode and KOH electrolyte. However, the second electrode of a NiMH cell is a hydrogen absorbing alloy instead of cadmium. This makes NiMH batteries more environmentally friendly. Furthermore, they have higher gravimetric energy densities ranging from 60 to 120 Wh/kg. They have a similar cell voltage of 1.25 V as NiCd batteries and their overcharging tolerance is also high. However, they have a higher self discharge rate and shorter cycle life than the NiCd technology.

Lithium-ion batteries

Lithium being the lightest metal and having the highest electrochemical potential make rechargeable lithium-ion (Li-ion) batteries superior. Li-ion battery cell has a nominal cell voltage in the range of 3.2-3.6 V depending on the exact chemistry and energy densities as high as 190 Wh/kg (although more typical numbers are in the range of 100-150 Wh/kg). Furthermore, Li-ion batteries have long cycle life and they are suitable for operation at any SOC without lifetime being significantly affected. Li-ion batteries can be manufactured from a wide range of electrode materials. Most commonly used materials for the positive electrode include lithium cobalt dioxide (LiCoO_2), lithium manganese oxide (LiMn_2O_4) and lithium iron phosphate (LiFePO_4). Graphite is the most common material for the negative electrode. Electrolyte material for Li-ion batteries is usually a lithium salt in an organic solvent.

Li-ion batteries currently dominate the consumer electronics market as they have been proved superior in low power applications. However, they are facing obstacles in penetrating into the high power applications market such as electric car batteries or power grid applications. Main obstacle they are facing is their high capital costs of about USD 600/kWh. Li-ion battery prices are expected to decrease as electric vehicle (EV) market reaches a more mature state and more manufacturers bring out their EV models equipped with Li-ion battery packs. Another issue with Li-ion batteries is their high safety requirements. Complex electrical and thermal battery management systems are required for Li-ion battery operation as lithium based batteries can catch fire or explode due to thermal runaways resulting from overcharging or ruptures.

Sodium sulfur batteries

Sodium sulfur battery is a type of high temperature battery, which operates at 290-380°C. It has sulfur at the positive electrode and sodium at the negative, both of which are at molten states. A beta-alumina solid electrolyte (BASE) membrane separates the electrodes from each other while also acting as the ion

transfer medium. Sodium sulfur batteries have a cell voltage of about 2 V. They have already been successfully used for stationary and mobile applications in the past and although this technology has lost its popularity for mobile applications, research and development for stationary applications still continues. Japan is leading the research in this technology and more than 20 MW of capacity is installed in this country.

Metal-air batteries

Metal-air battery technology is considered as a future prospect for electrical energy storage. It works on the principle that the metallic cathode material is oxidized by the air on the anode side. Ion conducting electrolyte is a salt of the metal used for the electrode. Zinc, aluminum, and lithium are highly considered metals for this type of batteries due to their high electrochemical potentials.

There are certain difficulties in mainly recharging but also in discharging operation of metal-air batteries. Major hurdles are electrolyte stability issues and mechanical stresses resulting from deposition of electrode material during operation. Although utilizing more stable ionic liquids as electrolyte material has been investigated, this would drive up costs significantly. Although non-rechargeable zinc-air batteries are already marketed for low power applications, further research is necessary for market introduction of rechargeable metal-air batteries.

Flow batteries

A flow battery is a type of secondary battery where one or both of the reactants are liquids stored in external tanks and flow through an electrochemical cell consisting of electrodes and separator structures. The cell is the component of a flow battery where the chemical reactions of charging and discharging occur. Electrolyte material stored in external tanks are pumped through the cell by the help of pumps. Reacting electrolyte returns to the tank in a closed circuit system, yet in a different chemical state. Figure 2.7 shows the operating principle of a flow battery. Electrodes are connected to conductive bipolar plates that act as current collectors. They are separated by an ion exchange membrane, which allows ions crossing from one side to the other during a charge or discharge reaction while preventing the mixing of positive and negative electrolytes and electrical short circuits.

Various types of flow batteries exist depending on their electrolyte materials. Some of these are zinc-bromine, zinc-chlorine, zinc-cerium, polysulfide bromine and vanadium redox flow batteries. In this study, the focus is on vanadium redox flow batteries (VRFB), which have solutions of vanadium as electrolyte material. The VRFB technology is explained further in the following section.

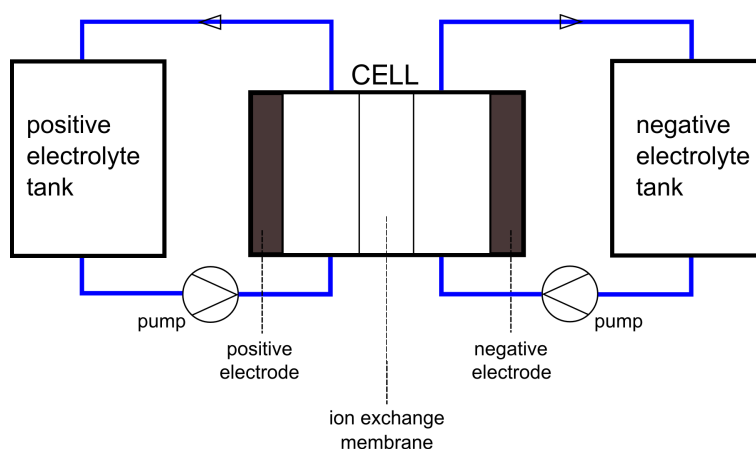


Figure 2.7 Schematic representation of a flow battery.

2.6.4 Vanadium redox flow batteries

Among flow batteries, vanadium redox flow batteries (VRFB) have certain advantages due to certain properties and this energy storage technology has drawn much attention in recent years [8]. Vanadium is an abundant material in nature and it is already widely mined and used by the steel industry. Furthermore, having vanadium based solutions in both electrolyte tanks bring simplicity to the system whereas having different couples of electrolytes could result in complex electrochemical reactions. One other advantage of using vanadium is the reversibility it brings to the electrolyte, meaning that the vanadium based electrolyte could be used over and over after some processing, which makes the electrolyte lifetime not an issue in the whole lifetime of a VRFB [57–60]. Table 2.3 compares some characteristics of VRFB to those of the widely used lead-acid battery.

Table 2.3 VRFB vs Lead-Acid Battery.

	VRFB	Lead-Acid Battery
Gravimetric energy density (Wh/kg)	20-25	25-50
Volumetric energy density (Wh/l)	30	30-50
Nominal cell voltage (V)	1.26	2.10
DC-DC round-trip Efficiency (%)	70-85	70-80
Lifetime (cycles)	10,000-16,000	200-1500
Operating temperature (°C)	10-45	-10-40

VRFB components

Electrolyte

Electrolytes in a VRFB are composed of vanadium ions in an aqueous acid solution. Sulfuric acid is the most commonly used acid type as vanadium species are highly soluble in it. Operating temperature of the electrolyte in vanadium redox flow batteries is between 0 °C and 40 °C as lower temperatures increase the viscosity of the electrolyte, making it more difficult to flow through the stacks while too high temperatures can cause V_2O_5 precipitation in the positive electrolyte [8, 57, 58].

Electrodes

Carbon felt is typically used for manufacturing VRFB electrodes. They are sometimes coated with niobium to avoid hydrogen evolution. The most important property of the electrodes is that they have a large surface area in order to provide high current densities [8, 57, 58, 61, 62].

Ion exchange membrane

Half cells in each cell are separated by an ion exchange membrane, which separates the positive and the negative electrolyte solutions. Ion exchange membrane must allow the ion transfer within the electrolyte while preventing electrons to pass through. Various membrane materials are used in VRFB. Nafion[®] is a commonly used commercial product for membranes. It was developed by DuPont [63].

Bipolar plates

Role of the bipolar plates is to separate adjacent cells in a stack physically while connecting them electrically to each other. It has to be made up of a highly conductive and chemically stable material to withstand the acidity. Plastic carbon electrodes are commonly used for this component [64].

Electrolyte tanks

Electrolyte is stored in external tanks outside the cell stack. Tanks should be made of materials that can resist the low pH environment. Typical tank construction materials are plastic and fiberglass [8].

Pumps and piping

Like the electrolyte tanks, pumps, valves, and piping components should also be resistant in low pH environments. Therefore, pumps with plastic impellers are highly preferred. For piping, polyvinyl chloride (PVC) is the most favorable material [8].

Electrochemistry and functioning

A VRFB is based on the four possible oxidation states of the vanadium, which are V^{2+} , V^{3+} , V^{4+} and V^{5+} . As it can be seen in Figure 2.8, V^{2+} is oxidized into V^{3+} and V^{5+} is reduced into V^{4+} during discharging while the opposite oxidation and reduction reactions take place during charging.

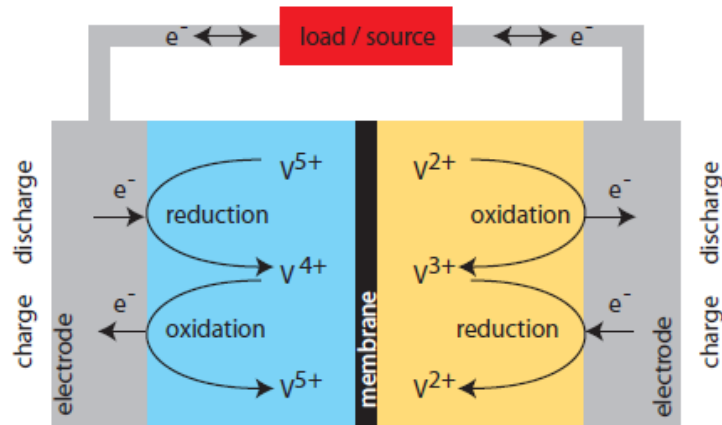
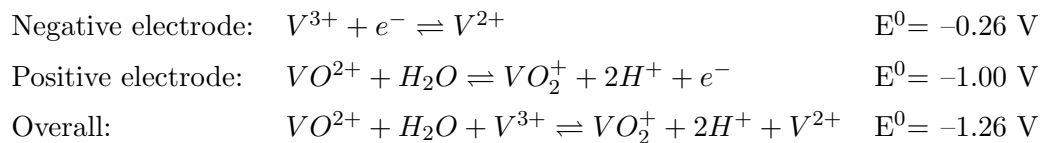


Figure 2.8 VRFB redox reactions during charging and discharging.

The VRFB stores and releases energy by utilizing the redox chemistry in an acid media between vanadium ions in different oxidation states (cathode: $V^{5+} \leftrightarrow V^{4+}$; anode: $V^{2+} \leftrightarrow V^{3+}$). Electrolytes are fed into the cell from external storage tanks by using pumping equipment. The power output, which is determined by the converting unit (cell stacks) and energy capacity which is defined by the size of the electrolyte tanks are decoupled, giving the VRFB a high degree of design flexibility.

Following reactions take place at each half cell of a vanadium redox flow cell. It should be noted that both electrolyte tanks are filled with vanadium ions at different oxidation states and dissolved in a sulfuric acid solution.



Operation parameters

Energy capacity

Concentration and amount of electrolyte in the tanks determine the energy capacity of a VRFB. Typical electrolyte has a volumetric energy density of 20 to 30 Wh/l.

Power capacity

Power capacity of a VRFB is determined by the number of stacks that make up the system. Essentially, stacks are made up of cells and as mentioned above, each cell has a nominal voltage of 1.26 V. Therefore the nominal voltage of a unit will be determined by the number of cells connected in series. Furthermore, the current capacity depends on the electrode area. Voltage and current capacity together define the nominal power of the VRFB unit. However, it should be noted that the state of charge (SOC) of the battery can play a role in the maximum available power from a stack.

Efficiency

Inefficiencies in VRFBs are related to the thermodynamics, reaction kinetics, and ohmic resistances. Pumps and power converters are other sources of overall efficiency reduction although new generation power converters have efficiencies as high as 95%. After the efficiency drops caused by other auxiliary equipment such as control systems and thermal management systems, overall round trip efficiency of VRFBs can be expected to be 60-70%.

Response time

Similar to other battery types, VRFBs have response times in the range of microseconds.

Lifetime

Ion exchange membrane is the most fragile component of a VRFB and might have to be replaced every few years [8, 63]. Other important component that determine the lifetime of a unit is the pump. VRFB units can operate for more than 20 years with replacement of some components and regular maintenance of others.

Pros and cons

In the recent years, in order to increase efficiency and reduce the self discharge rate of VRFBs, much attention was paid to the improvement of individual components of the power unit such as the electrodes, membranes and current collectors [61–63, 65]. Further focus has been on development of new electrolyte mixtures to increase the relatively low energy density of 25 Wh/l and the thermal stability of the battery [57]. Despite these drawbacks, the VRFB technology has certain advantages over other battery types:

- Energy and power capacity of flow batteries can be sized independently of each other. Energy rating of a flow battery depends on the amount of electrolyte,

therefore the size of the electrolyte tanks. Power rating on the other hand depends on the size and the number of cell stacks. Energy and power ratings can be upgraded by adding more electrolyte or more cell stacks to the systems respectively. This feature makes this technology very attractive for stationary applications where space requirement is not an issue.

- Flow batteries require low maintenance.
- They have a relatively long cycle life as the active material in their electrolyte does not degrade easily and can be reused. In addition, as the negative and positive electrolyte have the same chemistry (vanadium ions at different charge states), crossover process do not cause irreversible contamination of the electrolyte.
- Active thermal management can be provided in an easy way, prolonging the life of electrochemical components.
- State of charge (SOC) can be measured during battery operation with the help of an external cell setup.
- Flow batteries are more tolerant to overcharging and deep discharging conditions than other batteries.
- Electrolyte can be managed at system level as it is shared by all the cells in the whole stack whereas in conventional batteries, electrolyte of each cell is separate from another and it can be managed only at cell level.
- They have a low ecological impact with no toxic or hazardous components involved.

It has already been demonstrated in a number of projects in various locations that the VRFB technology can be successfully utilized in applications ranging in sizes from several kilowatts to some megawatts [37]. For instance, a 200 kW/800 kWh grid-connected vanadium battery was commissioned at the Kashima-Kita Electric Power station in Japan back in 1997. The system was tested for load leveling application. By the beginning of 1998 in less than 1 year of operation, it had already undergone 150 charge-discharge cycles and was continuing to show high energy efficiencies of close to 80% at current densities of 80-100 mA/cm² [58]. Similarly, a 250 kW/520 kWh VRFB system was demonstrated in Stellenbosch, South Africa for a number of applications such as sub-second UPS ride-through capabilities, power quality and emergency back-up [66]. Furthermore, a 1.5 MW system, which was realized by Sumitomo Electric Industries in Japan with the aim of voltage sag compensation for a semiconductor plant can be presented as an example of megawatt scale VRFB application [67]. In 2005, a larger system of 4 MW/6 MWh was installed at Subaru Wind Farm in Japan again by Sumitomo

Electric Industries. The battery has been utilized for wind energy storage and wind turbine output power stabilization [37].

Chapter 3

Vanadium Redox Flow Battery Model

3.1 Introduction

First part of this study is to simulate and characterize a megawatt scale vanadium redox flow battery (VRFB) unit, which is later to be utilized in a wind power integration application as discussed in the next chapter. As no megawatt scale VRFB systems are widely available yet, characterization is done by measurements on a commercially available kilowatt scale (10 kW) battery and a software model, which provides a precise upscaling and evaluation at the system level through simulating various system sizes via a modular battery approach.

The battery model mainly focuses on the efficiency of the VRFB system within its operating ranges. The main goal of the experimental work was to characterize a real life VRFB system as accurately as possible in order to have good input data for the megawatt scale battery modeling later on. It can be stated that the results that were obtained during the experiments with a real life unit contributed significantly to building the megawatt scale software model, which was developed in Matlab[™] Simulink[®] environment. The model estimates the optimal number of modules for certain power levels during charging and discharging operations.

Utilization of the built battery software model for wind power integration is achieved by using the output efficiency data as the key input for the hypothetical dedicated VRFB unit integrated with a 10 MW wind power plant. Efficiency of the battery is calculated for every instance of the power plant output as a function of the battery SOC and power. Details of the model utilization in a dedicated storage design is discussed further in the next chapter.

3.2 Experimental characterization of a VRFB unit

3.2.1 Overview

Battery characterization with the commercial unit is based on measurements during real life operation of the unit. It aims to determine the operating ranges and efficiencies of the battery based on various operation parameters. Operating ranges and efficiencies are evaluated both at string and system level. Several charge and discharge cycles at various operating points were realized with the battery in order to collect the necessary data for the calculations.

3.2.2 Description of the battery unit

The battery unit, which was used for the measurements was a Gildemeister¹ CellCube FB 10/100 with a nominal power of 10 kW and a nominal energy storage capacity of 100 kWh [68]. The unit is made up of the complementary systems, which are explained below. The complete unit is packaged in a container with a volume of about 24 m³. Figure 3.1 shows the CellCube schematic and the component locations in the container.

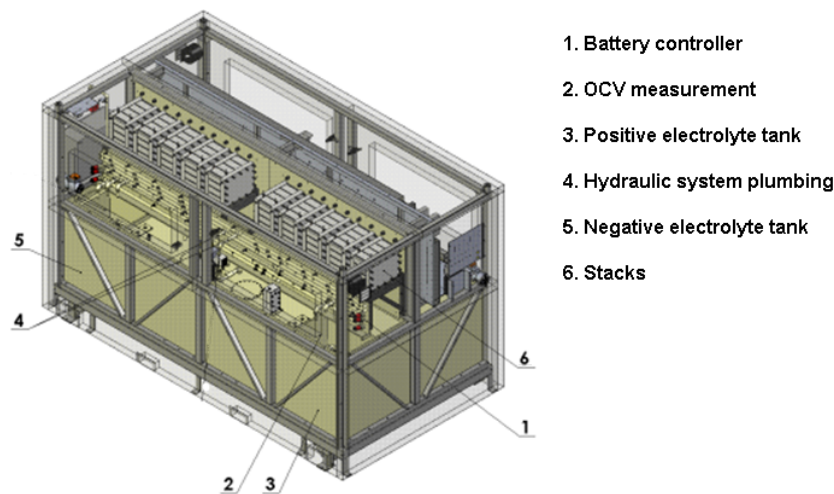


Figure 3.1 CellCube Schematic [5].

The battery unit is made up of cell stacks where the electrochemical conversions take place, hydraulic circuits that transport the electrolyte into the stacks, measurement sensors for battery management, and electrical connections.

In the stacks compartment, there are 10 stacks each made up of 20 bipolar cells. Two stacks are connected electrically in series and make up 1 *string*, nominal power of which is 2 kW. There are three hydraulic circuits. The primary

¹<http://www.gildemeister.com/energysolutions/en>

hydraulic system serves for the first string and the open circuit voltage (OCV) measurement cell. The other two hydraulic systems are utilized for the further four strings. Each hydraulic system has its own pair of pumps, one being for the flow of the positive electrolyte and the other for the negative. As all these hydraulic circuits are independent from each other, they can be switched on and off independently, based on the power demand. This configuration is aimed at avoiding lower overall efficiencies resulting from high pumping power demand during low power requirements. Strings are connected electrically in parallel to a common bus, which then connects to the power electronics components including the inverter/rectifier unit that is required for the AC/DC conversion. There are two tanks located at the bottom of the stack container for the positive and the negative vanadium based electrolyte. Each tank contains 2,500 liters of electrolyte fluid.

As already mentioned in the previous chapter, one of the advantages of flow batteries in comparison to other battery types is the possibility of monitoring the battery state of charge (SOC) during battery operation by measuring the open circuit voltage (OCV) at an external cell. Accordingly, the CellCube unit is equipped with an external OCV cell where the OCV was measured during the experimental work. Since the same electrolyte flows through the external OCV cell and that no load is connected to this, the open circuit voltage can be measured at this cell even if the main stack is in charging or discharging operation. The relationship between the OCV and the SOC can be defined by using the Nernst equation as follows:

$$OCV = E_{cell} = E_{cell}^0 + \frac{RT}{nF} \ln \frac{[SOC]^2}{[1 - SOC]^2} \quad (3.1)$$

where E_{cell} is the cell potential (V), E_{cell}^0 the cell potential at 50% SOC (V), R the gas constant ($8.314 \text{ JK}^{-1}\text{mol}^{-1}$), T the temperature (K), n the number of equivalents per mole of vanadium, F the Faraday's constant ($96.487 \text{ C mol}^{-1}$) and SOC the state of charge.

Based on the equation 3.1, the relationship between the OCV and the SOC for a 2 molar vanadium electrolyte VRFB system can be visualized as in Figure 3.2.

Alongside the AC/DC converters required for the connection to the 3-phase AC power grid, additional DC/DC converters are utilized in order to mitigate the highly fluctuating bus voltages.

Battery management system (BMS) is an essential component for the whole system and is made up of electronic components such as micro controllers, measurement sensors, and data logging equipment. Its function is electrical and thermal management of the system in order to provide the optimal operation modes for the battery while also guaranteeing safety during battery operation. Battery management system plays a key role in the energy exchange with the power grid and operating the battery at high efficiency. Efficiency optimization

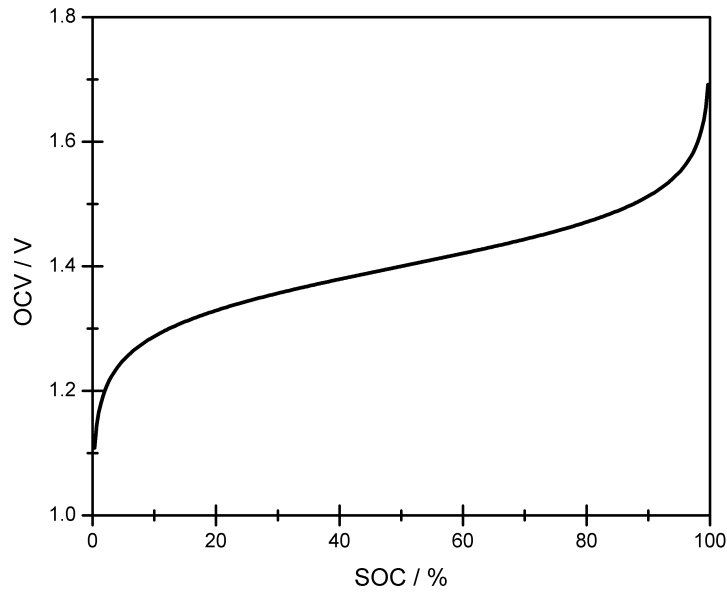


Figure 3.2 OCV vs SOC for a VRFB cell (2 M vanadium electrolyte, $E_{cell}^0=1.4$ V)

is realized mainly by managing the strings and hydraulic system in an effective way, which includes deciding the number of strings that need to be online or number of pumps that need to be operating. Safety of the entire system is also provided by the BMS, which detects possible problems such as overcharging, deep discharging conditions, electrolyte leakages, and overheating. In case such a condition is detected, BMS takes action by activating alarms or interrupting the battery operation. An additional function of the BMS is to provide data logging, real-time monitoring, and remote supervision capabilities.

3.2.3 Measurement strategy

The aim of the performed measurements was to obtain sufficient data to calculate the efficiency and determine the optimal operating modes of the battery. The CellCube unit, which was used for the measurements needs approximately 10 hours to be completely discharged and more than 10 hours to be fully recharged at nominal power. Due to limited time availability, no complete discharge/charge cycles could be performed. Alternatively, short cycles at different SOC and different charging and discharging powers were realized. For instance at 60% SOC, the battery was charged for 30 minutes at a 6 kW power level and then was discharged with the same power for the same duration. Similarly, the same procedure was applied with power values of 2 kW and 4 kW. Same strategy was

applied for SOCs of 20%, 40% and 75%.

Additionally, partial charge/discharge cycles at nominal power and several complete discharge runs with constant power were performed. The data, which were collected and analyzed for the construction of the model includes more than 171 hours of measurements with an average sample rate of about 2.14 seconds. The most important variables that were obtained during the measurements are listed in Table 3.1.

Table 3.1 Variables recorded during the measurements.

Variable	Unit	Description
Bus voltage	V	Voltage at the common point of all strings
Bus current	A	Current at the common point of all strings
Open circuit voltage (OCV)	V	Open circuit voltage measured at the OCV cell
State of charge (SOC)	%	State of charge (calculated)
String 1 current	A	Current flowing through the string 1
String 2 current	A	Current flowing through the string 2
String 3 current	A	Current flowing through the string 3
String 4 current	A	Current flowing through the string 4
String 5 current	A	Current flowing through the string 5
Pumping circuit 1 power	W	Power consumption of the hydraulic circuit 1
Pumping circuit 2 power	W	Power consumption of the hydraulic circuit 2
Pumping circuit 3 power	W	Power consumption of the hydraulic circuit 3

3.2.4 Efficiency calculations

Overall system efficiency in a VRFB unit is determined by considering the exergy losses at stacks during the electrochemical conversion and by the auxiliary power consumption of the hydraulic circuits, power conversion systems, control systems, and air conditioning system. Since the power demand of the control system and the air conditioning system would be negligible in a megawatt size system, losses resulting from these are not included in the efficiency calculations. Hence, the overall system efficiency calculations are based on the following three factors:

- Voltage efficiency
- Coulombic losses
- Pumping power

Overall system efficiency during the discharging process is determined by the ratio between the amount of discharged energy from the electrolyte and the

amount of energy fed into the power grid. For the charging process, the calculation is reversed. It should be noted that "OCV Power" is defined as the power that reaches the strings after overvoltage losses, which are described in the "Voltage efficiency of a string" subsection. OCV power is calculated by using the open circuit voltage values whereas "power to the strings" is calculated by using the voltage at the string terminals.

As mentioned before, the battery is made up of 5 strings, which are electrically connected in parallel. The strings are switched on and off depending on the power demand from the battery and the SOC of the battery at a certain moment. On the other hand, the first string, which shares the hydraulic system with the OCV cell is always on when the battery is in operation. Therefore, there were more available measurement data for this string than for the other four. For this reason, the string efficiency of the battery is calculated based on the measurements on the first string. Although this approach simplifies the calculation process to a certain extent, it also comes with some drawbacks. Firstly, the pumping power for this string is fixed and does not adapt to the power demand unlike the other four strings. Furthermore, the hydraulic circuit for this string supplies the OCV cell with electrolyte as well, making the energy consumption of the pumps higher for this string than the other four. In order to deal with this problem, the power demand of the pumps was measured for the entire battery and then scaled down to represent one string. Further details and discussion about this process can be found in the subsection "Pumping power demand". Following subsections describe the evaluation of the losses and the pumping power demand for the first string of the CellCube unit.

Coulombic losses

Amount of electric charge that flows into a battery during the charging process is not equal to the amount that leaves the battery during discharging. This loss of charge is associated with coulombic losses, which reduce the overall efficiency of a battery. Coulombic losses are caused by several phenomena such as ion diffusion processes (e.g. crossover), none reversible reactions (e.g. gassing), and shunt currents through the electrolyte.

Since the coulombic losses depend strongly on the hydraulic circuits and the number of online strings, they were calculated on the basis of segments of complete charge-discharge cycles where all strings are online, the power is constant and the hydraulic characteristics remain the same. It should be mentioned that in the measurements, these conditions were fulfilled at high SOC values. Coulombic losses were calculated on parts of charging and discharging cycles for the same starting and ending SOCs by deducting the voltage and pumping losses from the total losses, which were obtained as the difference between the total input and output energy. Based on the measurements, coulombic losses ranged from

50 to 60 W per string with an average value close to 58 W. The deviations can be explained by coulombic efficiency being SOC dependent. For the efficiency calculations, which are described in the following sections, a conservative value of 60 W per string was used.

Voltage efficiency of a string

In this study, voltage efficiency of a string is assumed to be only influenced by the losses that result from overvoltages during charging and discharging processes. Overvoltage losses can simply be defined as the losses resulting from the voltage difference between the open circuit voltage and the string voltage when a load is connected or when the battery is charging. Open circuit voltage tends to be lower than the string voltage during charging and higher when discharging.

Theory and mathematical equations

The equations for the efficiency calculations are described below. Charging power is calculated by the following equation:

$$P_{OCV_{chg}} = N_c \times V_{oc} \times I_{S_{chg}} \quad (3.2)$$

where $P_{OCV_{chg}}$ is the power that goes into the electrolyte after the overvoltage losses during charging, N_c is the number of cell per string (for CellCube, $N_c = 40$), V_{oc} is the open circuit voltage and $I_{S_{chg}}$ is the string current during charging. Power to the string during charging is calculated using the following equation:

$$P_{S_{chg}} = N_c \times V_{S_{chg}} \times I_{S_{chg}} \quad (3.3)$$

where $P_{S_{chg}}$ is the power that goes into the string, N_c is the number of cells per string, $V_{S_{chg}}$ is the voltage at the string terminals (measured at the bus) and $I_{S_{chg}}$ is the string current.

Similarly, power during the discharging process can be calculated as follows:

$$P_{OCV_{dschg}} = N_c \times V_{oc} \times I_{S_{dschg}} \quad (3.4)$$

$$P_{S_{dschg}} = N_c \times V_{S_{dschg}} \times I_{S_{dschg}} \quad (3.5)$$

where $P_{OCV_{dschg}}$ is the discharged power from the electrolyte after the coulombic losses and $P_{S_{dschg}}$ is the power from the string to the load.

As this efficiency model aims to characterize the behavior of the battery under stable conditions for a specific constant power, calculated power values can be integrated over certain period of times in order to calculate the efficiencies based on energy amounts. This approach would mitigate the unwanted variations in

power in the order of seconds to minutes. Accordingly, voltage efficiencies could be calculated by using the following equations:

$$\eta_{V_{chg}} = \left(\int_{t_1}^{t_2} P_{OCV_{chg}} dt \right) / \left(\int_{t_1}^{t_2} P_{S_{chg}} dt \right) \quad (3.6)$$

$$\eta_{V_{dschg}} = \left(\int_{t_1}^{t_2} P_{S_{dschg}} dt \right) / \left(\int_{t_1}^{t_2} P_{OCV_{dschg}} dt \right) \quad (3.7)$$

where $\eta_{V_{chg}}$ is the voltage efficiency during charging, $\eta_{V_{dschg}}$ is the voltage efficiency during discharging.

Calculation run

A calculation tool was programmed in Matlab[™] in order to deal with the large amount of data and perform the calculations. Following steps were taken during the calculations:

1. Time series of measurements were loaded and interpolated at regular intervals of 1 second.
2. Integral limits were set to 5 minutes.
3. If the change in power accounted for more than 100 W within an integration interval, that interval was discarded from the calculation run.
4. Integration intervals where maximum and minimum OCV vary more than 10 mV were discarded.
5. Efficiency calculations were performed according to the equations 3.2 to 3.7.
6. Missing data points due to measurement errors were substituted with synthetic data, which were obtained by three dimensional interpolation and extrapolation algorithms available in Matlab[™].

Power consumption of the pumps

Another important aspect to consider when evaluating the overall efficiency of the battery is the power demand for electrolyte pumping. This demand depends principally on the power demand of the load or charging power as well as the battery SOC.

Methodology

There are two possible ways of calculating the power needed for pumping as a function of the power demand and the SOC. The simplest approach is to consider only the first string, which is always online during battery operation. Nevertheless, this strategy has a major drawback as the pumps of the first hydraulic system can operate only at two power levels. Scaling up the pumping power for further power and SOC levels of the battery based on the first hydraulic circuit would mean using only two power levels for the entire battery, which would lead to a large error in pumping power evaluations.

The second option is to use the entire battery for calculating the power demand of the pumps. This method was preferred as there are more power levels to consider for evaluating the pumping power. Hence, the pumping demand as a function of power and SOC exhibits a more continuous characteristic, which is convenient for scaling up the power of the battery model. The average power demand of the pumps is calculated as follows:

$$\overline{P_{PB}} = \frac{\int_{t_1}^{t_2} P_{PB} dt}{t_2 - t_1} \quad (3.8)$$

where P_{PB} is the average power consumption of the pumps between t_1 and t_2 and $\overline{P_{PB}}$ is the instantaneous power consumption of the pumps for the entire battery.

Calculation run

Same Matlab[™] tool and the algorithm for calculating the string efficiency was used to calculate the average pumping power as a function of battery power demand and SOC. Time intervals of 5 minutes were used for the integration. Furthermore, the same algorithm for the calculation of the string efficiency was used for interpolating and extending the data to the entire operating range.

Finally, power demand of the pumps has to be scaled down to represent the pumping demand for one string. As the ratio between the nominal power of a string and the entire battery is 1/5, it was assumed that the pumping power needed for one string (P_{PS}) is one fifth of the pumping power required for the entire battery (P_{PB}) when the SOC and the *load level*² are constant. Accordingly, the pumping power drop for one string can be calculated with the following equation:

$$L_{p(SOC_i, P_{S_i})} = \frac{P_{PB(SOC_i, P_{B_i})}}{5} \quad (3.9)$$

²Load level is defined as the ratio between the actual and the nominal power of a string or the entire battery.

where $P_{PS(SOC_i, P_{S_i})}$ is the pumping power demand for a string, which is operating at the SOC of SOC_i and the power of P_{S_i} . P_{B_i} is the operating power of the whole battery unit.

Final string efficiency

Final string efficiency is calculated based on the coulombic losses (L_c), overvoltage losses (L_{ov}) and pumping losses (L_p), which are explained above.

As explained in the related section, coulombic losses (L_c) are assumed to be 60 W for each string, independent of SOC and power.

Overvoltage losses (L_{ov}) calculations are based on the charging and discharging voltage efficiencies, which are defined by the equations 3.6 and 3.7 respectively. They are calculated according to the following equation:

$$L_{ov(SOC_i, P_{S_i})} = (1 - \eta_V(SOC_i, P_{S_i})) \times |P_S| \quad (3.10)$$

where P_S is the string power and $\eta_V(SOC_i, P_{S_i})$ is the voltage efficiency at the state of charge of SOC_i and the string power of P_{S_i} . η_V represents the round-trip voltage efficiency, which is calculated from charging and discharging voltage efficiencies in the equations 3.6 and 3.7.

Since the stack power is used as the power reference for voltage and coulombic efficiencies as well as for pumping demand, this power value is also used to calculate the string efficiencies. The battery power during charging is calculated as follows:

$$P_{B_{chg}(SOC_i, P_{S_{chg_i}})} = P_{S_{chg_i}(SOC_i)} - L_p(SOC_i, P_{S_{chg_i}}) \quad (3.11)$$

where $L_p(SOC_i, P_{S_{chg_i}})$ is the pumping power demand (pumping losses) for a string, which is operating at SOC of SOC_i and power of $P_{S_{chg_i}}$. Similarly, the power during discharging is calculated as follows:

$$P_{B_{dchg}(SOC_i, P_{S_{dchg_i}})} = P_{S_{dchg_i}(SOC_i)} - L_p(SOC_i, P_{S_{dchg_i}}) \quad (3.12)$$

String losses for both charging and discharging are calculated as the sum of coulombic, overvoltage, and pumping losses according to the following equation:

$$L_S(SOC_i, P_{S_i}) = L_{ov}(SOC_i, P_{S_i}) + L_c(SOC_i, P_{S_i}) + L_p(SOC_i, P_{S_i}) \quad (3.13)$$

During charging, the power, which determines the energy stored in the electrolyte tanks in a certain time period can be calculated as the charging power at the DC terminals of the battery minus all the string losses as in the following equation:

$$P_{chg}(SOC_i, P_{S_{chg_i}}) = P_{B_{chg}(SOC_i, P_{S_{chg_i}})} - L_{S_{chg}}(SOC_i, P_{S_{chg_i}}) \quad (3.14)$$

where $P_{chg}(SOC_i, P_{S_{chg_i}})$ is the power that reaches the electrolyte tank (becoming the stored energy) at an SOC of SOC_i and a string power of $P_{S_{chg_i}}$, $P_{B_{chg}}(SOC_i, P_{S_{chg_i}})$ is the charging power at the battery terminals and $L_{S_{chg}}(SOC_i, P_{S_{chg_i}})$ is the losses at the corresponding SOC and string power.

Based on equation 3.14, the string efficiency during charging is calculated as follows:

$$\eta_{S_{chg}}(SOC_i, P_{S_{chg_i}}) = \frac{P_{chg}(SOC_i, P_{S_{chg_i}})}{P_{B_{chg}}(SOC_i, P_{S_{chg_i}})} \quad (3.15)$$

During discharging, the power, which is drawn from the electrolyte is calculated as the sum of the power that is fed into the grid at the DC terminals of the battery plus the losses according to the following equation:

$$P_{dschg}(SOC_i, P_{S_{dschg_i}}) = P_{B_{dschg}}(SOC_i, P_{S_{dschg_i}}) + L_{S_{dschg}}(SOC_i, P_{S_{dschg_i}}) \quad (3.16)$$

where $P_{dschg}(SOC_i, P_{S_{dschg_i}})$ is the power that is drawn from the electrolyte at an SOC of SOC_i and a string power of $P_{S_{dschg_i}}$, $P_{B_{dschg}}(SOC_i, P_{S_{dschg_i}})$ is the discharging power at the battery terminals and $L_{S_{dschg}}(SOC_i, P_{S_{dschg_i}})$ is the losses at the corresponding SOC and string power.

Based on equation 3.16, the string efficiency during discharging is calculated as follows:

$$\eta_{S_{dschg}}(SOC_i, P_{S_{dschg_i}}) = \frac{P_{dschg}(SOC_i, P_{S_{dschg_i}})}{P_{B_{dschg}}(SOC_i, P_{S_{dschg_i}})} \quad (3.17)$$

Final string efficiency is the most important parameter, which is obtained through the characterization work with the real life VRFB unit. It constitutes a base for the efficiency calculations of the megawatt scale battery unit model, which is discussed in the following section. This input parameter for the model plays an important role in the selection of string and module numbers, as well as operating ranges, which are described in detail in the following sections.

3.3 Megawatt scale VRFB model development

3.3.1 Overview

Based on the characterization work explained in the previous section, a megawatt scale VRFB software model was developed in Matlab™ Simulink® environment. The experimental results were imported into the Simulink® model in matrix form using a custom Matlab™ script. The matrix contains the calculated efficiency information for each SOC and power level. The model uses the data from the

matrix as input and scales the system up to megawatt level. It evaluates the energy efficiency and operating ranges of a hypothetical megawatt scale VRFB for an optimum design and does not take into consideration further aspects such as component degradation, ease of construction and ease of maintenance of a large scale system.

3.3.2 Design criteria

As explained earlier, power and energy capacities of a VRFB can be sized independently from each other. Since modifying the energy capacity of the battery can be achieved simply by increasing or reducing the amount of electrolyte and its related components, this megawatt scale battery model focuses on the power expansion part.

In this study, the software model of the megawatt class VRFB is based on the CellCube. As explained before, CellCube works under the principle of *multi-staging*, which means battery modules along with several hydraulic systems coming online and offline automatically depending on power and energy requirements. This characteristic makes this battery modular and therefore scalable to bigger capacities. Therefore, for modeling a megawatt class VRFB, the approach of increasing the size of a CellCube is taken. Instead of having three hydraulic circuits and one or two string per hydraulic circuit, more hydraulic systems and more strings per hydraulic system are simulated in the software model.

In order to decide the number of modules and strings, which should be utilized in a megawatt class battery, the benefits and drawbacks of having more or fewer modules have to be evaluated.

Another aspect of the model is the module size, as having different or identical modules in size has certain advantages and drawbacks. If all modules have the same size, the battery can be operated in a way that ensures the alternation of the modules for homogeneous component aging. Furthermore, with equally sized modules, inventory of spare parts that need to be available in real life conditions is much simpler. On the other hand, having different sizes for each module leads to better operational efficiencies by improved adjustment of the number of online stacks. However, as having different module sizes is not expected to bring a dramatic efficiency improvement and in order to keep the model simpler, this study follows the approach of utilizing equally sized modules.

3.3.3 General assumptions

Considering the design criteria, the megawatt class battery model is similar to a CellCube in most of its aspects. Therefore, the parameters, which define its operating ranges and its efficiency are similar. Efficiency evaluation is based on overvoltage losses, coulombic losses, and pumping losses.

As a megawatt class VRFB would need much more space, it would be installed inside a building instead of containers. A key aspect of this building is the temperature management due to the fact that an active heating or cooling system would considerably reduce the overall efficiency of the battery. In a real life battery, in order to minimize heating or cooling requirements, the building should be well insulated and have an intelligent low energy heating and cooling system. For this study, it was assumed that the temperature management does not require a significant amount of energy supply from the battery, the grid or any other electrical source. Accordingly, auxiliary power consumption resulting from possible real life thermal management systems was neglected and is not included in the calculations.

Space requirement for the electrolyte tanks were not considered as an issue in this study and the energy consumption of the control systems was neglected.

3.3.4 The software model

Based on the above mentioned criteria and assumptions, a software model of the battery was developed in Matlab[™] Simulink[®]. The software algorithm that is based on the efficiency matrix selects the optimal number of modules that should be online for achieving the best efficiency for every possible power demand and SOC. The optimization algorithm was performed using a modified Matlab[™] Level-2 C-Mex S-function (`msfuntmpl.basic.m`) with two constraints. First constraint sets the limits for the charging and discharging power for each SOC level while the second determines the operating range of the battery in terms of SOC (15-90%). In order to calculate an optimized battery model, the following steps were performed:

1. User defines the parameters maximum discharging power and number of modules.
2. Model sets the maximum charging power to the same value as the requested discharging power in step 1.
3. String efficiency table and operating ranges, which are obtained via VRFB characterization are loaded into the model as input parameters.
4. Number of strings per module is calculated as the maximum discharging power divided by the number of modules and the nominal power of a CellCube string (2 kW).
5. Operating range of the battery is defined as the operating range of a string multiplied by the number of strings. Operating ranges at a specific SOC are considered as in CellCube.
6. Specific power level and SOC are selected from a previously defined grid that covers the whole operating range of the battery.

7. Power demand and corresponding efficiency on every online string is calculated for every possible number of online modules.
8. The optimal number of modules for the specific power level and SOC selected in step 6 is determined as the minimum number of online modules, which can provide an efficiency that lies within the 5% of the highest possible efficiency value.
9. Steps 6 to 8 are repeated until the whole operating range of the battery is covered.

Using this algorithm, which was programmed in Matlab[™], battery systems with various nominal power levels were modeled and evaluated.

3.4 Results and discussion

3.4.1 Overview

This section shows and analyzes the results obtained by the battery characterization work with the commercial VRFB unit and the megawatt scale VRFB model simulated with Matlab[™] Simulink[®]. First two subsections discuss the operating range and the efficiency of the CellCube unit based on the data obtained by the experimental work and the calculations explained earlier. Third subsection focuses on the outcome of the module/string configuration after simulation runs while the last subsection analyzes the results of the test runs at high power levels.

3.4.2 Operating range of a string

Similar to other battery types, VRFB operating ranges, where a unit is capable of storing and delivering energy are set by various parameters such as voltage limitations, energetic efficiencies, degradation, and economy. These parameters need to be considered for the battery itself as well as for other system components including power converters and safety equipment. While operational voltage limits are difficult to overcome, other parameters including efficiency, economy, and time constraints are more adjustable and allow optimization of the battery operation.

Figure 3.3 shows the operating range of a string for the CellCube FB 10/100 unit as defined by the measurements and calculations. Positive values for power indicate discharging while negative values mean charging. Green zone indicates the operating range of a string in relation to SOC and power. Although the battery is able to operate in the red zones, due to several limitations considering the whole system, such operation is not recommended. Reasons for defining the red zones are described in detail later on.

Various measurements on the battery unit were performed in order to define the operating range of a string. Measurements were realized between the maximum

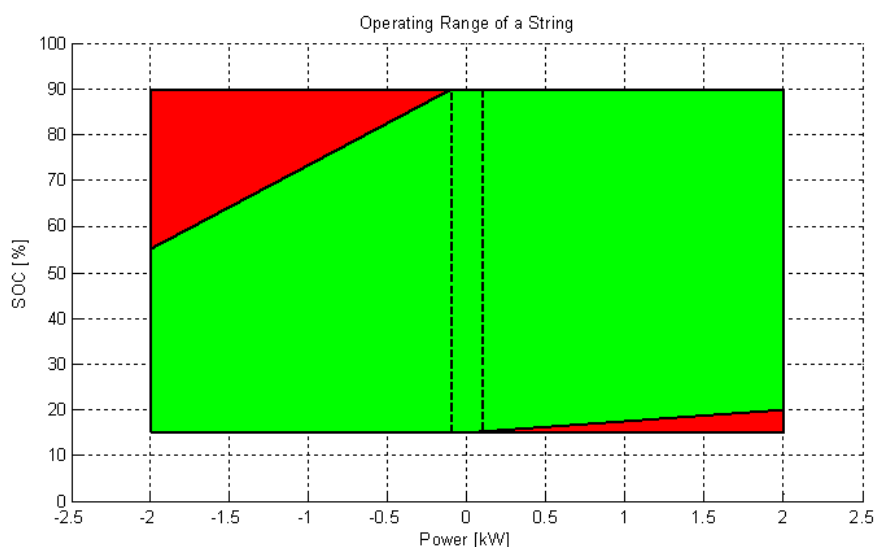


Figure 3.3 Operating range of a string [6].

discharging and charging powers of 2 kW and SOC levels between 15% and 90% for the reasons described below. States of charge above 90% were not taken into consideration and no measurements were performed as the charging power becomes very limited at these high SOC levels and the charging process slows down drastically, making the battery operation unreliable. According to certain analyses, this could be due to the need for avoiding side reactions such as gassing. Furthermore, high SOC levels accelerate the degradation within the battery due to higher corrosion rates caused by vanadium at charged oxidation states in the positive electrolyte. Due to these reasons, string was declared unsuitable for effective and reliable operation at SOC levels above 90%.

At states of charge below 15%, measurements were not possible due to the voltage limitations of the power electronics equipment. When the battery SOC goes below 15%, voltage at the battery terminals drops below the minimum voltage, which is required by the inverter/rectifier unit and a system start is deterred by the protection circuits. Accordingly, SOC levels below 15% were also kept out of the measurement runs.

Charging and discharging power was limited to 2 kW by the rectifier/inverter. At high power levels during charging, the power is limited due to the SOC as explained before, causing the rectifier/inverter unit operating below its nominal power for a majority of the string operating range. Therefore, sizing this component for higher discharging and charging power levels was not considered to be an economically viable option. However, it should be noted that the measurements with the CellCube unit showed that the discharging power for a single string can reach far beyond 2 kW. Nevertheless, in this study the charging and discharging power levels were limited to 2 kW per string, which corresponds to the CellCube

nominal power. After measurements and calculations with the unit, the green and red zones, along with the zone bordered by dashed lines in Figure 3.3 were defined with the following arguments:

- The red zone in the upper left corner was declared unsuitable for operation as the voltage at the terminals of the string was above the safety levels.
- The red zone in the lower right corner was declared unsuitable for operation as the output voltage was too low for other system components such as the inverters.
- Between the dashed lines, battery is capable of operating although it has a lower efficiency compared to the other operating ranges. It is highly probable that this low efficiency results from the pumping power and self discharge rates being high compared to the input (charging) or output (discharging) power in this region. However, it should be noted that this low efficiency region is rarely utilized as CellCube stacks can come online and offline on the fly to improve efficiency.

3.4.3 Efficiency of a string

Voltage efficiency of a string

Voltage efficiency of a string was calculated as explained earlier. Figure 3.4 shows the results obtained from the calculation run.

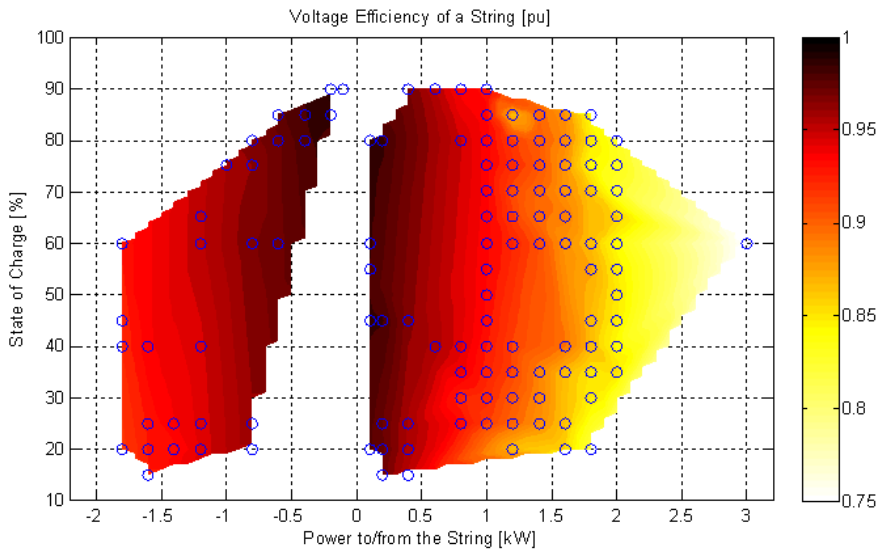


Figure 3.4 Voltage efficiency of a string as a function of SOC and power [6].

In this figure, voltage efficiency of a string is plotted as a function of power and SOC. Negative power values indicate the charging of the battery while

positive values indicate discharging. Efficiency at a certain operating point is visualized with a color, darker colors meaning higher efficiencies. Circles indicate the operating points where the efficiency could be calculated directly from the measurements. As the whole operating range could not be covered with experimental measurements due to time limitations, the remaining efficiency points were calculated by software interpolations.

Measurements and software interpolations provided 1677 data points for the string efficiency and after averaging the results in certain power and SOC intervals, efficiency values were obtained for 114 different power and SOC combinations. The reason for this grouping and averaging was to mitigate the short term fluctuations in the efficiency values, which were caused by time delays in the measurements of the OCV and changes in the electrolyte flow rates.

Furthermore, although the efficiency of a string was aimed to be determined for the whole operating range of a string, which is shown in Figure 3.3, it could only be calculated for some parts of the "green zone" due to time limitations and measurement errors. However, as it is crucial to cover the whole operating range of a string for a realistic megawatt scale VRFB software model, missing efficiency values in the remaining parts of the operating range were calculated by software extrapolation. In order to achieve an accurate extrapolation procedure, some efficiency values at the boundaries of the operating range were altered. Although this altering process was performed by preserving the tendency of the calculated values shown in Figure 3.4, it still introduces a small deviation from the real life measurement values. Nevertheless, this extrapolation process is essential for the modeling work and it can not be avoided. Besides, as the core of the efficiency calculations still relies on real measurement data, this extrapolation procedure is not expected to affect the final results coming out of the megawatt scale software model drastically. Figure 3.5 shows the voltage efficiency of a string for the entire operating range after the extrapolation procedure.

It can be clearly seen from the figure that the efficiency of a string has a much stronger dependency on the power rather than the SOC. As the SOC solely depends on the oxidation states of vanadium in the positive and negative electrolyte in a VRFB, this outcome meets the expectations based on theory. However, it can still be seen that the SOC has an influence on the efficiency at power levels above 1 kW during discharging. Although the string efficiency drops significantly as the power increases both during charging and discharging, this effect is more visible during discharging as the efficiency is reduced to values as low as 83%. Lower efficiencies at high power levels can be explained by high overvoltage losses as explained earlier. Equation 3.10 showed clearly that the overvoltage losses would increase with increasing string power both at charging and discharging as long as the efficiency is below 100%, which is always the case in real life.

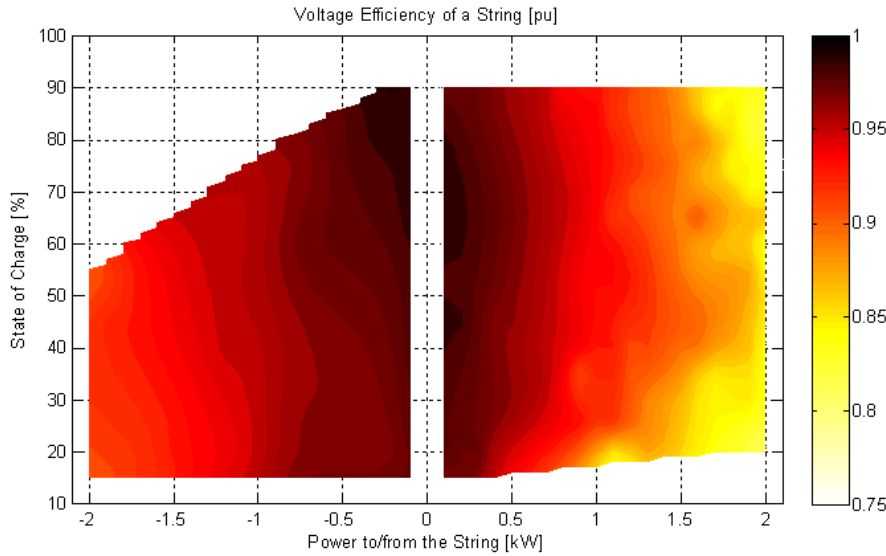


Figure 3.5 Voltage efficiency of a string as a function of SOC and power (with corrections and extrapolation to cover the entire operating range) [6].

It is challenging to explain the wavy form in the efficiency curve, which results from the influence of SOC. This effect can be seen especially in the discharging region where the power lies between 1 kW and 2 kW. Efficiency curve in this region is far from being uniform. Similar changes in efficiency can be observed in the low power region of the charging process. Although the SOC is not expected to have a direct effect on the efficiency according to theory, measurements with a real unit proved otherwise. As the dependency on SOC does not follow a certain trend, it is not possible to come up with a mathematical function, which reflects the SOC-efficiency relation. As it can be seen on the graph, efficiency becomes higher between the SOC of 40% and 55%, decreasing until about 60% and having another peak between 60% and 70%. This behavior can more likely be explained by the dynamics of the system during the measurements rather than a direct influence by the SOC. In other words, instead of covering the whole operating range of the battery continuously, if there were long enough pauses between the measurements of each power level and SOC, this efficiency trend would likely look different, without influenced strongly by changes in the SOC. Furthermore, the changes in efficiency with different SOC is not that strong compared to changes in different power levels.

Pumping power demand

Pumping power demand was attempted to be measured for the whole operating range of the battery. Figure 3.6 shows the results obtained from the experiments. It should be noted that the pumping power measurements were carried for the

entire battery instead of just one string as in the string efficiency measurements. Therefore, the power values range from -10 kW to 15 kW where the negative values indicate charging and the positive values discharging as before. Similar to the string efficiency plot without corrections and extrapolation, circled data points show the results obtained through measurements while data points in between these circles were acquired with interpolations.

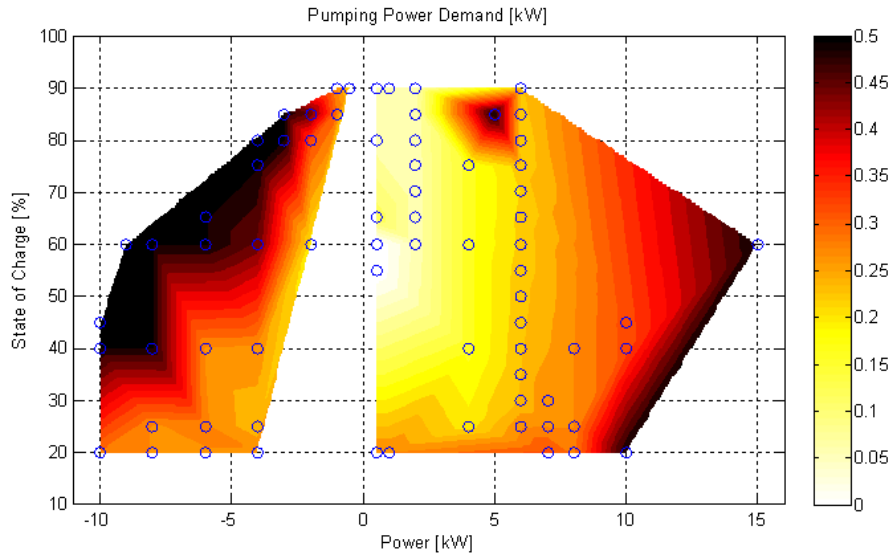


Figure 3.6 Pumping power demand of the battery as a function of SOC and power [6].

Figure 3.7 shows the pumping power demand of the entire battery after the extrapolation and correction procedure was applied.

As the pumping power demand of a single string was required for the final string efficiency calculations, results for the entire battery were normalized for one string with the Equation 3.9 as explained in before. The final outcome is shown in Figure 3.8.

It can be seen in Figure 3.8 that the pumping power on average during charging is higher than during discharging and is varied by the control system in a response to changes in SOC and power. On the contrary, direct influence of SOC on pumping power can hardly be seen during discharging and the variations depend mainly on the discharging power. This can be explained by the utilization of two different pumping strategies for charging and discharging.

As explained earlier, pumping is necessary in order to provide the electrolyte flow through the cell stacks during battery operation. Electrochemistry of a VRFB section explained that during charging, V^{3+} species in the electrolyte are reduced into V^{2+} while V^{4+} species are oxidized into V^{5+} . In order to sustain these redox reactions, the necessary amount of V^{3+} and V^{4+} species must be constantly supplied to the cell stack where the reactions take place. This is essentially

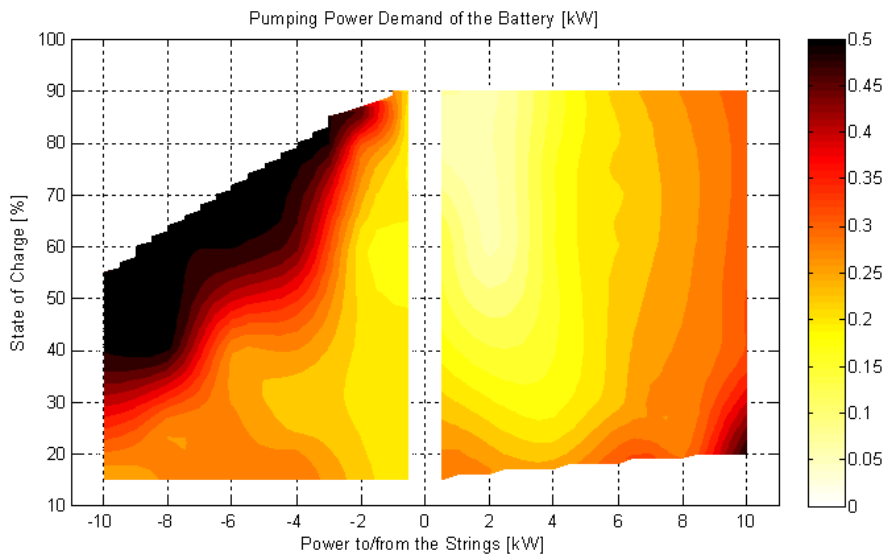


Figure 3.7 Pumping power demand of the battery as a function of SOC and power (with corrections and extrapolation to cover the entire operating range) [6].

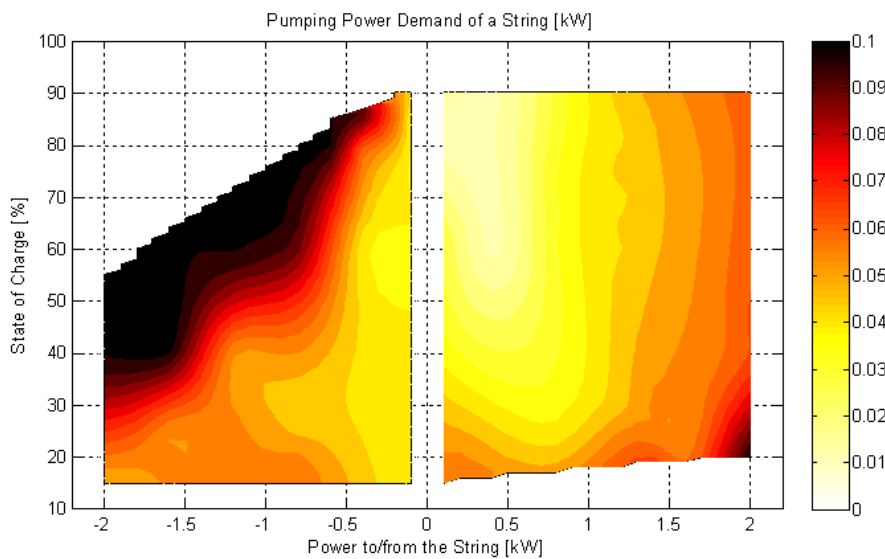


Figure 3.8 Pumping power demand for one string as a function of SOC and power [6].

provided by pumping the electrolyte, which includes these V^{3+} and V^{4+} species in the negative electrolyte tank and the positive electrolyte tank respectively. Electrolyte flow rate is adjusted by altering the pumping power depending on the amount of species needed by the reactions at the stacks. According to the theory, this flow rate would be dictated by the charging power. However, the experiments with the CellCube unit showed that in practice this procedure might not be that

straightforward.

Based on the experimental results and analyses, it can be stated that with increasing SOC of the battery, depletion of active vanadium species could occur in the stack during charging. This effect would be more apparent at high charging power. However, as long as a charging current is provided to the battery, the active vanadium species are strictly needed for the charging reactions to continue. In the case of active species depletion, the applied charging current starts electrolyzing the water in the aqueous solution of sulfuric acid, which then leads to the build up of hydrogen gas (H_2) and oxygen gas (O_2) at the negative and the positive electrode sides respectively. Both these gases and especially oxygen is highly aggressive toward the battery stack and might cause irreversible damage. Therefore, the pumping power is increased to avoid this depletion of species situation and continue with the normal charging operation at the cost of consuming more power for pumping. This situation is more apparent at high SOCs of the battery as the V^{2+} and V^{5+} concentrations in the negative and positive electrolyte tanks are much higher compared to low SOCs. Hence, a higher average pumping power can be observed with increasing SOC level during charging, which is reflected by the horizontal gradients in the graph in Figure 3.8. Similarly, more pumping power is necessary for higher charging powers as the conversion of species take place at higher rates, which also require higher flow rates for supplying new V^{3+} and V^{4+} species from the tanks. As it can be seen in the graph, highest pumping power during charging occur at SOCs above 40% and powers above 500 W for a single string.

Pumping power also increases with increasing power during discharging. This is clearly visible in the figure by the vertical gradients in the discharging region. However, unlike in the charging process, horizontal gradients, which represent the change in pumping power by changing SOC cannot be observed except at low SOC levels, namely below 30%. This is due to the fact that deep discharging is not causing irreversible damages in the battery. If the concentration of V^{2+} and V^{5+} species decrease drastically by being converted into V^{3+} and V^{4+} , the discharging will still continue by further redox reactions of V^{3+} and V^{4+} species being converted into V^{2+} and V^{5+} . Although this deep discharging situation is unwanted, it does not constitute a critical condition like in the case of gassing as the redox reactions of vanadium species are totally reversible. In the experiments, an increase in the pumping power for providing the load with the necessary current was only necessary when the SOC went below 30% and the V^{2+} and V^{5+} concentrations in the electrolyte were reduced significantly.

Final string and system efficiency

Final string efficiency was calculated by considering the voltage efficiency, pumping power demand, and coulombic losses. Voltage efficiency and pumping power

demand calculations were based on measurements with the CellCube unit while coulombic losses were taken constant (60 kW) due to the reasons explained earlier. Figure 3.9 shows the final outcome of the string efficiency calculations. Final string efficiency of a CellCube string is plotted as a function of power and SOC.

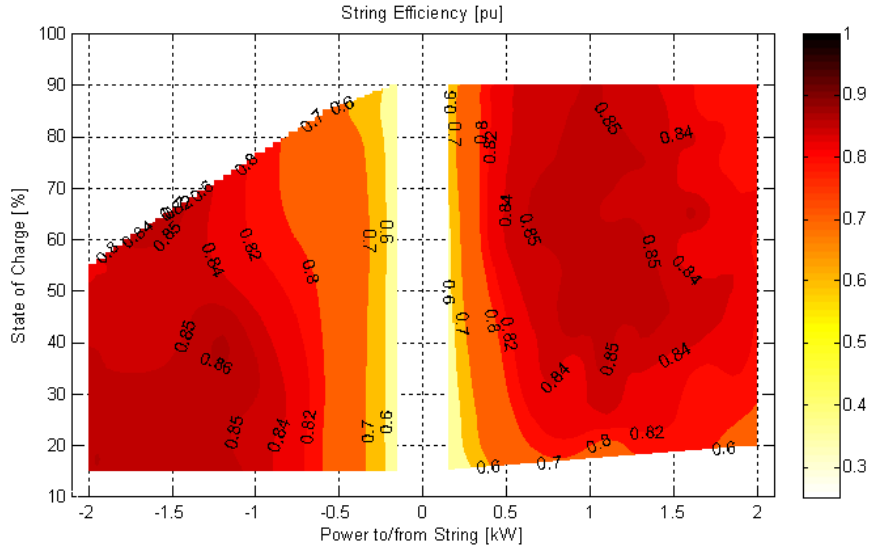


Figure 3.9 String efficiency as a function of SOC and power [6].

It can be seen from the plot that the string efficiency goes as low as 60% and as high as 86% both during discharging and charging. Lowest efficiencies are recorded at very low power levels where the power is less than 500 W. This is due to the fact that the losses that result from the pumping demand has a big impact on the overall efficiency in this region. As the ratio between the string power and the pumping power, which is necessary to sustain charging and discharging becomes smaller, pumping losses start playing a more significant role. As the charging or discharging power increases, pumping power increases at a comparatively slower rate, making them less significant in the overall picture.

Effect of SOC on the final string efficiency is negligible within the operating range as it can be seen in the plot. Nevertheless, slightly lower efficiencies are observed at higher SOC during charging. This mainly results from the higher pumping power demand at high SOC during charging, which was discussed earlier. The main conclusion here is that, operating a string at less than 25% of its rated power should be avoided in order not to experience low efficiencies.

It can also be seen that at the discharging region, the highest efficiencies (96%) are achieved at the 1 kW power mark rather than at the rated string power. This is a direct effect of the combination of low voltage efficiency and high pumping power in the nominal power region of the operating range. A similar effect is not observed during charging region since the voltage efficiency tends to be higher.

This higher voltage efficiency mitigates the extra exergetic losses, which result from high pumping power demand at this region. It should be mentioned that the additional losses resulting from higher pumping power at high charging powers are not as big as the losses resulting from low voltage efficiencies at high discharging powers. Therefore, it can be concluded that the major influence on the final string efficiency results from the voltage efficiency of a string. Pumping power demand on the other hand has a very small if not negligible effect on the overall picture.

3.4.4 Choosing the number of modules

The first task with the megawatt scale VRFB modeling tool was to determine the number of modules for an optimal operation with the highest system efficiency.

One string of the CellCube has a nominal power of 2 kW and the number of total strings would eventually decide the nominal power of the whole battery. However, the distribution of the strings by the number of modules results in different efficiency values within the operating range of the battery. Various battery operation scenarios were simulated in order to find the optimal conditions for battery operation as long as the number of modules and strings were concerned and the benefits and drawbacks of having more or fewer modules were evaluated.

Due to the reasons explained in the efficiency evaluation sections, it is certain that the larger number of modules allows a better efficiency adjustment. Furthermore, having more modules improves the reliability of the battery due to the fact that only a smaller part of the battery is affected in case of a failure of a single module. On the contrary, having less hydraulic circuits makes the battery simpler and cheaper as there are fewer hydraulic system components such as pipes, valves, and pumps. Although utilizing additional modules lead to higher efficiencies, the efficiency improvement rate declines as the total number of modules increases. In other words, bigger the number of already existing modules, more negligible is the efficiency improvement, which can be achieved by adding another module. Hence, a good design criterion for defining the number of modules should aim to achieve a high efficiency and reliability with as few modules as possible.

As the battery efficiency was not constant for the entire operating range of the VRFB unit, an *average efficiency* was defined in order to compare different configurations. Average efficiency was defined and calculated as the weighed average of several efficiencies in an area, which is located within the operating range, so called "the green zone". Each single area was defined as a short interval where the SOC and power are quasi continuous. According to the measurements and calculations, the average efficiency does not get affected by the power capacity of the battery as long as the number of modules stay constant and only the number of strings per module is altered. This can be seen in Table 3.2 where batteries with nominal powers of 1 MW, 2 MW, and 4 MW are compared. Results show

that in order to increase the battery power, only the number of strings per module is increased and the overall efficiency of the battery follows the string efficiency.

Table 3.2 Effect of battery power on efficiency.

Battery nominal power (kW)	1000	2000	4000
Number of modules	20	20	20
Strings per module	25	50	100
Number of total strings	500	1000	2000
Power per module (kW)	50	100	200
Average charging efficiency	0.84	0.84	0.84
Average discharging efficiency	0.82	0.82	0.82

Table 3.3 shows the average charging and discharging efficiencies at different configurations of modules and strings for a 1 MW unit. It can be seen that the efficiency increases with increasing number of modules. However, in accordance with the statement in the previous paragraph, the efficiency increase by switching from 10 modules to 20 modules is less than the increase by switching from 5 to 10. Furthermore, the efficiency increases that are achieved by doubling the number of modules are around 1% and would not have a drastic effect on the evaluations with wind power integration model. Therefore, the number of modules for a VRFB unit was selected as 10 for this study and further calculations throughout the study were carried with a 10 module configuration.

Table 3.3 Effect of module/string configuration on efficiency.

Number of modules	5	10	20
Strings per module	100	50	25
Number of total strings	500	500	500
Power per module (kW)	200	100	50
Battery power (kW)	1000	1000	1000
Average charging efficiency	0.824	0.835	0.841
Average discharging efficiency	0.821	0.821	0.818

Figure 3.10 shows the number of modules brought online by the control system depending on the SOC and the power for a 1 MW battery model. As it can be seen, number of modules during discharging is solely dictated by the requested power with the SOC having no significant effect on it. On the other hand, during charging, the configuration is affected by the SOC as it gets above 55%. This is a direct effect of the change in the pumping power demand and a reference to Figure 3.8 could help recognizing the correlation. Since the pumping has to be increased due to the effects explained in the section regarding the pumping power demand,

new modules have to be brought online to cope up with the power. The losses resulting from additional pumping power demand could then be compensated by bringing these additional modules online. As it can be seen in the figure, 10 online modules are only necessary when the power exceeds 900 kW during discharging regardless of the SOC, while the same number of online modules is already required at power levels as low as 400 kW if the SOC approaches 80%.

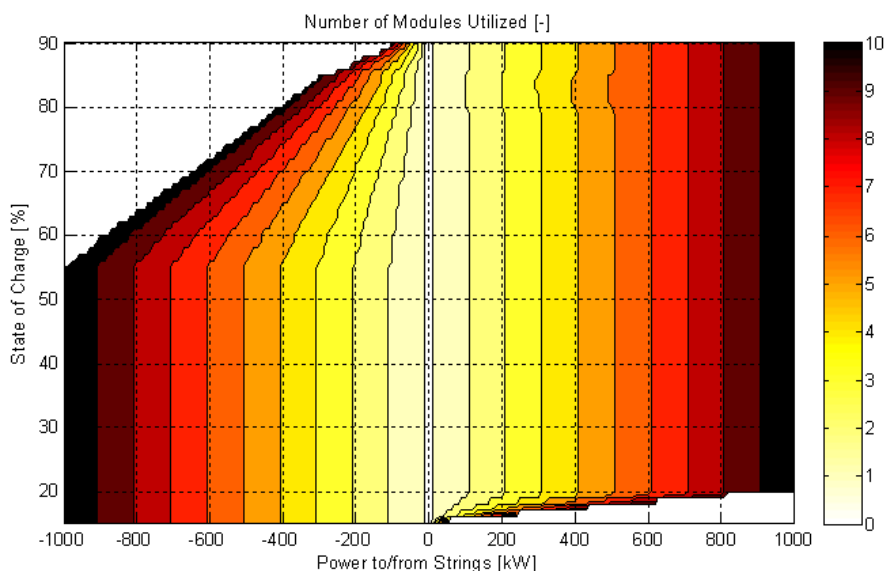


Figure 3.10 Number of utilized modules as a function of SOC and power [6].

3.4.5 Test runs with the model

In order to test the software model, various test runs, which include several charging and discharging cycles were simulated. Figure 3.11 shows the outcome of a sample cycle with a simulated battery, which has a nominal power of 2.5 MW and an energy capacity of 20 MWh.

Both the charging and discharging power were set as 2 MW for the test cycle. First, a 15-hour charging at 2 MW was requested by the power reference, which is represented by the red dashed line. The control system reacts to this *power reference* and charges the battery as long as it is technically possible. It can be seen that the charging power starts decreasing once the SOC increases as discussed in the previous sections and eventually the charging stops as the battery SOC reaches 90%, the maximum allowed by the operating range. Immediately afterwards, the battery starts discharging with a power of 2 MW as requested by the power reference input until it reaches 15% SOC, the operating range minimum. It can be seen that the charging process takes longer than the discharging due to the higher limitations on charging power.

Green line represents the actual power reaching the electrolyte tanks after losses during charging and the net power going out of the tanks during discharging. Accordingly, the yellow areas between the black and green lines represent the losses in the system. Explicit steps than can be seen on both black and green lines are a result of the low resolution of the input values for efficiency and operating range. In a real battery, these curves could be expected to be smoother.

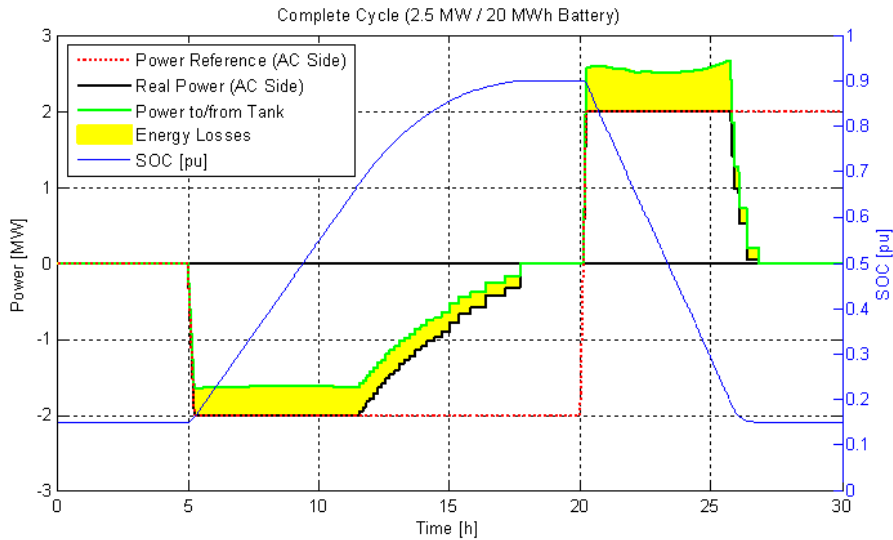


Figure 3.11 Full cycle simulation of a 2.5 MW/20 MWh VRFB [6].

Further test runs with the model were realized at different power and SOC levels in order to evaluate the overall system efficiency for these different operation parameters. The system was tested for power levels in the range of 1 MW and 12 MW with 1 MW intervals and for SOC levels between 15% and 90% (the whole operating range) with 5% intervals. A maximum power of 10 MW was selected, as this value represents the maximum power capacity, which could be expected for the wind power integration operation, which is discussed in the next chapter. As no drastic effects were observed at different power levels, overall system efficiency at megawatt scale was displayed in Figure 3.12 as a function of the SOC using the results at 5-6 MW power level. However, it should be noted that the whole efficiency table (with all the power levels) as acquired by the simulation runs was used to provide the efficiency input data when utilizing the battery for wind power integration that is discussed in the next chapter.

It can be seen that both charging and discharging efficiency curves have two peaks although they occur at different SOC intervals. Charging efficiency is at its maximum value (82.6%) when the battery SOC is at the lowest value within the operating range. The second peak is then at the 60-65% SOC level with a value of 82%. The decreasing efficiency trend after this second peak is explained by the

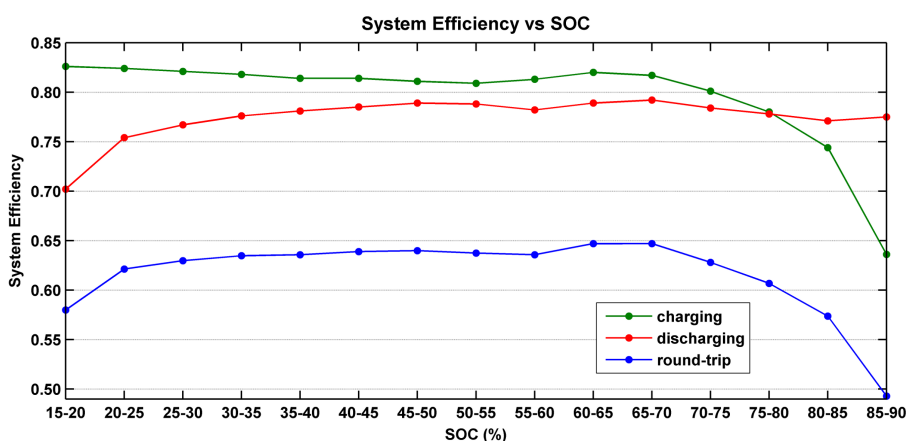


Figure 3.12 Overall system efficiency as a function of SOC at megawatt scale.

highly increasing pumping power demand with the efficiency eventually reaching a minimum of 63.6% at the 90% SOC.

Discharging efficiency has a more stable stance when compared to the charging efficiency. The efficiency is almost constant throughout the operating range with the exception of low efficiencies (lowest 70.2%) when the SOC is approaching its minimum. These low efficiencies as at low SOC's are as expected due to the reasons discussed in the previous sections. Although the discharging efficiency also peaks twice, the efficiency increases at these maximums are not significant and have no big impact on the overall system operation.

As long as the round-trip efficiency is concerned, it can be concluded that the overall system efficiency is likely to remain constant for most of the operating range, exceptions being the battery SOC approaching its minimum and maximum values. The main reason for lower efficiencies at these operating regions is the high pumping power demand with the string efficiency characteristics having a secondary effect.

3.5 Summary

Main goal of the battery characterization and modeling work was to obtain the operating range and efficiency of a real life VRFB unit. This information is essential for the construction of a software model of a megawatt class VRFB.

The data used in the calculations were recorded by measurements with a CellCube FB 10/100 VRFB unit manufactured by Gildemeister. Battery unit is made up of modules, which include several strings. Operating range of a battery string was determined by a series of cycling tests. Recorded data were evaluated and the optimal operating range was defined. Efficiency calculations involved the evaluation of three parameters: overvoltage losses, power demand of the pumps,

and coulombic losses. Latter of the three was assumed to be constant (60 W per string) while the former two were calculated based on measurements. Auxiliary power consumption of complementary systems such as the thermal management units and control systems were not taken into account in the efficiency calculations as they would not reflect the possible auxiliary consumption of a megawatt scale unit.

The data obtained throughout this experimental battery characterization work were then used in the building of the megawatt scale VRFB model. The megawatt scale model was developed in Matlab™ Simulink® environment and with the aim of evaluating the possible operation characteristics of a hypothetical unit. Model was used to define the efficiency characteristics of the whole VRFB system when used in grid connected high power applications.

Acquired efficiency characteristics and data provide a basis for utilizing a hypothetical VRFB unit for easier power grid and market integration of wind power at a single wind farm level, which is discussed in the next chapter. Efficiency of the VRFB at each operating point determined by the power and SOC is calculated by the model and an efficiency matrix is generated within the battery operating range determined through the experimental work. As the wind power integration operation with a dedicated VRFB unit requires the battery to operate at a different power and SOC frequently, the efficiency matrices generated by the model is then used as input for the overall efficiency calculations during discharging and charging of the dedicated battery used in a single wind farm setup.

Chapter 4

Wind-VRFB Model

4.1 Introduction

In this second part of this study, facilitating power grid and electricity market integration of wind power at a single wind farm level by utilizing a hypothetical VRFB has been evaluated. Real wind power output data from a 10 MW wind farm and wind power forecasting data obtained by state-of-the-art forecasting methods were used in the calculations. VRFB system was simulated using the developed software model, which was described in the previous chapter. Efficiency of the battery at each operating point as requested for smooth wind power integration was calculated by the VRFB software model. Calculations were based on a scenario, in which a single wind farm participates with its power output in an electricity market bidding structure, similar to a conventional power plant. The aim was to evaluate the economic benefits of utilizing a VRFB unit in a market mechanism where inaccurate bids resulting from forecast errors are financially penalized. Figure 4.1 shows the objectives diagram with the above explained inputs, used for the dedicated VRFB model for utilization with the wind farm, highlighted in red.

4.2 Input data and parameters

4.2.1 Wind power data

In this study, real life wind power data was used for the calculations. Considering the scale of the vanadium redox flow battery model (VRFB), which is discussed in the previous chapter and existing real life wind-storage installations, a wind power plant with an installed power in the range of 10-20 MW was approached. After considering several wind farms and consulting operators for obtaining recorded

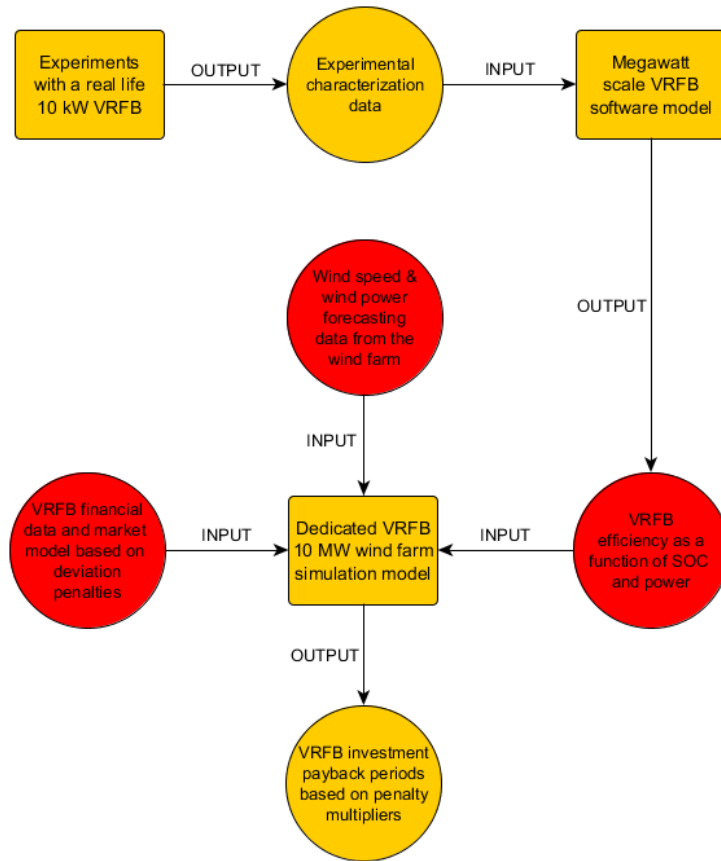


Figure 4.1 Objectives diagram with highlighted Wind-VRFB model inputs.

data in northwest Germany, a 10 MW wind farm (5 turbines with 2 MW rated power each) was selected for the study. Layout of the turbines in the wind farm is shown in Figure 4.2 although the exact wind farm location and detailed turbine information cannot be disclosed due to confidentiality reasons. Turbines shown in the layout are numbered from 1 to 5.

Power measurements from the wind farm were available for the whole year of 2009 with 10 minute intervals. However, there were some missing data points in the data set due to measurement errors or equipment malfunctions. These missing data points were mitigated by generating synthetic power output data based on averages from the closest good measurements available, making 52560 power output data points available for the calculations. Following lines provide more information on the wind data with graphical representations of the important wind farm parameters.

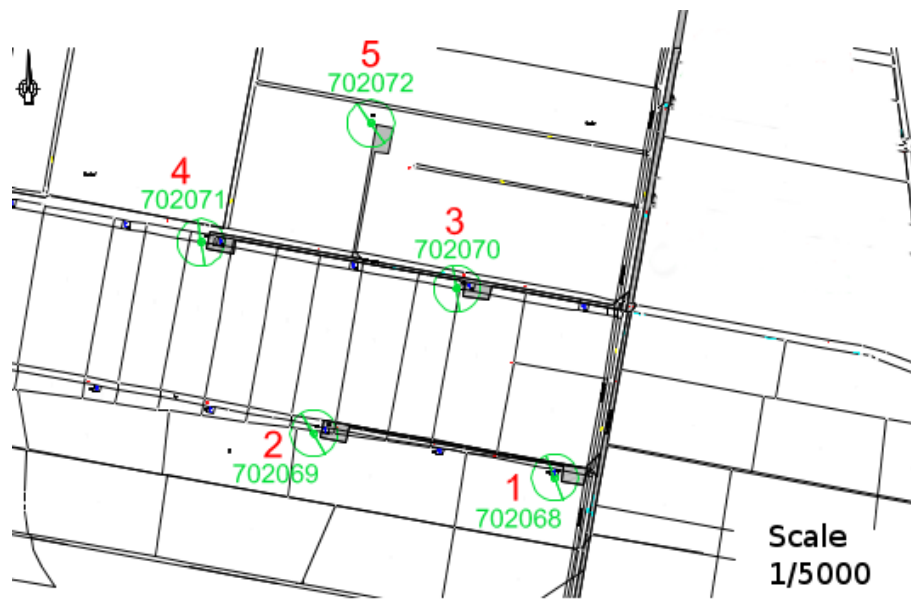


Figure 4.2 Wind farm layout.

Installed power

The wind farm has an installed power of 10 MW with 5 wind energy converters of 2 MW each.

Power output

Power output of the wind farm varies strongly due to the variable nature of the wind as expected. Figure 4.3 shows the power output from the wind farm for each quarter of the year 2009. It can be seen from the graphs that the variability is present throughout the year and does not necessarily follow a certain pattern with the output varying continuously between 0 and 10 MW.

Figure 4.4 shows the wind power output histogram for the whole year where the frequency of the output levels can be seen.

Figure 4.5 shows the daily power output pattern of the wind farm for the year 2009. The power output values for each hour of the day were obtained by calculating the average power output values for the relevant hourly interval throughout the year.

Energy output

Total energy generated by the wind farm in 2009 accounts for 28,521 MWh. Figure 4.6 shows the monthly distribution of the energy generation. It can be seen that

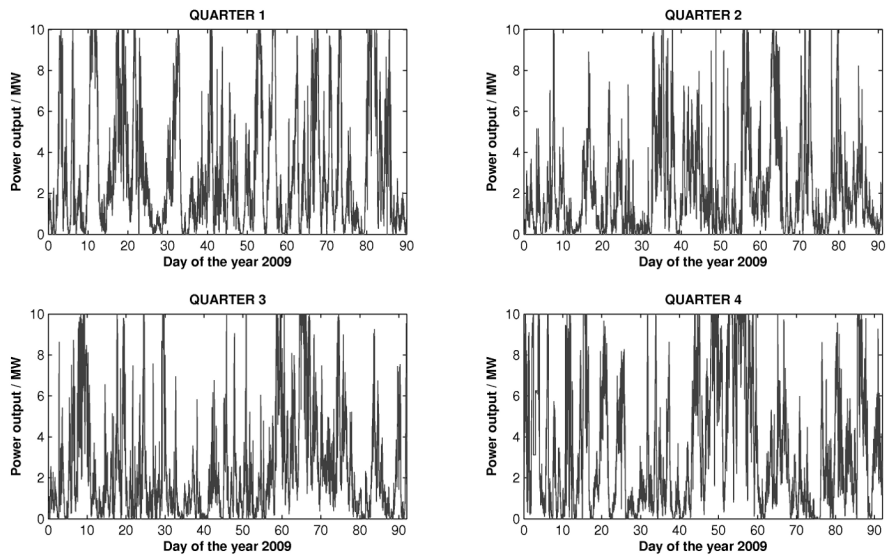


Figure 4.3 Quarterly wind power output patterns for 2009 [7].

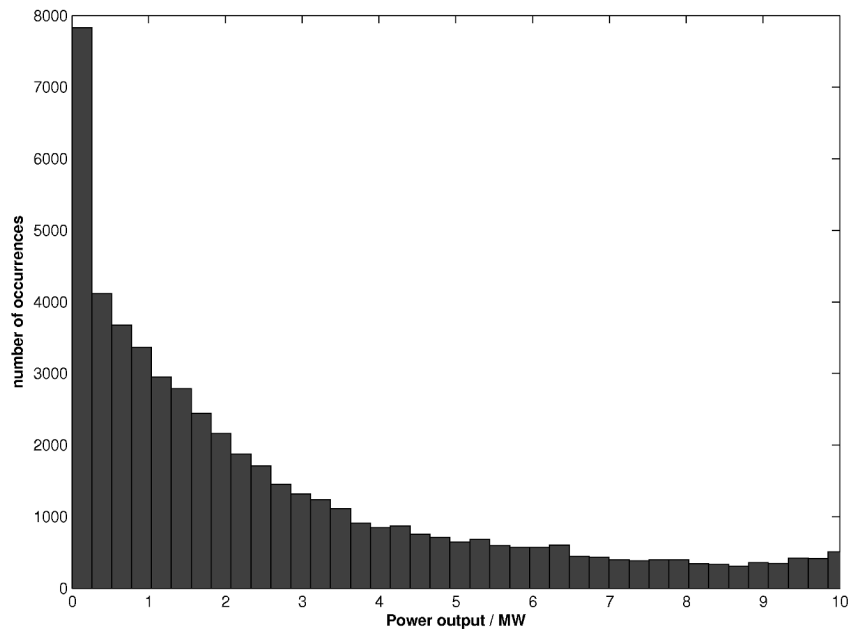


Figure 4.4 Power output histogram for 2009 [7].

the most energy was generated in quarters 1 and 4 with the summer months being the low generation periods due to weaker winds.

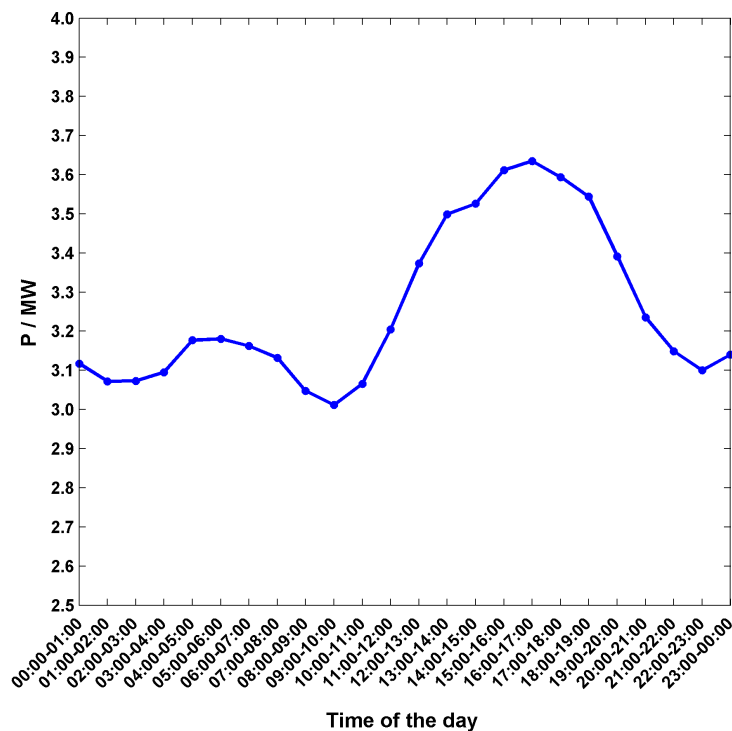


Figure 4.5 Hourly power output averages for 2009.

Capacity factor

The total energy generation of 28,521 MWh means a wind farm capacity factor of 27.13% for the year 2009. This number lies within the typical capacity factor values for the onshore wind farms in northern Germany.

It is clear that the data set used for the simulations represents only a single year of operation and these patterns and figures can vary from year to year. Nevertheless, historical data indicate that wind patterns follow similar long-term (monthly/seasonal) and short-term (daily/weekly) behaviors in the geographical region where the wind farm is located. Therefore, although differences in power patterns and capacity factor are expected every year, these would not be drastic changes, which would strongly alter the analysis results when evaluating the wind power integration utilizing a VRFB.

4.2.2 VRFB data

Technical data

The VRFB characterization and megawatt scale modeling results from Chapter 3 constitutes the base for the inputs into the model, which is used for evaluating the

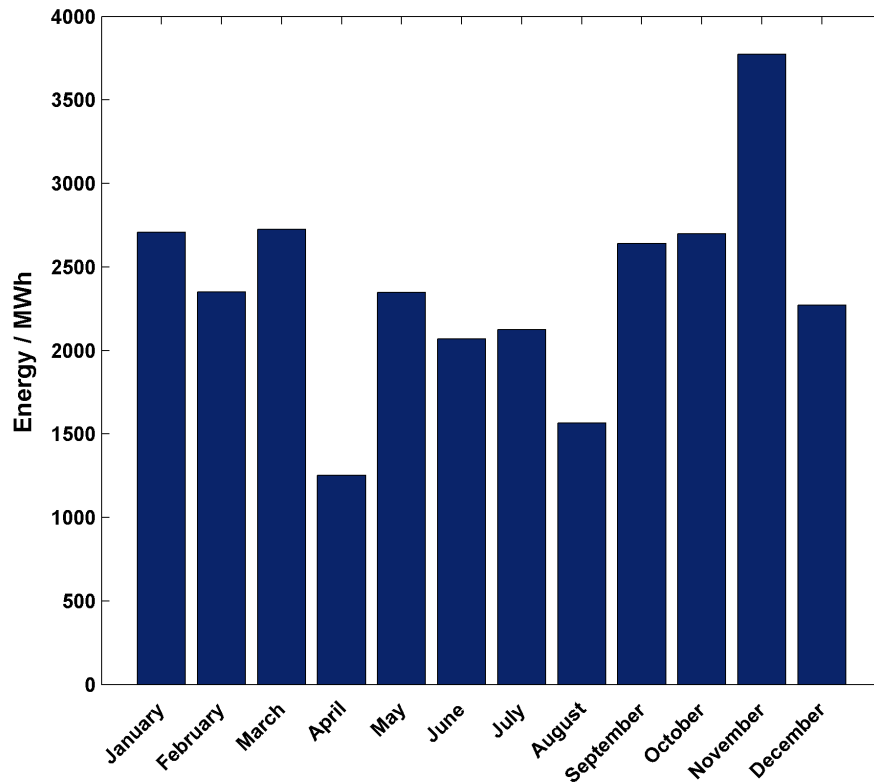


Figure 4.6 Monthly wind energy generation for 2009.

power grid and market integration of wind power by utilizing a VRFB at single wind farm level. Operating range and the efficiency input values are obtained from the matrices, which were generated by the megawatt scale VRFB software model.

Generated matrices consist of battery efficiency values for every single operation point of the VRFB unit within its operating range. Therefore, each SOC and power value at both discharging and charging operations relate to a specific efficiency value as calculated by the battery model explained in the previous chapter. As the requested power for discharging or charging of the battery is set according to the wind power output, the battery model calculates the efficiency for this power value and state of charge of the battery at that interval. In addition, the efficiency values of the auxiliary components such as the inverters and rectifiers determine the final power values. This technical functioning of the battery is then combined with the economics in order to determine the battery operating strategies which are described in the upcoming sections.

Financial data

Financial data concerning the megawatt scale VRFB unit is difficult to estimate. This is due to the fact that not many real life systems are existent worldwide and accordingly the lack of a wide scale business model or an established VRFB market. Therefore, the estimated costs for the calculations in this study are based on the current kilowatt scale battery market prices and own estimations, which were based on consultations and evaluations of financial projections regarding the VRFB technology. These projections rely on several aspects of the technology, which include prices of materials that are used to build up VRFB units, cost of construction, and cost of auxiliary systems required for battery operation.

Financial evaluations that are discussed in the report titled "Vanadium Redox Flow Batteries - An In-depth Analysis", which was published by Electric Power Research Institute (EPRI) were used as a basis in building own estimations on VRFB finances. However, as the EPRI report dates back to 2007 and that no further comprehensive analysis was done on VRFB finances since then, evaluations and considerations, which were done by the colleagues at NEXT ENERGY Energy Storage Department helped improving the financial evaluations on VRFB and enabling more accurate estimations on present time VRFB prices.

Capital cost

As power and energy capacities of a VRFB are independent from each other, overall capital cost of a system also scales with the power and energy capacities. However, there is also a third cost component, which does not scale with the size of the system. Examples that contribute to this third cost component could include transport costs, earthwork costs before the construction work and insurance costs. The first two capital cost components depend directly on the costs of the individual system components. Therefore, the commodity prices play a big role in calculating the manufacturing costs of a VRB system.

Another important issue on capital cost calculations of VRFB systems is the cost gaps, which were discussed in detail in the above mentioned EPRI report. Cost gaps result from confidentiality and secrecy followed by manufacturers and vendors, as well as from future commodity costs, which are most of the time difficult to estimate.

Figure 4.7 shows the capital cost breakdown for VRFB systems according to the EPRI study. It can be seen that the major contributions to the overall capital cost are by the vanadium electrolyte at 35% and the cell stacks at 26%. Accordingly, it can be concluded that the energy side of the system contributes with a higher weight to the overall capital cost in comparison to the power side. The remaining 40% in the breakdown can be considered as the costs that do not scale or scale to a lesser extent with either power or energy size of a system.

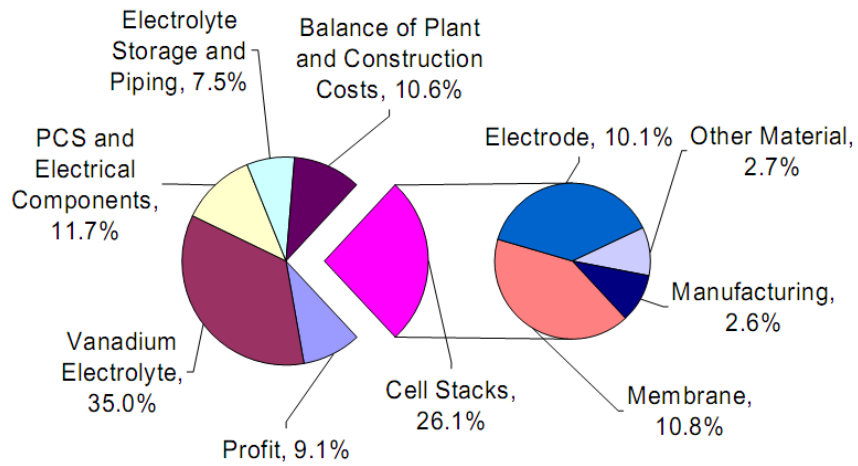


Figure 4.7 Capital cost breakdown for a 1 MW, 8 MWh unit [8].

Furthermore, Figures 4.8 and 4.9 show the electrolyte and cell stack cost breakdowns for a VRFB unit respectively. It can be clearly seen that the electrolyte cost is dominated by the price of vanadium pentoxide while the membrane is responsible for almost half of the cell stack costs. Therefore, market price of vanadium pentoxide along with the prices of current and future membrane materials would have a significant impact on VRFB system costs.

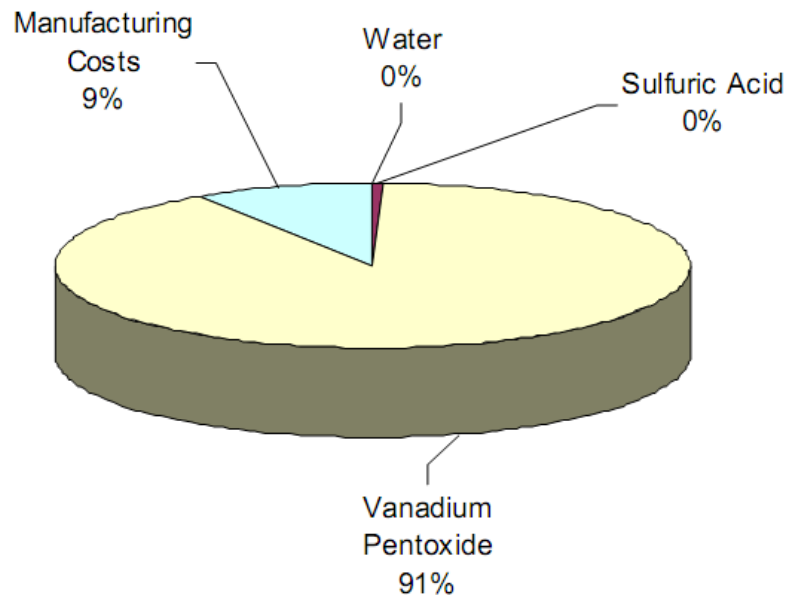


Figure 4.8 Cost breakdown for vanadium based electrolyte [8].

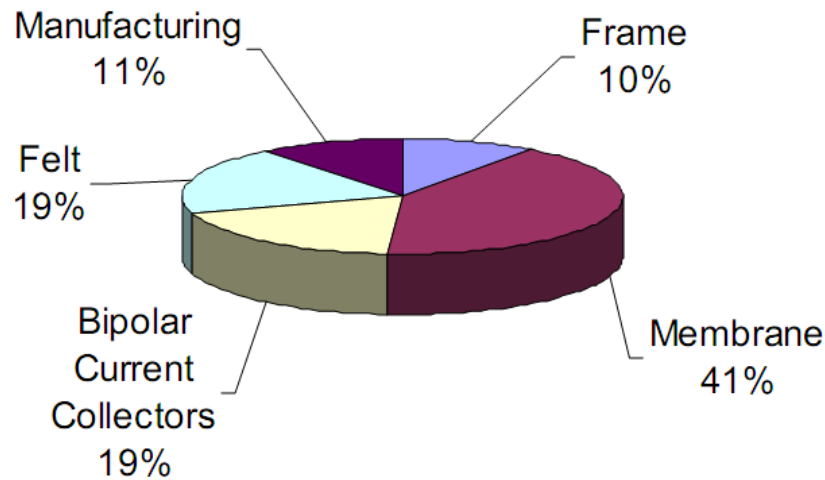


Figure 4.9 Cost breakdown for vanadium redox battery cell stack [8].

In the EPRI report, capital cost of a VRFB system was described by the following equation:

$$\text{Capital Cost} = x \times (\text{cost/kW}) + y \times (\text{cost/kWh}) + z \quad (4.1)$$

where x corresponds to the costs scaling with power capacity, y with the energy capacity of a system, whereas z represents the costs that do not scale with size. As explained earlier, costs that scale with power capacity include those for the cell stack, the power conditioning and pumping systems while the costs that scale with the energy capacity include those for the electrolyte storage tanks and the electrolyte itself. Costs that do not scale with either power or energy capacity include construction management, transport, earthwork and insurance.

Based on the Equation 4.1, EPRI report makes present day (2007) and future (2013) capital cost estimations for a 1 MW / 8 MWh VRFB system. For the 2007 estimations, commodity prices, service costs and other financial parameters for the year 2007 are used while the 2013 capital cost estimation was based on projections for commodity prices and future costs for components. Estimations go as follows:

Estimation for 2007

$$\text{Capital Cost} = \text{USD}2,300 \times (\text{kW rating}) + \text{USD}300 \times (\text{kWh rating}) + \text{USD}250,000$$

Estimation for 2013

$$\text{Capital Cost} = \text{USD}1,250 \times (\text{kW rating}) + \text{USD}210 \times (\text{kWh rating}) + \text{USD}280,000$$

For the capital cost calculations in this study, above described EPRI estimations could not have been used as they are, due to the following reasons:

1. The EPRI report titled "Vanadium Redox Flow Batteries - An In-Depth Analysis" dates back to year 2007 and since then there have been significant changes in the global economy (not to mention a global financial crisis and recession), which had direct strong impacts on commodity prices, construction and energy sectors that are directly related to developing and building a VRFB system.
2. Power and energy cost components are for a 1 MW / 8 MWh system and they might not scale for effective capital cost estimations for larger systems that are modeled in this study.
3. Fixed cost component definitely do not scale for larger systems and has to be calculated from scratch for each system size.

Accordingly, using a similar approach as in the EPRI report, own estimations on power and energy cost components were made. For these new estimations, up-to-date commodity prices, recent developments in the flow battery market, projections on the future costs for components and several other financial indicators were used.

As several system energy component sizes ranging from 10 to 200 MWh and high power levels ranging up to 6 MW were modeled in this study made an accurate estimation of the fixed cost component very difficult. Therefore, a different approach from the EPRI study was taken and the fixed cost component was eliminated from the cost estimation calculations. Costs that contribute to the fixed cost component were instead reflected on the power and energy cost components. Finally, the VRFB capital cost calculations in this study were done according to the following equation:

$$\text{Capital Cost} = \text{EUR}1,500,000 \times (\text{MW rating}) + \text{EUR}300,000 \times (\text{MWh rating})$$

Running costs

It is even more difficult to estimate the running costs of a VRFB systems due to the fact that there have not been plenty of long-term running systems around until now. Accordingly, the running costs or the O&M costs are yet unclear for present and future VRFB systems.

O&M requirements of a VRFB system can be split into 3 categories. These would be the O&M requirements at the stack side, at the electrolyte side, and at the auxiliary components. In principle, maintenance or replacement requirements of each individual component at any part of the battery system contribute to

the overall O&M costs. Therefore, it is necessary to have a look at the main components of the system in order to come up with reasonable estimations of overall O&M costs.

It is safe to say that the electrolyte side of the system is mainly maintenance free due to the reversible character of the vanadium based electrolyte, performance of which does not degrade much during years or thousands of cycles of operation. Electrolyte tanks, which are manufactured using of state of the art materials are also maintenance free for many years of operation. Finally, the building containing these tanks can be considered to require low maintenance throughout the lifetime of the battery system.

As for the auxiliary components, pumps, piping, and valves, which make up the hydraulic systems require the most maintenance while power electronics and air conditioning systems can run maintenance free for as much as the lifetime of the battery or require very small maintenance. In VRFB systems, pumps are expected to need replacement every 2 years due to the corrosive effects of the electrolyte and the degradation of the mechanical parts within them. Therefore, among all auxiliary components, pumps can be expected to have the biggest impact on the overall O&M costs.

Cell stack is clearly the most maintenance requiring part of a VRFB system due to the existence of more fragile components such as the membrane and the bipolar plates. Other main components at the stack side are electrodes and mechanical parts although they can operate for long periods of time without any maintenance or replacement requirements. So that leaves the membrane and the bipolar plates as the two components that in fact need to be replaced after a certain amount of degradation. However, as long-term running systems are inexistent so far, lifetimes of these components are mostly unclear. Several membrane materials are being tried out by manufacturers to reduce degrading effects and prolong lifetime but there is still no ultimate material for membrane manufacturing. Similarly, bipolar plates degrade with use but the exact causes of degradation are not known. Small scale experiments in our labs with one-cell setups showed that bipolar plate degradation accelerates when the entire operating range of the battery is in use. It is believed that advanced materials in the coming years might reduce degradation of this component and prolong its lifetime.

To summarize, the estimated cost information in Table 4.1 was used to make the calculations regarding the market integration of wind power while utilizing a VRFB unit. It should be noted that conservatively high values for both investment and running costs were estimated for this study and VRFB costs are expected to drop in the near future as the technology becomes more widespread, higher production volumes are reached, and advancements in VRFB components lead to further cost reductions.

Table 4.1 Estimated cost information for a megawatt scale VRFB unit.

Cost type	Cost in EUR
Capital expenditures (CAPEX)	1000/kW + 200/kWh
Running costs	5/kW/year
Other (e.g. insurance)	5/kW/year

4.3 Simulation model and methodology

4.3.1 Wind power forecasts

In order to simulate the bidding procedure in a hypothetical market and to evaluate storage management, wind power forecasts are required. The accuracy of wind power forecasts up to three days ahead has increased considerably in the last years. Wind power forecasts for the analyzed wind farm have been performed at ForWind, University of Oldenburg using mesoscale wind forecasts and the Farm Layout Program FLAP.

Operational wind forecasts of the mesoscale model COSMO¹ provided by the German Weather Service (DWD) were used to compute the wind power forecasts for the wind farm. The horizontal resolution is 4.1 km in zonal and 7 km in meridional direction. The wind components u,v in 68.8 m height have been interpolated to the geographical position of the wind farm. In the following, the u,v wind components have been converted into wind speed and wind direction. The model started at 00 UTC and data for the year 2007 to 2009 have been considered. The forecast horizon is +72 hours in hourly steps. The forecasts would naturally improve as the forecast horizon decreases. Based on the available weather data and the conservative approach taken with the model, 48-hour and 24-hour forecasts were not evaluated. Intraday market connections have also been excluded in order to see how the battery reacts to the deviation problem in a scenario where intraday corrections are difficult to implement or financially less beneficial. Considering today's market structure, even though excluding these might result in more battery utilization and possibly lower battery efficiencies for mitigating the deviation penalties, it can be stated that the effects and benefits of utilizing a VRFB for wind power integration at single wind farm level could still be evaluated effectively.

The wind farm power forecast and *real* production is simulated with FLAP, which was developed at the University of Oldenburg. The program implements state-of-the-art wind turbine wake models and has been validated for onshore and offshore conditions. The software takes the time series of the wind direction and the inflow wind speeds at hub height and calculates the internal wake effects and eventually the power production of each wind turbine within the wind farm.

¹<http://www.cosmo-model.org/>

The actual layout of the wind farm and the operational specifications of the wind turbines, such as thrust coefficient curves, have been set for the simulations. FLaP has been run with hourly time series of wind speed and wind direction from the COSMO model. The simulations have been performed applying the well established PARK model. Two wake expansion coefficients have been used, namely $k_1 = 0.08$ and $k_2 = 0.10$. In a final step, the individual power productions of all wind turbines have been added up in order to obtain the power output of the whole wind farm.

4.3.2 Market structure and deviation penalties

In Spain, being a balance responsible party puts more pressure on the wind power operators in terms of accurate power forecasting. Hence, having a wind farm dedicated storage unit, which could mitigate the deviations resulting from inaccurate forecasts could be of interest for a wind farm operator in this country. Therefore, a market mechanism similar to the Spanish electricity market was assumed for the calculations in this study and relevant market price data and deviation penalty information from the Spanish market were used.

4.3.3 Power dispatch strategy by utilizing the VRFB unit

In order to match the bids in the day-ahead market, the battery should be able to respond to deviations between the actual wind power output and the placed bid in the amount of the wind power to be sold. As the forecast power could deviate from the actual output in both negative and positive directions, it would be convenient to maintain the battery state of charge (SOC) at a level close to 50%. Therefore, the hourly bids in the market for each day should take into consideration the wind power forecast and the battery SOC, aiming to keep it at around 50%. Such a bidding strategy, which takes into account the wind power forecasts and the battery operation as well as the desired SOC is defined by the following equations for charging and discharging cases of the battery:

For charging,

$$(FE_i - BE_i) \times \eta_c = \Delta SOC_i \times BEC \quad (4.2)$$

For discharging,

$$(FE_i - BE_i) = \eta_d \times \Delta SOC_i \times BEC \quad (4.3)$$

where FE_i is the forecast and BE_i is the bid energy in kWh for the i^{th} day of the year, η_c and η_d are charging and discharging efficiencies respectively as calculated by the VRFB model. Finally, ΔSOC_i is the desired change in SOC in percentage while BEC is the energy capacity of the battery in kWh.

Calculations are done for all 24 hours of each day and finally the bids, which must be submitted by the wind farm/VRFB operator are calculated accordingly.

If for any given hour of a day, the battery is expected to be charging, the following formula can be used in order to determine the bid for that interval:

$$BE_i = FE_i - \frac{\Delta SOC_i \times BEC}{\eta_c} \quad (4.4)$$

$$BE_i = FE_i - \eta_d \times \Delta SOC_i \times BEC \quad (4.5)$$

In a typical day-ahead electricity market, the bids for the next day must be submitted until noon. Accordingly, an estimation of the battery SOC for the end of the day can be done by using the last day-ahead forecast and calculating the expected SOC levels for each hour as in the following equation:

$$SOC_{d,23} = SOC_{d,11} + \sum_{i=12}^{23} \frac{\eta_x \times (FP_{d,i} - BP_{d,i}) \times \Delta t}{BEC} \quad (4.6)$$

where the summation is calculated from 12:00 to 23:00 for the day d . FP is the forecast power and BP is the bid power whereas Δt is the time interval for converting power values into energy. In this case, Δt is always equal to 1, representing 1 hour. η_x is the efficiency factor, which is equal to η_c for charging and $1/\eta_d$ for discharging operation of the battery. Considering the VRFB always operates in an SOC range that is predefined by the battery model, there is a buffer zone for errors resulting from the SOC predictions for the bids. For instance, if the SOC is predicted to be 45% at a given interval, the efficiency value for this SOC would be taken from the 40-50% SOC zone. Accordingly, the efficiency values for a specific SOC range could be assumed to be accurate enough most of the time.

Based on the above described equations, the amount of energy, which is to be bid and sold in the market next day can be determined by the following equations for charging and discharging cases of the battery:

For charging,

$$BE_{d+1} = FE_{d+1} - \frac{\Delta SOC_{d+1} \times BEC}{\eta_c} \quad (4.7)$$

For discharging,

$$BE_{d+1} = FE_{d+1} - \eta_d \times \Delta SOC_{d+1} \times BEC \quad (4.8)$$

It should be noted that these equations assume a permanent charging or discharging of the battery in the course of a day. It is also worth mentioning that the Equation 4.7 suggests that the "sold energy" might be negative in some cases when both the SOC of the battery and the expected wind energy output for the following day is quite low. This would theoretically mean buying energy from the grid in order to charge the battery until the desired SOC is reached. However, in practice this situation could be avoided by placing lower bids in the market for

the next day and avoiding penalties that could result from a mismatch. Battery can then be recharged in the next possible time interval when there is sufficient wind energy generation.

Yearly avoided deviation was calculated as:

$$AD = ED_o - ED_b - L_b \quad (4.9)$$

where AD is the yearly avoided deviation, ED_o is the yearly energy deviation without a battery, ED_b is the yearly energy deviation with battery and L_b is the battery losses during the battery operation in the course of a year. Battery losses result from the charging and discharging cycles of the battery and the values depend on the efficiency figures calculated by the VRFB model, which was explained in the previous chapter.

As the price paid for inaccurate bids is the deviation penalty in the above explained market structure, battery utilization is aimed at avoiding as much of these deviations as possible. Based on the avoided energy deviation numbers, financial benefits obtained from avoided penalty payments were calculated. The penalty, which is paid for a deviation between the forecast and the actual energy sold at a given time interval (each hourly interval in the course of a day, so 24 penalty calculations per day) is calculated as follows:

$$DP = ED \times EP \times PM \quad (4.10)$$

where DP is the deviation penalty in EUR, ED is the energy deviation between the forecast and the actual energy delivered in MWh, EP is the wholesale electricity price in EUR/MWh for the considered time interval and PM is the penalty multiplier, which defines the final penalty price as a percentage of the market price.

In order to calculate the total amount of avoided penalty payments, market price of the electricity and the penalty multiplier values are necessary. For the baseline calculations in this study, the most recent available price information from the Spanish wholesale electricity market (49 EUR/MWh in 2011) were used. Further calculations were done for a decreasing electricity price scenario as well as an increasing price one. Although there have been some positive and negative spikes in the trend over the last 14 years, general tendency indicates an average market price increase at about 5%. Therefore, in the increasing price scenario, a 5% yearly increase was applied whereas similarly a 5% drop in the price was assumed for the decreasing price scenario. Penalty multiplier value was also varied in steps of 0.20 between 0.20 and 2.00 in order to compare low and high penalty scenarios.

Based on the VRFB cost data and annual revenue savings by utilizing a VRFB and avoiding penalties, profitability of the system was evaluated for each battery

size, deviation penalty multiplier and different electricity price trend scenarios. A Matlab™ based tool was used to simulate different scenarios.

Although the above mentioned calculations and equations specify how the energy bidding can be done with the use of forecasts and the battery, management of power that can be adjusted hour by hour should also be explained. Power output of a wind farm can be in several different combinations without affecting the final hourly or daily energy output. One power output strategy from the wind farm could be keeping the power constant at all times. This strategy would be the easiest to implement with the battery storing energy whenever there is more wind power than the fixed constant output and discharging during low wind periods. However, this strategy has the disadvantage of the battery not being able to provide the required power due to low SOC during long periods of no or low wind. This situation can be avoided by oversizing the battery, which would increase the costs significantly.

Another strategy could be a price oriented one where the wind energy is stored when the electricity prices are low and dispatched at higher prices, so called arbitraging. This strategy would optimize the income and be financially most preferred. However, such an operation may result in a situation, in which the battery operates close to its operating range limits where the efficiencies are low and the power is limited. Similar to the previous strategy, battery oversizing could be necessary for maximum flexibility to adapt price variations.

A third strategy and also the one followed for the calculations in this study is a forecast oriented one. In this approach, the bid power in the electricity market follows the same shape as the forecast but the forecast power values at each interval are multiplied by a factor. Multiplication factor is kept constant for a single day and is calculated by considering the power forecast and battery SOC parameters. For instance, if the battery SOC is relatively low, multiplication factor is generally below 1.00 in order to bid and sell less power in the market but charge the battery. On the contrary, if the battery SOC is at a high value, multiplication factor is larger than 1.00 and bid/sold power at a fixed interval is higher than the wind power output from the farm being supported by discharging the battery. As this strategy takes into consideration the SOC of the battery beforehand, higher efficiencies are achieved and the losses from the battery operation are reduced. On the other hand, the strategy does not optimize the income from electricity sales, which could be considered a disadvantage.

4.4 Results and discussion

As the sizing of the battery depends on power and energy parameters as well as the economics of the system, a starting point for the simulations had to be defined. This was done by evaluating the wind power data. It could be seen from

the power output histogram in Fig. 4.4 that there is an exponential decline in the number of occurrences as the power output value increases. Based on this information, the power capacity for the VRFB was selected as 4 MW for the baseline simulation. In order to see the effects of utilizing a battery immediately, a generous 100 MWh energy capacity was used in this baseline simulation.

Fig. 4.10 shows the results for a representative 3-day run of the yearly simulation where the VRFB (4 MW/100 MWh) is utilized to compensate for the deviations resulting from the forecasts and the actual output. Any deviation penalty, which has to be paid by the wind power generator can be avoided during this 3-day period by utilizing the VRFB. On the other hand, it is also clear that some inefficiencies result from the battery operation depending on the battery efficiency at a particular operating point. Relevant efficiency values are determined by the VRFB model for every charging and discharging operation taking place during the simulation and they depend primarily on the battery power and SOC for the moment the battery is operating. Even though the battery operating strategy favors keeping the battery SOC close to 50% in order to compensate positive and negative deviations effectively, battery can be at a fully charged or a fully discharged state at certain times. If this becomes the case, deviations cannot be mitigated and penalties have to be paid.

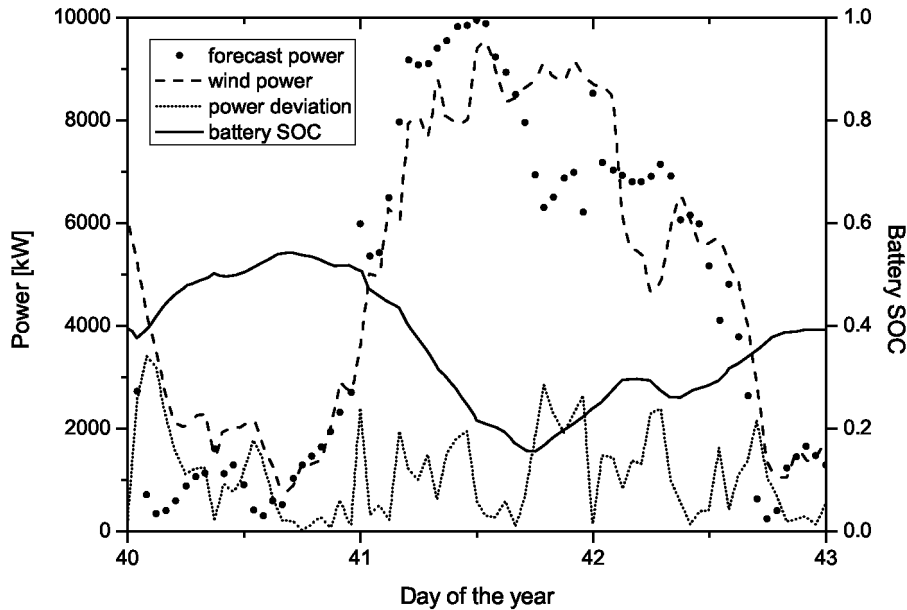


Figure 4.10 Battery (4 MW/100 MWh) response to deviations between forecast and actual output.

Table 4.2 shows that a significant 85% reduction in power deviations can be achieved by utilizing a 4 MW/100 MWh VRFB. The saved deviation of over 8 GWh is as big as 32% of the yearly energy output of the wind farm, which would

mean an important financial benefit due to the avoided penalties.

Table 4.2 Comparison of energetic values with and without a battery.

	no VRFB	4 MW/100 MWh VRFB
Wind farm energy output [MWh/year]	24416	24416
Battery losses [MWh/year]	0	1958
Energy fed into the grid [MWh/year]	24416	21955
Penalized deviation [MWh/year]	9711	1480

On the other hand, the financial benefits, which are gained by avoiding deviation penalties depend also on the investment costs to install a dedicated VRFB unit. As it was presented earlier in Table 4.1, capital expenditures and running costs of a VRFB depend on the rated power and energy capacities. Hence, sizing of the battery was done in a way that the maximum benefit could be achieved in terms of avoiding deviations while requiring the smallest possible capital expenditures and running costs. In order to determine the optimal power capacity of the VRFB for the simulations, the wind farm data and the forecasting data were analyzed and the deviations for the whole year were evaluated. In order to convert energy deviation values into power values, each hourly deviation was averaged out to reflect an hourly power value. Although this approach means a certain amount of approximation as various hourly intervals would have different deviation characteristics in terms of power and time, the error introduced does not affect the results for the yearly scale drastically. As it can be seen in Fig. 4.11, power deviations remain within a 2 MW range for most of the year. Therefore, a VRFB unit with a power capacity of 2 MW was selected to be utilized for further calculations.

As explained earlier, it was assumed that the energy capacity of a VRFB unit does not affect the VRFB running costs significantly. Hence, the contribution to the running costs by the energy capacity was neglected. However, the energy capacity of the battery unit contributes to the capital expenditures although with a lower impact compared to the power capacity. In order to determine the feasible energy capacity for the wind farm under consideration, various energy capacity values were evaluated. Following the same battery operation strategy for compensating the deviations between the forecast and the actual output, energy capacity of the VRFB was varied by 6 MWh steps between 6 and 30 MWh. The starting value was selected as 6 MWh since the data show that a minimum storage duration of 3 hours at 2 MW power would be necessary to cope up with the short-term power deviations within a day. Obtained results are shown in Fig. 4.12 and it can be seen that the increase rate of avoided deviation by adding more battery capacity is not as high as the rate, which capital expenditures for the VRFB unit increase for this particular wind farm size. Avoided extra deviation by

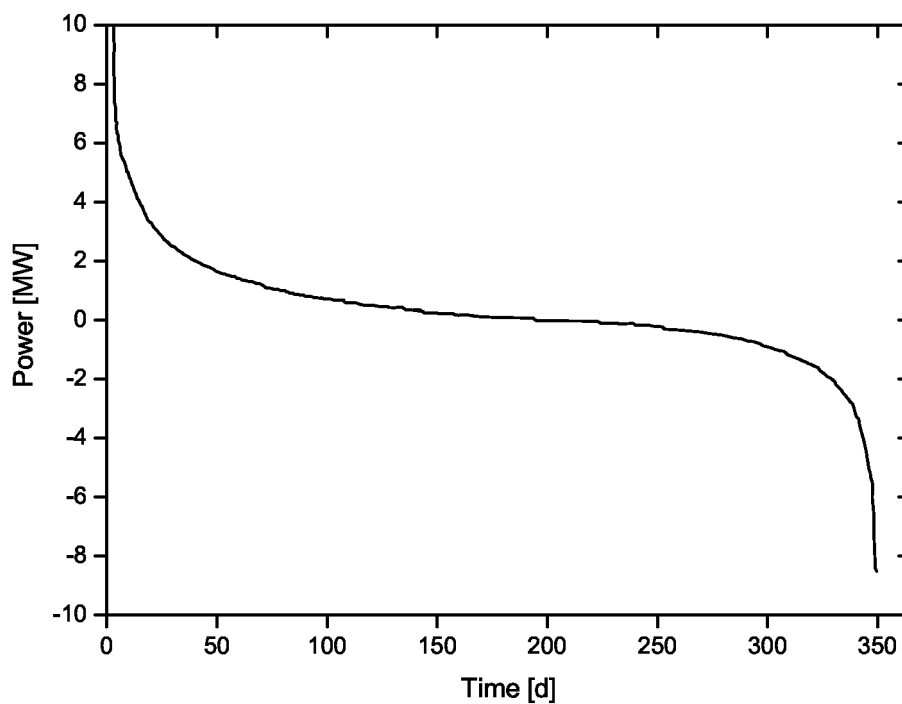


Figure 4.11 Yearly duration curve of the wind power deviation (without battery) [7].

adding 6 MWh to the battery energy capacity is just 3-6% higher at each increase whereas the rise in capital expenditures ranges from 20% to 40%. Therefore, a 6 MWh energy capacity for the VRFB was decided to be the most feasible for the wind farm under consideration.

Size of the battery

Physical size of a VRFB mainly depends on the size of the electrolyte tanks and therefore the energy capacity. For a 2 meter tank height, following illustration shows an approximation of the area covered by the electrolyte tanks for various VRFB sizes. Red squares represent the space required by the tanks with the numbers indicating the energy capacity in MWh.



Based on the financial savings due to the avoided deviation penalties along with the capital expenditures and running costs of the hypothetical VRFB unit, payback periods for such an installation were calculated for three electricity price scenarios and different penalty multipliers. Electricity price scenarios include a baseline scenario with the current (2011) average market price in Spain. Other scenarios assume a 5% increase and a 5% decrease in the average market price every year. The results are shown in Fig. 4.13 and it can be seen that only with a relatively high penalty multiplier of 1.50, payback periods around 10 years can be achieved. Furthermore, if electricity prices enter a decreasing trend in the coming years, payback periods would get much longer with presently assumed VRFB prices.

Findings in this study show that the capital expenditures constitute the larger share of the overall costs for a VRFB system. Following the discussed deviation penalty strategy similar to the one in the Spanish electricity market, payback periods, which are around 10 years are only achievable at relatively high penalty

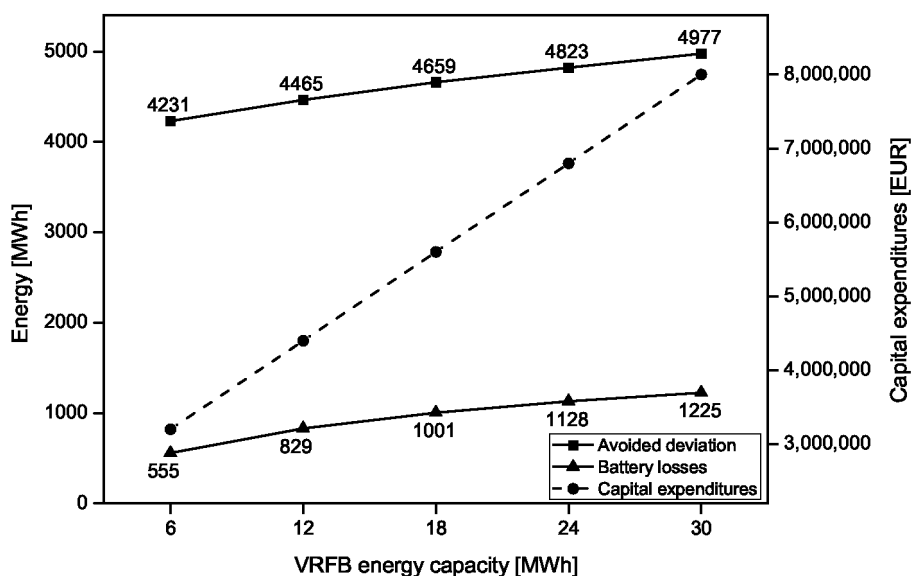


Figure 4.12 Avoided deviations, battery losses, and capital costs for different battery capacities [7].

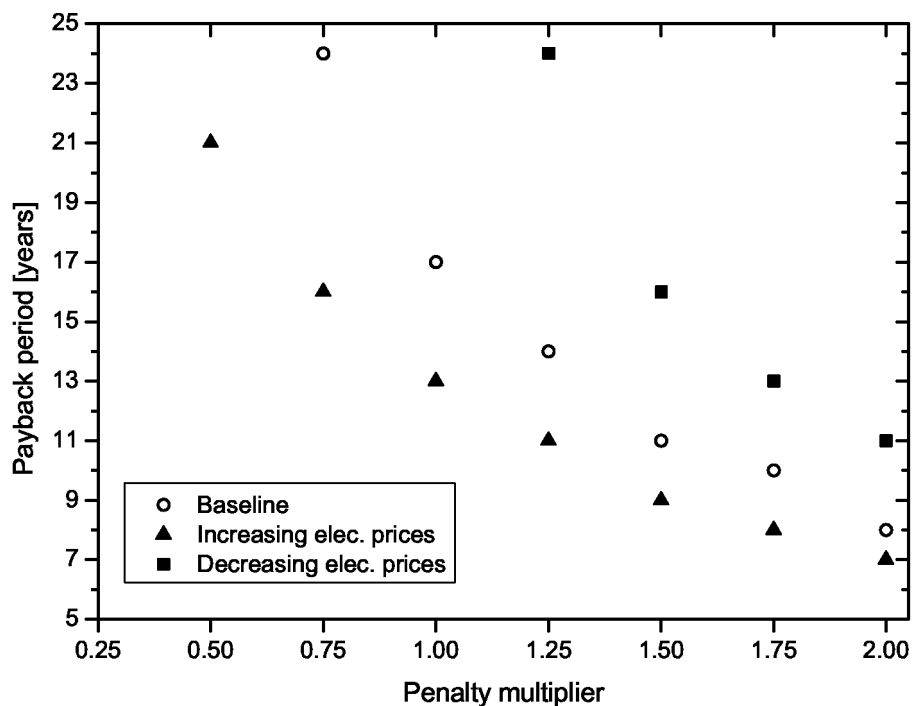


Figure 4.13 Payback periods for different penalty multipliers and electricity price scenarios [7].

multiplier values, which do not compare to today's lower multiplier values in the Spanish market. This would mean that such an investment on a VRFB system

would unlikely be made by wind farm operators under current market conditions. Unless there is a significant drop in the capital expenditures necessary for the installation of a VRFB in the near future, a strong support mechanism would be necessary to encourage wind power generators to employ dedicated VRFB units. On the other hand, once a larger global VRFB market with high power units is established, capital costs are expected to decrease due to higher production volumes and more market competition. In addition, as the technology advances and system components become more reliable and longer lasting, running costs would also drop significantly. Therefore, until the prices go down, energy storage support schemes could be introduced to encourage wind power and even other renewable energy generators to utilize VRFB units for leveling out fluctuations and mitigating market and grid integration issues resulting from intermittent generation.

4.5 Summary

This study investigated the utilization of a VRFB in an attempt to mitigate power grid and market integration issues resulting from variable nature of wind power. Real wind power data from a 10 MW wind farm, synthetic wind power forecasting data and a megawatt scale VRFB software model was used to simulate the system. Spanish electricity market, which employs deviation penalties was taken as an example to replicate the market structure. A parameter study of battery size and level of deviation penalty was performed in an attempt to respond to deviations between day-ahead forecasts and the actual energy output from the wind farm in order to match the bids placed in the market to avoid paying deviation penalties. Although the methodology proposed in this study could be applied to evaluate the benefits of utilizing other types of batteries for a similar market integration approach for wind power, it should be noted that the battery utilization rates for other technologies could differ significantly due to different efficiency characteristics.

Chapter 5

Conclusion and outlook

This study investigated the utilization of a vanadium redox flow battery (VRFB) for mitigating power grid and market integration issues resulting from variable nature of wind power. Real wind power data from a 10 MW wind farm, synthetic wind power forecasting data, and a megawatt scale VRFB software model was used to make technical and financial evaluations. Spanish electricity market, which employs deviation penalties was taken as an example to replicate the market structure.

The main idea was to model a megawatt scale energy storage unit and then utilize this hypothetical unit in an application where a medium sized single wind farm and the storage system are integrated for a dedicated storage utilization. As for the storage technology, VRFB was chosen because of its advantages, including sizing flexibility concerning power and energy, low maintenance, tolerance to overcharging and deep discharging conditions, and long cycle life.

As there has not been any modeling studies at system level up until now, a new approach of modeling a megawatt scale system based on real-life data from a kilowatt scale unit was taken. Accordingly, the megawatt scale VRFB software model was developed based on characterization data, which were obtained through experiments with a commercial kilowatt scale battery unit, namely CellCube FB 10/100. Experimental results reveal strong correlation between SOC, power, and overall efficiency. Pumping losses seem to be crucial at very low power levels. Based on the experimental results, a megawatt scale model was simulated in Matlab™ Simulink® environment. Charging and discharging operations of megawatt sized VRFBs were evaluated and operational strategies for achieving higher efficiencies were proposed. Further research could be aimed at evaluating ways of increasing the overall system efficiency by reducing the pumping losses even at low power levels, possibly by looking at the fluid dynamics characteristics of the electrolyte circulation. In addition, it can be expected that improved

materials for the electrodes and the membrane would contribute significantly to efficiency improvements in the near future.

In order to see the effects of utilizing a megawatt scale VRFB on wind power integration, a parameter study of battery size and level of deviation penalty was performed in an attempt to respond to deviations between day-ahead forecasts and the actual energy output from the wind farm in order to match the bids placed in the market to avoid paying deviation penalties. Using the developed megawatt scale model and running further power plant simulations, the hypothetical VRFB unit was considered to be utilized as a dedicated storage unit for mitigating the possible incorrect bidding in the power market due to the wind power forecasting errors. Deviation penalty system used in the Spanish electricity market was taken as an example and the VRFB economics were assessed by referring to existing financial models since it is still extremely difficult to access real-life cost information on this technology. As for the wind power and wind forecasting data, a real-life data from a 10 MW wind farm data was used and the hypothetical bids were generated based on the wind power forecast simulations by the FlaP software.

Simulation results reveal that a significant amount of power deviations could be mitigated by utilizing a 2 MW/6 MWh battery for the wind farm under investigation. Financial analyses were performed by considering the VRFB investment and running costs and current electricity market prices. As payback periods shorter than 10 years could only be achieved with deviation penalty values of about four times the Spanish market, the attractiveness for investors considering current market models is not at the highest level. Nevertheless, on road to a 100% renewable energy scenario where more variable and fluctuating energy production is expected, energy storage would play an important role in keeping power grids stable. As the costs related to grid stability services are generally high and that the ongoing research on stack components will further reduce the costs related to VRFB manufacturing, this technology could be expected to become a profitable option for investors in the near future.

Although the methodology proposed in this study could be applied to evaluate the benefits of utilizing other types of batteries for a similar market integration approach for wind power, it should be noted that the battery utilization rates for other technologies could differ significantly due to different efficiency characteristics. Some unique features of VRFBs, especially the externally stored and pumped electrolyte cause varying efficiency values for different power levels and states of charge. It should also be mentioned that the decoupled power and energy ratings of VRFBs provide an important design flexibility feature. Accordingly, sizing of the battery energy capacity for other technologies would not be as straightforward as VRFBs, which only require larger external electrolyte tanks and more electrolyte material for bigger storage capacities. Hence, the proposed procedure and the

model concerning the economics and sizing of the system should be considered specific to VRFBs.

Even though the VRFB utilization in this study was limited to a single application, it can easily be said that future megawatt scale VRFB systems could be utilized in a wide range of applications. Considering the renewable energy share within the global electricity generation will keep increasing, energy storage can be expected to maintain its importance for tackling the challenge of variable and intermittent generation. Considering the advantages of the VRFB technology over other energy storage alternatives, VRFB systems could be utilized in power plant dedicated applications as well as centralized power grid management ones. They could also be utilized in combination with other storage technologies for providing ancillary services, supplying balancing power, and serving as backup power systems in buildings. Furthermore, there has already been some demonstration projects concerning the utilization of VRFBs to provide energy at electric vehicle charging stations. This is an indication that the technology might become useful not only in the electricity supply system but also in electric transport applications in the near future. Further research on these possible applications of the VRFB technology and also the combinations of them could be considered extremely useful for evaluating the further benefits of the technology in small and large scale applications.

To conclude, it can be stated that the future of the VRFB technology will be decided by the growing importance of grid connected energy storage systems and the ability of the technology to break its way into the power markets in a successful way. This will depend on the advancements in the technology, which will lead to price reductions in manufacturing and operating the VRFBs as well as on the possible support schemes, which could be introduced by the decision mechanisms to accelerate the inclusion of new generation grid connected energy storage technologies. It is safe to say that uninterrupted, secure, affordable, and most importantly green and carbon free supply of energy in the near future can only be achieved by successful implementation of energy storage technologies along with grid upgrades, new generation smart grid systems, and energy efficiency measures.

Chapter 6

Zusammenfassung und Ausblick

Diese Studie erforschte die Anwendung einer Vanadium Redox Flow Batterie (VRFB) um die Probleme von Netz- und Strommarktintegration, die durch den schwankenden Charakter der Windenergie entstehen, zu lösen. Tatsächliche Windenergiedaten eines 10 MW Windparks, synthetische Windleistungsvorhersagen sowie ein Softwaremodell einer VRFB in der Größenordnung von Megawatt wurden benutzt um technische und wirtschaftliche Evaluierungen durchzuführen. Der Strommarkt in Spanien, der Abweichungsstrafen verwendet, wurde als Beispiel genommen um die Marktstruktur nachzubilden.

Der Kern des Konzeptes war die Modellierung eines Energiespeichers in der Größenordnung von Megawatt und ebendieses Modell in einer Anwendung mit einem integrierten und fest zugeordneten Speichersystem für einen Windpark zu nutzen. Als Speichertechnologie wurde VRFB ausgewählt, da diese Technologie gegenüber anderen mehrere Vorteile bietet. Zu erwähnen sind hier unter anderem die unabhängige Dimensionierung von Leistung und Energie, der geringe Wartungsaufwand, gute Toleranz gegenüber Überladung und Tiefentladung zeigt als auch eine gute Lebensdauer.

Da bisher keine Modellierungsstudie existierte, wurde ein neues Vorgehen zur Modellierung eines megawattgroßen Systems, basierend auf einer realen kilowattgroßen Einheit realisiert. Deshalb wurde ein entsprechendes VRFB Softwaremodell auf Grundlage experimenteller Charakterisierungsdaten einer realen kilowattgroßen VRFB, dem CellCube FB 10/100 von Cellstrom, entwickelt. Experimentelle Ergebnisse zeigen eine starke Korrelation zwischen SOC (Ladezustand), Leistung und Gesamt-Wirkungsgrad. Die Verluste der Elektrolytpumpen sind bei niedrigen Leistungen sehr relevant. Auf Basis dieser experimentellen Ergebnisse wurde mit Matlab[™] Simulink[®] ein Softwaremodell entwickelt. Lade- und Entladeprozesse wurden evaluiert und Strategien für höhere Wirkungsgrade vorgeschlagen. Weiterführende Forschung könnte sich auf flüssigkeitsdynamische Charakterisierung

der Elektrolytpumpen konzentrieren um den Gesamtwirkungsgrad durch die Reduzierung von Pumpverlusten zu erhöhen. Weiterhin kann festgestellt werden, dass verbesserte Elektroden- und Membranmaterialien in Zukunft zu höheren Wirkungsgraden führen werden.

Um die Effekte der Verwendung einer VRFB für Windenergieintegration zu untersuchen, wurde eine Parameterstudie von Batteriegröße und Abweichungsstrafen durchgeführt. Das VRFB-Modell wurde benutzt, um die Abweichungen zwischen Energieverbrauchsvorhersagen (1 Tag) und der tatsächlichen Generation im Strommarkt zu korrigieren. Mit dem megawattgroßen Modell und der Kraftwerkssimulation wurden die hypothetischen VRFB benutzt um die Vorhersagefehler abzuschwächen. Das Abweichungsstrafensystem im spanischen Strommarkt wurde als Beispiel benutzt. Da reale Kosteninformationen für diese Technologie noch immer schwierig zu erhalten sind, wurden existierende Finanzmodelle für die VRFB genutzt. Als Windenergiekosten wurden reale Leistungsdaten eines 10 MW Windparks und synthetische, hypothetische Strommarkt Kostenvorschläge basierend auf Simulationen von FlaP Software verarbeitet.

Die Ergebnisse der Simulationen zeigen, dass eine maßgebliche Menge der Abweichungen des evaluierten Windparks mit einer 2 MW/6 MWh VRFB abgeschwächt werden könnten. Wirtschaftliche Analysen wurden in Form der Evaluierung der VRFB Investitions- und Betriebskosten und aktuelle Strompreise durchgeführt. Amortisationsperioden von weniger als 10 Jahre sind nur möglich, wenn die Abweichungsstrafen viermal größer als die heutigen Werte im spanischen Strommarkt sind. Aus diesem Grund ist die Attraktivität von VRFB für Investoren derzeit noch begrenzt. Ungeachtet dieser Tatsache könnte diese Technologie in Zukunft sehr attraktiv werden, da für ein Szenario von 100% erneuerbare Energien der Bedarf an Energiespeichern weiter steigen wird und reduzierte Kosten durch bessere Produktionstechnik und günstigere Materialien zu gesteigerter Wirtschaftlichkeit beitragen werden.

Obwohl die in dieser Studie vorgeschlagene Methodik benutzt werden könnte, um die Vorteile von Batterieanwendungen für ähnliche Studien zur Marktintegration von Windenergie zu evaluieren, sollte beachtet werden, dass die Batterienutzungsraten für andere Batterietypen stark abweichen können. Dies liegt an ihren unterschiedlichen Wirkungsgradcharakteristiken. Einige Eigenschaften von VRFB, insbesondere der extern gelagerte und gepumpte Elektrolyt, verursachen unterschiedliche Wirkungsgrade bei verschiedenen Leistungen und Ladezustände. Darüber hinaus bietet die voneinander unabhängige Leistungs- und Energiekonfiguration von VRFB eine wichtige Designflexibilität. Deswegen wäre die Dimensionierung unter Verwendung anderer Batterietypen nicht so einfach wie VRFB. Daher sollte das vorgeschlagene Modell für Dimensionierung und wirtschaftliche Evaluierung lediglich für VRFB eingesetzt werden.

Obwohl die Modellierung der VRFB im Rahmen dieser Studie auf eine einzige

Anwendung limitiert war, kann man sagen, dass zukünftig VRFB-Systeme für verschiedene Anwendungen zur Verfügung stehen werden. Wenn über zukünftige Energiesysteme mit steigendem Anteil erneuerbarer Energie nachgedacht wird, kann man erwarten, dass Energiespeichersysteme für Netz- und Marktintegration der fluktuierenden Energie eine große Rolle spielen werden. Durch die Vorteile von VRFB-Technologie im Vergleich zu anderen Speichertechnologien, könnten erstere in Kraftwerken sowie für zentrale Anwendungen auf Verteilnetzebene genutzt werden. Sie können auch in Kombination mit anderen Speichertechnologien Netz-Reserveleistung und Backupleistung von Gebäuden zur Verfügung stellen. Ferner gibt es bereits Pilotprojekte mit VRFB-Ladestationen für Elektroautos. Dies zeigt, dass die VRFB-Technologie in Zukunft auch für Elektromobilität wichtig sein könnte. Weitere Forschung im Bereich dieser möglichen Anwendungen von VRFB wären sehr wertvoll um die Vorteile von dieser Technologie bei kleinen und großen Anwendungen zu evaluieren.

Abschließend ist zu sagen, dass die Zukunft der VRFB-Technologie von der Wichtigkeit der netzintegrierten Speicher abhängt. Weiterhin ist die Frage der erfolgreichen Marktadaption diese Technologie offen. Diese wird von Förderungen, Kostenreduzierungen in Herstellung und Betrieb von VRFB sowie der finanzielle Unterstützung durch Strategiepläne für VRFB und andere Speichertechnologien abhängig sein. Man kann eindeutig feststellen, dass grüne und Kohlenstoff-freie Energie in Zukunft nur nach erfolgreicher Implementierung von Energiespeichern, Smart Grid-Systemen und Innovationen für höhere energetische Wirkungsgrade möglich sind.

Bibliography

- [1] Key World Energy Statistics. Technical report, International Energy Agency, 2013.
- [2] Renewables 2013 Global Status Report. Technical report, REN21, 2013.
- [3] 2012 Half-year Report. Technical report, The World Wind Energy Association, 2012.
- [4] Tony Burton, Nick Jenkins, David Sharpe, and Ervin Bossanyi. *Wind Energy Handbook*. John Wiley & Sons, 2nd edition, 2011.
- [5] CellCube FB10/100 Technical Description - 2009-02-23. Technical report, Cellstrom GmbH, 2009.
- [6] Burak Turker, Sebastian Arroyo Klein, Eva-Maria Hammer, Bettina Lenz, and Lidiya Komsysiyska. Modeling a vanadium redox flow battery system for large scale applications. *Energy Conversion and Management*, 66:26–32, 2013.
- [7] Burak Turker, Sebastian Arroyo Klein, Lidiya Komsysiyska, Juan Jose Trujillo, Lueder von Bremen, Martin Kuehn, and Matthias Busse. Utilizing a vanadium redox flow battery to avoid wind power deviation penalties in an electricity market. *Energy Conversion and Management*, 76:1150–1157, 2013.
- [8] S. Eckroad. Vanadium Redox Flow Batteries - An In-Depth Analysis. Technical report, Electric Power Research Institute, 2007.
- [9] Godfrey Boyle, editor. *Renewable Electricity and The Grid - The Challenge of Variability*. Earthscan, 1st edition, 2007.
- [10] J. Usaola and E. Castronuovo. *Wind Energy in Electricity Markets with High Wind Penetration*. Nova Science Publishers, Inc., New York, 2009.

- [11] F. Hulle, N. Fichaux, A. Sinner, P. Morthorst, J. Munksgaard, S. Ray, C. Kjaer, J. Wilkes, P. Wilczek, G. Rodrigues, and A. Arapogianni. Powering Europe: wind energy and the electricity grid. Technical report, The European Wind Energy Association, 2010.
- [12] Lion Hirth. The market value of variable renewables: The effect of solar wind power variability on their relative price. *Energy Economics*, 38:218–236, 2013.
- [13] Patrick J. Luickx, Erik D. Delarue, and William D. D’haeseleer. Considerations on the backup of wind power: Operational backup. *Applied Energy*, 85(9):787–799, 2008.
- [14] C. Hiroux and M. Saguan. Large-scale wind power in european electricity markets: Time for revisiting support schemes and market designs? *Energy Policy*, 38(7):3135–3145, 2010.
- [15] Grid Codes for Wind Power Integration in Spain and Germany: Use of Incentive Payments to Encourage Grid-Friendly Wind Power Plants. Technical report, Fichtner, 2010.
- [16] J. Parkes, J. Wasey, and A. Tindal. Wind Energy Trading Benefits Through Short Term Forecasting. Technical report, GL Garrad Hassan, 2006.
- [17] J. Rodriguez, O. Alonso, M. Duvison, and T. Domingez. The integration of renewable energy and the system operation: The Special Regime Control Centre (CECRE) in Spain. In *IEEE Power and Energy Society General Meeting - Conversion and Delivery of Electrical Energy in the 21st Century*, 2008.
- [18] Oliver Grothe and Felix Musgens. The influence of spatial effects on wind power revenues under direct marketing rules. *Energy Policy*, 58:237–247, 2013.
- [19] Yannick Perez and Francisco Javier Ramos-Real. The public promotion of wind energy in Spain from the transaction costs perspective 1986-2007. *Renewable and Sustainable Energy Reviews*, 13(5):1058 – 1066, 2009.
- [20] M. Bustos. The new payment mechanism of RES-E in Spain. Technical report, APPA - Spanish Renewable Energy Association, 2004.
- [21] Peter J. Hall. Energy storage: The route to liberation from the fossil fuel economy? *Energy Policy*, 36(12):4363–4367, 2008.
- [22] Jim McDowall. Integrating energy storage with wind power in weak electricity grids. *Journal of Power Sources*, 162(2):959 – 964, 2006.

- [23] Patrick Sullivan, Walter Short, and Nate Blair. Modeling the Benefits of Storage Technologies to Wind Power. In *WindPower 2008 Conference*, Houston, Texas, 2008.
- [24] J. Paatero and P. Lund. Effect of Energy Storage on Variations in Wind Power. *Wind Energy*, 8:421–441, 2005.
- [25] P. Denholm, E. Ela, B. Kirby, and M. Milligan. The Role of Energy Storage with Renewable Electricity Generation. Technical report, NREL - National Renewable Energy Laboratory, 2010.
- [26] M. Swierczynski, R. Teodorescu, C. Rasmussen, P. Rodriguez, and H. Vikelgaard. Overview of the Energy Storage Systems for the Wind Power Integration Enhancement. In *Proceedings of the IEEE International Symposium on Industrial Electronics*, pages 3749–3756. IEEE Press, 2010.
- [27] S. Eckroad. Energy Storage for Grid Connected Wind Generation Applications. Technical report, Electric Power Research Institute, 2004.
- [28] Jorge Marquez Angarita and Julio Garcia Usaola. Combining hydro-generation and wind energy: Biddings and operation on electricity spot markets. *Electric Power Systems Research*, 77(56):393 – 400, 2007.
- [29] Henrik Lund. Large-scale integration of wind power into different energy systems. *Energy*, 30(13):2402–2412, 2005.
- [30] Ruddy Blonbou, Stephanie Monjoly, and Jean-Francois Dorville. An adaptive short-term prediction scheme for wind energy storage management. *Energy Conversion and Management*, 52(6):2412 – 2416, 2011.
- [31] Baoming Ge, Wenliang Wang, Daqiang Bi, Craig B. Rogers, Fang Zheng Peng, Anibal T. de Almeida, and Haitham Abu-Rub. Energy storage system-based power control for grid-connected wind power farm. *International Journal of Electrical Power & Energy Systems*, 44(1):115–122, 2013.
- [32] Liliana E. Benitez, Pablo C. Benitez, and G. Cornelis van Kooten. The economics of wind power with energy storage. *Energy Economics*, 30(4): 1973 – 1989, 2008.
- [33] H. Holttinen. Optimal electricity market for wind power. *Energy Policy*, 33 (16):2052–2063, 2005.
- [34] Magnus Korpaas, Arne T. Holen, and Ragne Hildrum. Operation and sizing of energy storage for wind power plants in a market system. *International Journal of Electrical Power & Energy Systems*, 25(8):599–606, 2003.

- [35] Claus Krog Ekman and Soren Hojgaard Jensen. Prospects for large scale electricity storage in Denmark. *Energy Conversion and Management*, 51(6): 1140 – 1147, 2010.
- [36] Dimitrios Zafirakis, Konstantinos J. Chalvatzis, Giovanni Baiocchi, and George Daskalakis. Modeling of financial incentives for investments in energy storage systems that promote the large-scale integration of wind energy. *Applied Energy*, 105:138–154, 2013.
- [37] M. Skyllas-Kazacos, M. H. Chakrabarti, S. A. Hajimolana, F. S. Mjalli, and M. Saleem. Progress in Flow Battery Research and Development. *Journal of The Electrochemical Society*, 158(8):R55–R79, 2011.
- [38] Ao Tang, Simon Ting, Jie Bao, and Maria Skyllas-Kazacos. Thermal modelling and simulation of the all-vanadium redox flow battery. *Journal of Power Sources*, 203:165–176, 2012.
- [39] H. Al-Fetlawi, A. A. Shah, and F. C. Walsh. Non-isothermal modelling of the all-vanadium redox flow battery. *Electrochimica Acta*, 55(1):78–89, 2009.
- [40] Xiangkun Ma, Huamin Zhang, and Feng Xing. A three-dimensional model for negative half cell of the vanadium redox flow battery. *Electrochimica Acta*, 58:238–246, 2011.
- [41] A. A. Shah, M. J. Watt-Smith, and F. C. Walsh. A dynamic performance model for redox-flow batteries involving soluble species. *Electrochimica Acta*, 53(27):8087–8100, 2008.
- [42] A. A. Shah, R. Tangirala, R. Singh, R. G. A. Wills, and F. C. Walsh. A dynamic unit cell model of the all-vanadium redox flow battery. *Journal of The Electrochemical Society*, 158(6):A671–A677, 2011.
- [43] M. Vynnycky. Analysis of a model for the operation of a vanadium redox battery. *Energy*, 36(4):2242–2256, 2011.
- [44] Ao Tang, Jie Bao, and Maria Skyllas-Kazacos. Thermal modelling of battery configuration and self-discharge reactions in vanadium redox flow battery. *Journal of Power Sources*, 216:489–501, 2012.
- [45] Dongjiang You, Huamin Zhang, Chenxi Sun, and Xiangkun Ma. Simulation of the self-discharge process in vanadium redox flow battery. *Journal of Power Sources*, 196(3):1578–1585, 2011.
- [46] Izumi Tsuda, Ken Nozaki, Koichi Sakuta, and Kosuke Kurokawa. Improvement of performance in redox flow batteries for PV systems. *Solar Energy Materials and Solar Cells*, 47:101–107, 1997.

- [47] Luiz Augusto Barroso, Teofilo Cavalcanti, Paul Giesbertz, and Konrad Purchala. Classification of electricity market models worldwide. 2005. On behalf of CIGRE Task Force C5.2.1.
- [48] Julio Usaola. Participation of wind power in electricity markets. 2008.
- [49] Erik Ela, Brendan Kirby, Eamonn Lannoye, Michael Milligan, Damian Flynn, Bob Zavadil, and Mark O'Malley. Evolution of Operating Reserve Determination in Wind Power Integration Studies. *IEEE*, 2010.
- [50] H. Agabus and H. Tammoja. Estimations of wind power production through short-term forecast. *Oil Shale*, 26(3):208–219, 2009.
- [51] Jan Dobschinski, Arne Wessel, Bernhard Lange, and Lueder von Bremen. Reduction of wind power induced reserve requirements by advanced shortest-term forecasts and prediction intervals. 2009.
- [52] Ulrich Focken, Matthias Lange, Kai Monnich, and Hans-Peter Waldl. A statistical analysis of the reduction of the wind power prediction error by spatial smoothing effects. .
- [53] U. Focken, M. Lange, and B. Graeber. Grid Integration of Wind Energy in Germany - Towards Managing 25 GW Offshore Wind Power. In *Fifth International Workshop on Large-Scale Integration of Wind Power and Transmission Networks for Offshore Wind Farms*, Glasgow, UK, .
- [54] Ulrich Focken, Matthias Lange, Kai Moennich, Hans-Peter Waldl, Hans Georg Beyer, and Armin Luig. Short-term prediction of the aggregated power output of wind farms - a statistical analysis of the reduction of the prediction error by spatial smoothing effects. *Journal of Wind Engineering and Industrial Aerodynamics*, 90(3):231–246, 2002.
- [55] Gregor Giebel, Poul Sorensen, and Hannele Holttinen. Forecast error of aggregated wind power. Technical report, TradeWind, 2007.
- [56] Jason Makansi and Jeff Abboud. Energy Storage - The Missing Link in the Electricity Value Chain. 2002. ESC White Paper.
- [57] Aishwarya Parasuraman, Tuti Mariana Lim, Chris Menictas, and Maria Skyllas-Kazacos. Review of material research and development for vanadium redox flow battery applications. *Electrochimica Acta*, 101:27–40, 2013.
- [58] M. Skyllas-Kazacos. Vanadium redox flow batteries. *Encyclopedia of Electrochemical Power Sources*, pages 444–453, 2009.

- [59] Nobuyuki Tokuda, Takashi Kanno, Takushi Hara, Toshio Shigematsu, Yasumitsu Tsutsui, Atsuo Ikeuchi, Takefumi Itou, and Takahiro Kumamoto. Development of a redox flow battery system. *SEI Technical Review*, 50: 88–94, 2000.
- [60] C. Ponce de Leon, A. Frias-Ferrer, J. Gonzalez-Garcia, D. A. Szanto, and F. C. Walsh. Redox flow cells for energy conversion. *Journal of Power Sources*, 160(1):716–732, 2006.
- [61] B. Sun and M. Skyllas-Kazacos. Chemical modification of graphite electrode materials for vanadium redox flow battery application - part II. Acid treatments. *Electrochimica Acta*, 37(13):2459–2465, 1992.
- [62] B. Sun and M. Skyllas-Kazacos. Modification of graphite electrode materials for vanadium redox flow battery application - I. Thermal treatment. *Electrochimica Acta*, 37(7):1253–1260, 1992.
- [63] Xiangguo Teng, Yongtao Zhao, Jingyu Xi, Zenghua Wu, Xinpeng Qiu, and Liqun Chen. Nafion/organically modified silicate hybrids membrane for vanadium redox flow battery. *Journal of Power Sources*, 189(2):1240–1246, 2009.
- [64] Peng Qian, Huamin Zhang, Jian Chen, Yuehua Wen, Qingtao Luo, Zonghao Liu, Dongjiang You, and Baolian Yi. A novel electrode-bipolar plate assembly for vanadium redox flow battery applications. *Journal of Power Sources*, 175(1):613–620, 2008.
- [65] T. Sukkar and M. Skyllas-Kazacos. Modification of membranes using polyelectrolytes to improve water transfer properties in the vanadium redox battery. *Journal of Membrane Science*, 222(1-2):249–264, 2003.
- [66] John M. Hawkins and Tim Robbins. A field trial of a vanadium energy storage system. In *INTELE*, 2001.
- [67] T. Shigematsu, T. Kumamoto, H. Deguchi, and T. Hara. Applications of a vanadium redox-flow battery to maintain power quality. In *IEEE PES Transmission and Distribution Conference and Exhibition (2002)*, volume 2, pages 1065–1070. IEEE, 2002.
- [68] Martha Schreiber, Martin Harrer, Adam Whitehead, Herbert Bucsich, Matthias Dragschitz, Ernst Seifert, and Peter Tymciw. Practical and commercial issues in the design and manufacture of vanadium flow batteries. *Journal of Power Sources*, 206:483–489, 2012.
- [69] Mary Black and Goran Strbac. Value of storage in providing balancing services for electricity generation systems with high wind penetration. *Journal of Power Sources*, 162(2):949 – 953, 2006.

- [70] Martin Braun. Technological control capabilities of DER to provide future ancillary services. *International Journal of Distributed Energy Resources*, 3(3):191–206, 2006.
- [71] M. H. Chakrabarti, R. A. W. Dryfe, and E. P. L. Roberts. Evaluation of electrolytes for redox flow battery applications. *Electrochimica Acta*, 52(5): 2189–2195, 2007.
- [72] Dongyang Chen, Shuanjin Wang, Min Xiao, and Yuezhong Meng. Synthesis and properties of novel sulfonated poly(arylene ether sulfone) ionomers for vanadium redox flow battery. *Energy Conversion and Management*, 51(12): 2816–2824, 2010.
- [73] Haisheng Chen, Thang Ngoc Cong, Wei Yang, Chunqing Tan, Yongliang Li, and Yulong Ding. Progress in electrical energy storage system: A critical review. *Progress in Natural Science*, 19:291–312, 2009.
- [74] Rafael Cossent, Tomas Gomez, and Pablo Frias. Towards a future with large penetration of distributed generation: Is the current regulation of electricity distribution ready? regulatory recommendations under a european perspective. *Energy Policy*, 37(3):1145 – 1155, 2009.
- [75] Alexandre Costa, Antonio Crespo, Jorge Navarro, Gil Lizcano, Henrik Madsen, and Everaldo Feitosa. A review on the young history of the wind power short-term prediction. *Renewable and Sustainable Energy Reviews*, 12(6):1725 – 1744, 2008.
- [76] Joseph F. DeCarolis and David W. Keith. The economics of large-scale wind power in a carbon constrained world. *Energy Policy*, 34(4):395 – 410, 2006.
- [77] Erik D. Delarue, Patrick J. Luickx, and William D. D’haeseleer. The actual effect of wind power on overall electricity generation costs and CO₂ emissions. *Energy Conversion and Management*, 50(6):1450 – 1456, 2009.
- [78] K. C. Divya and Jacob Ostergaard. Battery energy storage technology for power systems - An overview. *Electric Power Systems Research*, 79:511–520, 2009.
- [79] Ronan Doherty and Mark O’Malley. Quantifying Reserve Demands due to Increasing Wind Power Penetration. In *IEEE Bologna Power Tech Conference*, 2003.
- [80] Prudent Energy. Prudent Energy - case study: VRB Technology in Japan.

- [81] Jean-Michel Glachant, Ute Dubois, and Yannick Perez. Deregulating with no regulator: Is the German electricity transmission regime institutionally correct? *Energy Policy*, 36(5):1600–1610, 2008.
- [82] Eric Hirst and Brendan Kirby. Separating and measuring the regulation and load-following ancillary services. *Utilities Policy*, 8(2):75–81, 1999.
- [83] Eric Hirst and Brendan Kirby. Operating reserves and bulk-power reliability. *Energy*, 23(11):949–959, 1998.
- [84] Hannele Holttinen, Michael Milligan, Brendan Kirby, Tom Acker, Viktoria Neimane, and Tom Molinski. Using standard deviation as a measure of increased operational reserve requirement for wind power. *Wind Engineering*, 32(4):355–378, 2008.
- [85] H. Ibrahim, A. Ilinca, and J. Perron. Energy storage systems - characteristics and comparisons. *Renewable and Sustainable Energy Reviews*, 12(5):1221 – 1250, 2008.
- [86] Tryggvi Jonsson, Pierre Pinson, and Henrik Madsen. Day-Ahead Electricity Prices in Denmark: The Impact of Wind Power Forecasts.
- [87] J. de Joode, J.C. Jansen, A.J. van der Welle, and M.J.J. Scheepers. Increasing penetration of renewable and distributed electricity generation and the need for different network regulation. *Energy Policy*, 37(8):2907 – 2915, 2009.
- [88] Soren Krohn, Poul-Erik Morthorst, and Shimon Awerbuch. The Economics of Wind Energy. Technical report, The European Wind Energy Association, 2009.
- [89] B. Lange, H. Waldl, A. Guerrero, D. Heinemann, and R. Barthelmie. Modelling of Offshore Wind Turbine Wakes with the Wind Farm Program FLaP. *Wind Energy*, 6(1):87–104, 2003.
- [90] Matthias Lange and Ulrich Focken. State-of-the-Art in Wind Power Prediction in Germany and International Developments.
- [91] Wenyue Li, Jianguo Liu, and Chuanwei Yan. Graphite-graphite oxide composite electrode for vanadium redox flow battery. *Electrochimica Acta*, 56(14):5290–5294, 2011.
- [92] Qinghua Liu, Alice Sleightholme, Aaron Shinkle, Yongdan Li, and Levi Thompson. Non-aqueous vanadium acetylacetonate electrolyte for redox flow batteries. *Electrochemistry Communications*, 11(12):2312–2315, 2009.

- [93] Peter Lund. Large-scale urban renewable electricity schemes - Integration and interfacing aspects. *Energy Conversion and Management*, 63:162–172, 2012.
- [94] M. R. Milligan. A Chronological Reliability Model to Assess Operating Reserve Allocation to Wind Power Plants. In *European Wind Energy Conference*, 2001.
- [95] Mario Ragwitz and Claus Huber. Feed-In Systems in Germany and Spain and a comparison. Technical report, Fraunhofer Institute Systems and Innovation Research.
- [96] K. Rohrig, B. Lange, A. Gesino, M. Wolff, R. Mackensen, J. Dobschinski, A. Wessel, M. Braun, C. Quintero, J. Mata, and R. Pestana. Wind Power Plant Capabilities - Operate Wind Farms like Conventional Power Plants. In *EWEC 2009*, 2009.
- [97] Lina Ruiz. Integration of wind power in the electricity market: Impact of the RES-E support mechanism. In *20th International Conference on Electricity Distribution*, Prague, 2009.
- [98] Nadja Saleck and Lueder von Bremen. Wind power forecast error smoothing within a wind farm. *Journal of Physics*, 75, 2007.
- [99] A. Sarasua, M. Molina, D. Pontoriero, and P. Mercado. Wind energy and energy storage in power systems. In *XIII ERIAC Decimo Tercer Encuentro Regional Iberoamericano de CIGRE*, 2009.
- [100] Frank Sensfuss, Mario Ragwitz, and Massimo Genoese. The Merit-order effect: A detailed analysis of the price effect of renewable electricity generation on spot market prices in Germany. Technical report, Fraunhofer Institute Systems and Innovation Research, 2007.
- [101] Ingo Stadler. Power grid balancing of energy systems with high renewable energy penetration by demand response. *Utilities Policy*, 16(2):90–98, 2008.
- [102] Theresa Sukkar and Maria Skyllas-Kazacos. Water transfer behaviour across cation exchange membranes in the vanadium redox battery. *Journal of Membrane Science*, 222:235–247, 2003.
- [103] E. Sum and M. Skyllas-Kazacos. A study of the V(II)/V(III) redox couple for redox flow cell applications. *Journal of Power Sources*, 15(2-3):179–190, 1985.
- [104] J. Trujillo, A. Wessel, I. Waldl, and B. Lange. Online modelling of wind farm power for performance surveillance and optimisation. In *EUROMECH*, 2005.

- [105] Vilayanur Viswanathan, Alasdair Crawford, David Stephenson, Soowhan Kim, Wei Wang, Bin Li, Greg Coffey, Ed Thomsen, Gordon Graff, Patrick Balducci, Michael Kintner-Meyer, and Vincent Sprenkle. Cost and performance model for redox flow batteries. *Journal of Power Sources*, 2012.
- [106] Ping Zhao, Huamin Zhang, Hantao Zhou, Jian Chen, Sujun Gao, and Baolian Yi. Characteristics and performance of 10 kW class all-vanadium redox-flow battery stack. *Journal of Power Sources*, 162(2):1416–1420, 2006.
- [107] Wind Energy and Electricity Prices - exploring the 'merit order effect'. Technical report, Poyry, 2010.
- [108] Bottling Electricity: Storage as a Strategic Tool for Managing Variability and Capacity Concerns in the Modern Grid. Technical report, The Electricity Advisory Committee, 2008.
- [109] ERGEG Guidelines of Good Practice for Electricity Balancing Markets Integration. Technical report, European Regulators Group for Electricity and Gas, 2006.
- [110] European Electricity Market Perspectives. Technical report, Finnish Energy Industries Federation, 2003.

Studentische Arbeiten

In der vorliegenden Arbeit sind Ergebnisse enthalten, die im Rahmen der Betreuung folgender studentischer Arbeiten entstanden sind:

Sebastián Arroyo Klein, Technical and Economic Assessment of Utilizing Vanadium Redox Flow Batteries for Grid Integration of Wind Power

Biography

Burak Türker

burak.turker@uni-oldenburg.de

Türker received his B.Sc. Electrical Engineering and M.Sc. Renewable Energy degrees from Yildiz Technical University and University of Oldenburg respectively. He worked on biomass gasification and fuel cell technologies for his master thesis at Delft University of Technology (TU Delft) Process & Energy Department. After having worked at the University of Oldenburg as a research assistant for one year, he started his energy storage research at NEXT ENERGY - EWE Research Centre for Energy Technology. Simultaneously, he pursued his PhD degree at the University of Bremen. At NEXT ENERGY, he worked on Li-ion and Vanadium Redox Flow battery technologies as well as on grid integration of renewable energy and electric transport.

Türker has made presentations at several international seminars and conferences in the energy field. His recent areas of interest are energy efficiency, sustainable living, environmental issues, and energy policy.

Publications

- B. Turker, S. A. Klein, L. Komsijska, J. J. Trujillo, L. von Bremen, M. Kühn, M. Busse, Utilizing a vanadium redox flow battery to avoid wind power deviation penalties in an electricity market, *Energy Conversion and Management*, 2013;76
- B. Turker, S. Arroyo Klein, E. Hammer, B. Lenz, L. Komsijska, Modeling a vanadium redox flow battery system for large scale applications, *Energy Conversion and Management*, 2013;66

- B. Turker, Importance of Utilizing Local Energy Resources for Electricity Generation, Renewable Energy 2030 - Experts' Visions Conference 2012, Oldenburg, Germany
- P.V. Aravind, C. Schilt, B. Turker, T. Woudstra, Thermodynamic Model of a Very High Efficiency Power Plant based on a Biomass Gasifier, SOFCs, and a Gas Turbine, International Journal of Renewable Energy Development, 2011;1(2)
- S. Arroyo Klein, B. Turker, J. Trujillo, M. Kühn, B. Lenz, Technical and Economic Assessment of Utilizing Vanadium Redox Flow Batteries for Grid Integration of Wind Power, International Flow Battery Forum 2011, Edinburgh, UK
- B. Turker, B. Lenz, Using Vehicle-to-Grid (V2G) Technology to Compensate for Wind Power Forecasting Errors, World Wind Energy Conference 2010, Istanbul, Turkey